FLOW CHARACTERISTICS OF REFRIGERANT INSIDE DIABATIC CAPILLARY TUBE

A thesis submitted in partial fulfilment of the requirement for the award of degree of

MASTER OF ENGINEERING
IN
CAD/CAM & ROBOTICS

Submitted By
Akash Deep Singh
Roll No. 80781001

Under the guidance of

Mr. Sumeet Sharma

Sr. Lecturer, Deptt. of Mechanical Engg.

Thapar University, Patiala

DEPARTMENT OF MECHANICAL ENGINEERING
THAPAR UNIVERSITY
PATIALA-147004, INDIA

DECLARATION

I hereby declare that the work in this thesis entitled **"Flow Characteristics of Refrigerant Inside Diabatic Capillary Tube"** in partial fulfillment of requirement for the award of the master degree in **CAD/CAM & Robotics** submitted in the Mechanical Engineering Department, Thapar University, Patiala, is an authentic record of the initial work carried out by me under the guidance of **Mr. Sumeet Sharma, Sr. Lecturer, Mechanical Engineering Department, TU, Patiala.**

The matter embodied in this report has not been submitted in part or full to any other university or institute for the award of any degree.

Dated: 15/7/09

(Akash Deep Singh)

This is to certify that above declaration made by the student concerned is correct to the best of my knowledge & belief.

Mr. SUMEET SHARMA
Sr. Lecturer
Mechanical Engineering Department
Thapar University
Patiala-147004

Countersigned by

Dr. S.K.MOHAPATRA
Professor and Head
Mechanical Engineering Department
Thapar University
Patiala-147004

Dr. R.K.SHARMA
Dean of Academic Affairs
Thapar University
Patiala-147004

ACKNOWLEDGEMENT

I am highly grateful to the authorities of Thapar University, Patiala for providing me this opportunity to carry out the thesis work.

I would like to express a deep sense of gratitude and thank profusely to my thesis guide Mr. Sumeet Sharma for their sincere & invaluable guidance, suggestions and attitude, which inspired me to submit thesis in the present form. His dynamism and diligent enthusiasm have been highly instrumental in keeping my spirits high. His flawless and forthright suggestions blended with an innate intelligent application have crowned my task with success.

I am also thankful to Dr. S.K.Mohapatra (H.O.D.), all faculty, and staff members of Mechanical Engineering Department (MED), and staff of central library, TU, Patiala for their intellectual support.

I would also like to offer my sincere thanks to Dr. Mohd. Kaleem Khan, IIT Patna without the help of him it might not be possible for me to come up to this level.

Last but not least, I thank my family members and my friends for always being there when I needed them most, and for supporting me through all these months.

Akash Deep Singh

ABSTRACT

In the present investigation, an attempt is made to develop a mathematical model of diabatic capillary tube. The mathematical model has been developed by using equations of conservation of mass, momentum and energy. We need to calculate both single phase and two phase length for predicting the length of diabatic capillary tube. Flow of refrigerants inside a capillary tube is a complex phenomenon and is further complicated by heat exchange region in case of diabatic capillary tube. The presence of heat exchange region causes a delay of vaporization. When the vaporization starts pressure falls sharply. Friction Factor also plays an important role in the pressure drop. Moody (1944) correlation is used to calculate the friction factor. McAdams et al. (1942) viscosity correlation has been used to evaluate the two phase viscosity of the refrigerant. Input parameters have been taken from the data of Mendoca et al. (1998). Further a geometric model is developed in Pro-E and the mesh is created in Ansys ICEM CFD and analysis is carried out in Ansys CFX which has three modules CFX-Pre, Solver and CFX-Post.

Finally the results of mathematical model are validated with Ansys CFX and found to be in fair agreement.

LIST OF FIGURES

LIST OF TABLES

Contents

Chapter 4: Results and Discussion

Appendix

Nomenclature: -

d capillary tube internal diameter, m

D coil diameter, m

D_s suction line diameter, m

ΔT_{sub} degree of subcooling, K

e roughness height, m

f friction factor

G mass velocity, kg/m2/s

L capillary tube length, m

m mass flow rate, kg/s

P pressure, Pa

T temperature, _C

Greek letters

μ viscosity, kg/m/s

ρ density, kg/m3

Subscripts

hx heat exchanger

in capillary tube inlet

k condenser

o evaporator

out outlet

Chapter 1

Introduction

In this chapter, the capillary tubes, their classifications and the flow phenomena associated with capillary tube diabatic capillary tubes have also been discussed. The objectives of the proposed work have also been mentioned.

1.1 Capillary tube and its classification

In a vapour compression cycle, the refrigerant vapours emerging from the evaporator after producing the cooling effect enters the compressor. The compressor activates the refrigerant to high temperature and high pressure superheated vapours. These high temperature vapours get condensed inside the condenser. The saturated liquid refrigerant enters the capillary tube where the expansion pressure from high pressure to low pressure takes place. After expansion the refrigerant re-enters the evaporator and the cycle continues.

Capillary is used as an expansion device in a refrigerant in low capacity vapour compression systems like domestic refrigerators, freezers, window type air conditioners etc. A capillary tube is a 1 - 6 m long tube of drawn copper with an inside diameter generally from 0.5 to 2 mm, which connects the outlet of the condenser to the inlet of the evaporator. The capillary tube has low cost and is simple in construction. The refrigeration system employing capillary tube requires low starting torque motor as the pressure across the capillary tube equalizes.

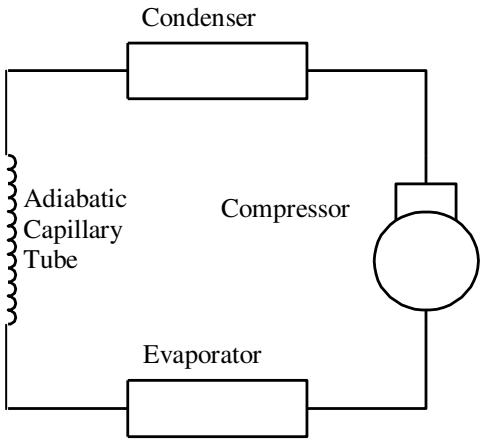

Fig. 1.1 Vapour Compression System

Depending upon the flow, the capillary tubes can be classified as follows:

- adiabatic capillary tube and
- diabatic capillary tube

In adiabatic arrangement, the capillary tube is thermally insulated and the heat exchange with the ambient is negligible.

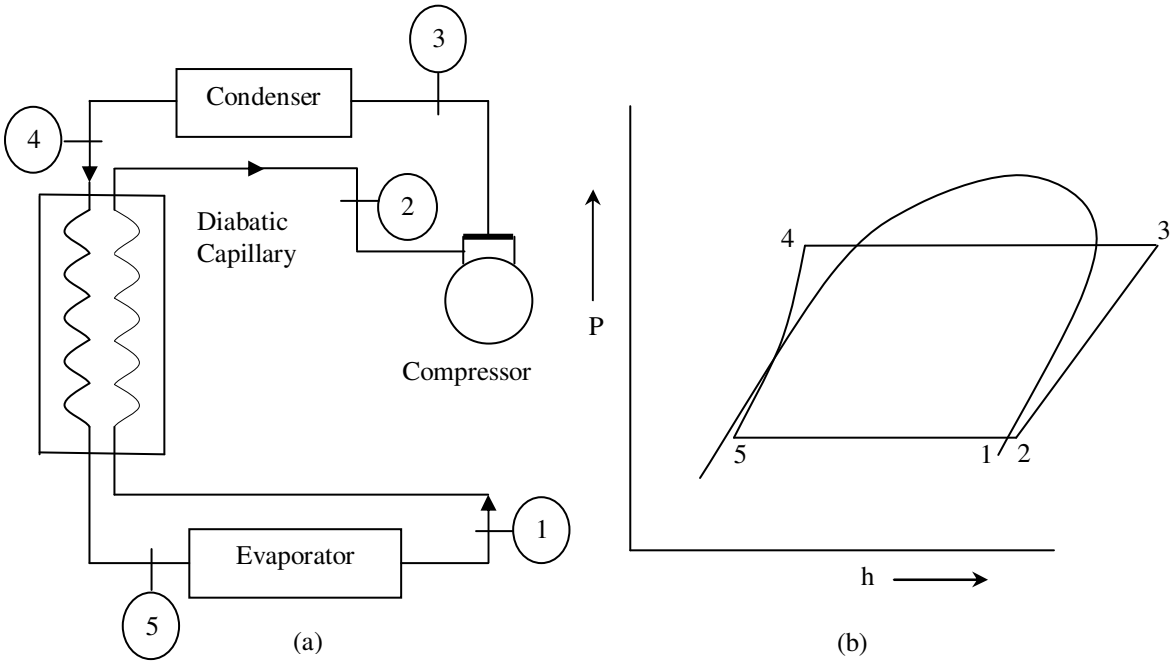

Fig. 1.2 (a) VCS using diabatic capillary tube (b) P-h diagram

In a diabatic flow arrangement, shown in Fig. 1.2., the capillary tube is bonded with the cold compressor suction line in a counter flow arrangement. Employing diabatic capillary tube in a refrigeration system results in higher refrigerating effect, thus, a better system performance is achieved. As shown in Fig. 1.2, the enthalpy of liquid refrigerant flowing in the capillary tube continuously falls in the single phase region as well due to heat exchange with the cold suction line of compressor. With the result the enthalpy of the refrigerant falls continuously throughout the capillary tube length. The presence of heat exchanger produces considerable subcooling in the liquid region, and consequently, causes a delay in flash point. Unlike adiabatic capillary tubes where the refrigerant temperature in the single phase region is constant, heat transfer to the suction line causes the temperature of refrigerant and, hence, the saturation pressure of the liquid refrigerant to fall. The reduction in saturation pressure causes a delay in the onset of flashing, and thus results, a longer single phase liquid length.

The thermal contact between the capillary tube and the compressor suction line can be attained in two ways viz., lateral and concentric arrangement. The two arrangements are shown in Fig. 1.3. In lateral configuration, the capillary tube is bonded with the

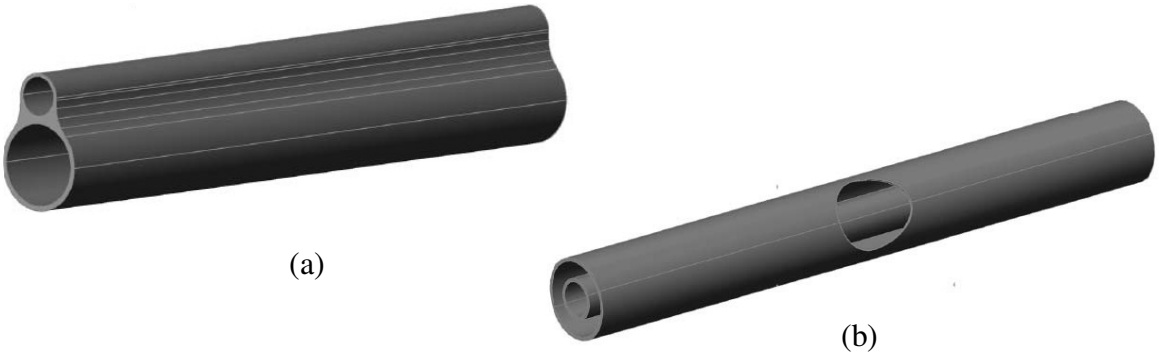

Fig. 1.3 (a) Lateral arrangement (b) Concentric arrangement

compressor suction line by means of a solder or brazing joint. Further, the copper tape is wound around the two bonded tubes so that the walls of the tubes could attain thermal equilibrium. In concentric arrangement, the capillary tube occupies the core of compressor suction line as shown in Fig. 1.3 (b). In the concentric arrangement, the capillary tube is surrounded by the cold vapors of the suction line emerging from the evaporator. Thus, the capillary tube is in direct contact with the vapors, a higher heat transfer from the capillary tube to the suction line vapors will take place. Therefore, the concentric arrangement is preferred over the lateral arrangement as the contact thermal resistance is smaller and a better system performance is achieved.

Normally, the refrigerant temperature inside the capillary tube is higher than the refrigerant vapour temperature inside the suction line. Therefore,

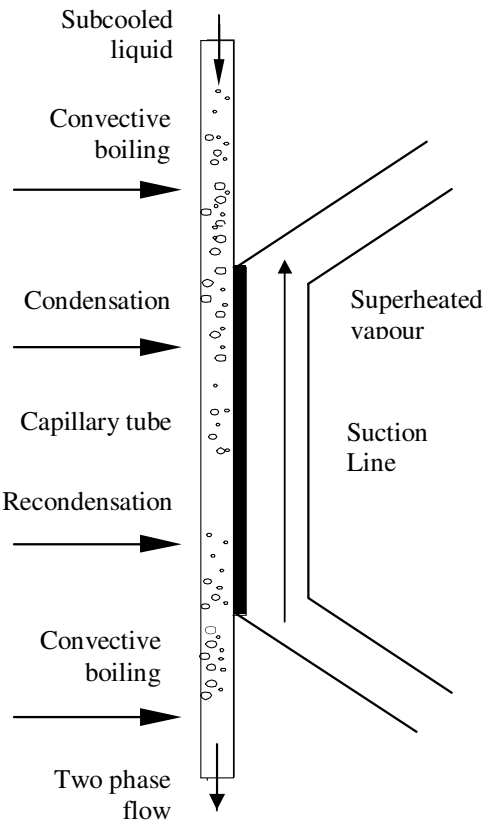

Fig. 1.4 Flow pattern along with capillary tube-suction line heat exchanger

earlier studies assumed the two-phase convective heat transfer coefficient to be infinite and based on condensation. In fact, as per the relative position of refrigerant flow inside the capillary tube-suction line heat ex-changer, it can be categorized into three different states: convective boiling, condensation, and liquid state. As can be seen from Fig. 1.4, the inlet and outlet region of the capillary tube-suction line heat exchanger is fully adiabatic and hence subcooled refrigerant entering the capillary can cause the flashing to occur due to strong pressure drop effect. This can be termed convective boiling in the tube. On the other hand, the flow pattern for two-phase refrigerant entering the tube within the adiabatic capillary tube inlet region is similar to that described for sub cooled inlet. When the refrigerant flows into the capillary tube-suction line heat exchange region, it loses heat to the suction line side, its quality decreases and at times the refrigerant can be in complete condensation state. Due to the strong heat transfer effect, the refrigerant quality may reduce to zero, leading the re-condensation phenomenon to occur.

1.2 Objectives of the proposed work

- To develop the numerical models for diabatic capillary tube using finite difference methods (FDM).
- To develop same model using ANSYS CFX module.
- To validate the developed numerical model with the developed ANSYS CFX module.

Chapter 2

Literature Review

The literature of diabatic capillary tubes can be grouped under two categories, viz. experimental investigation numerical investigations as shown in Fig. 2.1. Historically, tubes were sized in a number of ways e.g. empirically, by interpolation, extrapolation from previous experience of the capillary designers, or through charts produced by various agencies such as ASHRAE and commercial companies.

Since the present work mainly deals in numerical part, focus will be more on numerical investigations. The experimental investigations have been reviewed just for the sake of validation of the models to be developed using FDM and ANSYS CFX module.

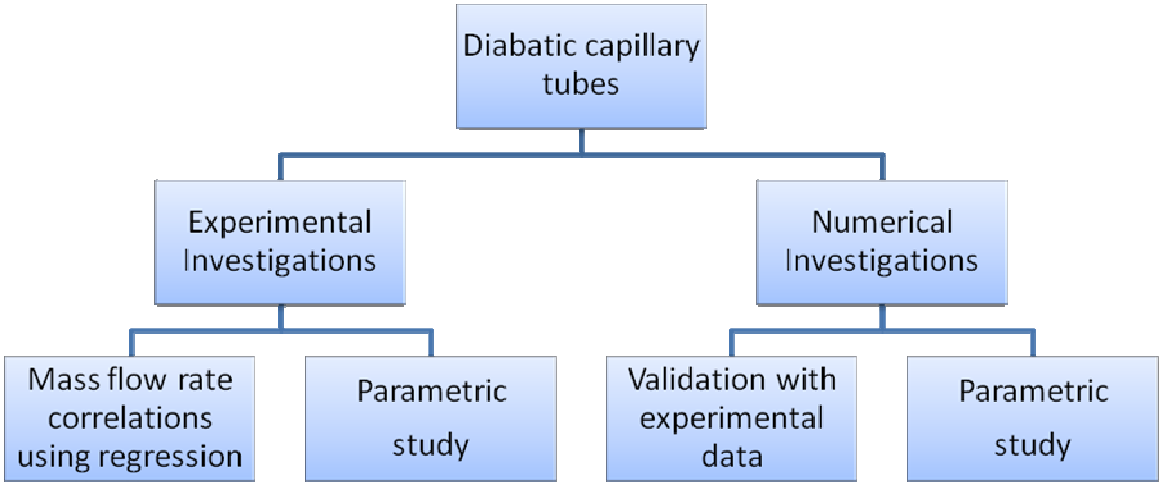

Fig. 2.1 Organization of literature on diabatic capillary tube

2.1 Experimental Investigations

The experimental investigations involve the experimental work conducted by different researchers to evaluate the performance of diabatic capillary tubes using different refrigerants. Table 2.1 shows some of experimental studies of various other researchers.

The experimental work on diabatic capillary tubes was pioneered by Staeblar [20]. The capacity balance characteristics to determine the length of diabatic capillary tube for R-12 and R-22 were proposed. The characteristics curves were plotted for 1.067 mm capillary tube diameter at two condenser temperatures, 30 ^{o}C and 42.2 ^{o}C and evaporator temperatures ranging from -28.9 ^{o}C to -1.1 ^{o}C.

Table 2.1 Experimental investigations on diabatic capillary tube

author(s) (year)	*refrigerant(s)*	*range of parameters*	*characteristics/ correlations*	*remarks*
Staeblar[20] (1948)	R-12 R-22	d = 0.787 to 1.397 mm T_o = -28.9 ^{o}C to -1.1 ^{o}C T_k = 30 ^{o}C and 42.2 ^{o}C	capacity balance	length is determined
Bolstad and Jordan[5] (1949)	R-12	d = 0.66 to 1.397 mm L = 1.83, 3.66, 5.49 m P_k = 827.4, 965.3, 1103.3 kPa P_o = 103.4 kPa	temperature and pressure profile	friction factor relations
Pate and Tree[16] (1984)	R-12	d = 0.71 mm Ds = 6.35 mm L_{hx} = 2.086m L = 2.953 m	temperature and pressure profiles	observed metastable flow in adiabatic capillary tube but not in diabatic
Khan et al.[11] (2007)	R-134a	p = 40, 60, 80 mm T_k = 40 _C DT_{sub} = 10 _C m = 8.28 kg/h d = 1.07 mm;	Comparison of the results of spiral capillary tube with straight capillary operating under similar conditions	Homogeneous two-phase flow

Bolstad and Jordan[5] investigated capillary tubes of diameters ranging from 0.66 mm to 1.397 mm for three inlet pressures of 827.4 kPa, 965.3 kPa and 1103.3 kPa. It was concluded that the effect of changes in evaporator pressure on the mass flow rate of R-12 was insignificant. The refrigerant temperature fell rapidly in the heat exchange region as the suction line of compressor is at a lower temperature than the capillary tube while the pressure fell linearly up to certain length and as the flashing began the drop in pressure is accelerated. Finally, friction factor characteristics, demarcating the laminar and turbulent regimes, were drawn for the flow of water inside the same capillary tube. Pate and Tree [16] analyzed the diabatic flow of R-12 through the straight capillary tube with air flowing in the suction line in counter flow direction forming an open loop. The same tube acted as an adiabatic capillary tube as the air flow was shut-off. It was found that the behavior of capillary tube with heat transfer was considerably different from that of an adiabatic capillary tube. When comparing the pressure profiles of diabatic capillary tube with adiabatic capillary tube, the higher degree of inlet subcooling resulted in a greater mass flow rate and a steeper pressure profile. It was due to the increased subcooling

causing the delay in vaporization and a shorter two-phase flow region was resulted. This, in turn, resulted in less flow restriction and a higher mass flow rate.

2.2 Numerical Investigations

Table 2.2 shown below shows the work of different authors on diabatic capillary tubes by using numerical techniques.

Table 2.2 Numerical investigations on diabatic capillary tube

author(s) (year)	*refrigerant(s)*	*range of parameters*	*characteristics/ correlations*	*methodology*
Valladares et al. [24] (2002)	Refrigerants and mixtures	-	one dimensional steady and transient numerical simulation	homogeneous two-phase flow model, finite volume method
Valladares et al. [25] (2002)	Refrigerants and mixtures	-	parametric study for concentric diabatic capillary tube	validation of numerical model with data of previous researchers
Xu and Bansal[27] (2002)	R-134a	d = 0.66 mm; T_k = 48 ^oC D_s = 6.6 mm; L_{hx} = 1.0 m; T_o = -15 5 ^oC; ΔT_{sub} = 1 ^oC	mathematical modeling, validation and parametric study	finite volume method
Bansal and Xu[2] (2003)	R-134a	d = 0.66 mm L_{hx} = 1.0 to 2.5 m; T_k = 32 to 47 ^oC T_o = -10 to -20 ^oC ΔT_{sub} = 1,2 and 3 ^oC	parametric study	finite volume method
Valladares[26] (2004)	R-407C	-	numerical simulation	review of his own numerical models [24-25]
Chen and Gu[6] (2005)	CO_2	d = 1.85 mm T_{in} = 45 ^oC T_{out} = -5 to 10 ^oC	pressure, temperature enthalpy and entropy profiles	finite volume method
Bansal and Yang[3] (2005)	R-134a R-600a	d = 0.867 mm; D_s = 6.6 mm; L_{hx} = 1.0 m; T_k = 42 ^oC; T_o = -13 ^oC; ΔT_{sub} = 1 ^oC	parametric study	finite volume method
Bansal and Yang[4] (2005)	R-134a R-600a	d = 0.867 mm; D_s = 6.6mm; L_{hx}=1 m T_k = 42 ^oC, T_o = -13 ^oC ΔT_{sub} = 1 ^oC	proposed a thermodynamic equation to determine the pressure drop per unit length during re-condensation	finite difference scheme and successive substitution method
Khan et al.[11] [2007]	R-134a	p = 40, 60, 80 mm T_k = 40 _C DT_{sub} = 10 _C m = 8.28 kg/h d = 1.07 mm	Comparison of the results of spiral capillary tube with straight capillary operating under similar conditions	Homogeneous two-phase flow

Bansal and Rupasinghe[17] developed an empirical model for sizing capillary tubes.

This paper presents an empirical model that has been developed to size adiabatic and non-adiabatic capillary tubes for small vapour compression refrigeration systems, in particular, household refrigerators and freezers. The model is based on the assumption that the length of a capillary tube is dependent on five primary variables, namely the capillary tube inner diameter, the mass flow rate of the refrigerant in the capillary tube,

the pressure difference between highside and lowside, the refrigerant subcooling at capillary inlet and the relative roughness of the capillary tube material. The model is validated with previous studies over a range of operating conditions and is found to agree reasonably well with the experimental data for HFCI34a.

Sami, Maltais and Desjardins[19] studied the Influence of Geometrical Parameters on Capillary Behavior with New Alternative Refrigerants.

In this paper, the experimental data obtained on capillary tube behavior, using various new alternatives under different geometrical parameters are presented and analyzed. Capillary geometrical parameters include length, diameter, as well as entrance conditions. The results clearly showed that the pressure drop across the capillary tube is significantly influenced by the diameter of the capillary tube, inlet conditions to the capillary and refrigerant type. The data demonstrated that the capillary pressure drop decreases with the increase of the capillary diameter and that alternatives in general experience higher pressure drop than that of R-22.

Wongwises, Songnetichaovalit, Lokathada, Kritsadathikarn, Suchatawat and Pirompak [23] did a comparison of the flow characteristics of refrigerants flowing through adiabatic capillary tubes.

This paper presents theoretical comparison of the flow characteristics of many pairs of refrigerants flowing through adiabatic capillary tubes. The two-phase flow model developed was based on homogeneous flow assumption. Two-phase friction factor was determined from Colebrook correlation. The viscosity model was also based on the recommendations from the previous literature. For all pairs, numerical results showed that the traditional refrigerants consistently gave lower pressure drops for both single-phase and two-phase flow than the environmentally acceptable alternative refrigerants which resulted in longer tube lengths.

Sinpiboon and Wongwises[22] did numerical investigation of refrigerant flow through diabatic capillary tubes.

A mathematical model is developed to study flow characteristics in diabatic capillary tubes. The theoretical model is based on conservation of mass, energy and momentum of fluids in the capillary tube and suction line. The mathematical model is categorized into three different cases, depending on the position of the heat exchange process. The first case is considered when the heat exchange process starts in the single-phase flow region, the second case is determined when the heat exchange process starts at the end of the single-phase flow region, and the last case is considered when the heat exchange process takes place in the two-phase flow region. A set of differential equations is solved by the explicit method of finite-difference scheme. The model is validated by comparing with the experimental data obtained from previous works. The results obtained from the present model show reasonable agreement with the experimental data. The present diabatic capillary tube model can be used to integrate with system models working with alternative refrigerants for design and optimization.

Zhang and Ding[9] to approximate analytic solutions of adiabatic capillary tube.

Approximate analytic solution of capillary tube is valuable for theoretical analysis and engineering calculation. In this work, two kinds of approximate analytic solutions of adiabatic capillary tube have been developed. One is the explicit function of capillary tube length. Another is the explicit function of refrigerant mass flow rate. In these solutions, the choked flow condition is taken into account without iterative calculations. The approximate predictions are found to agree reasonably well with experimental data in open literatures.

Bansal and Yang[4] developed a model for HFC-134a and HC-600a to study heat transfer phenomena in non-adiabatic capillary tubes.

A numerical simulation model for lateral capillary tube-suction line heat exchangers is presented to analyze its performance characteristics in small vapour compression refrigeration systems (e.g. domestic refrigerators). Appropriate heat transfer correlations have been used to illustrate the heat transfer phenomena inside the tubes. Some convergence problems were encountered during the execution of the model when lower vapour temperature inside the suction line caused the two-phase refrigerant inside the

capillary tube to re-condense within the heat exchange region. The modeling was performed with two refrigerants, namely HFC-134a and HC-600a. Further, a simple theoretical equation has been developed to express the re-condensation phenomenon in diabatic capillary tubes.

Yang and Bansal[3] presented Numerical investigation of capillary tube-suction line heat exchanger performance.

This paper presents the numerical results of the effect of different parameters on the performance of capillary tube-suction line heat exchangers (CT-SLHX), including condensing and evaporating temperatures, degrees of subcooling and superheat, tube diameter, tube length, and refrigerant flow inlet quality. The heat transfer rate from the capillary tube to the suction line has been simulated for two environmentally friendly refrigerants, namely HFC-134a and HC-600a. The simulation model also postulates the situation where heat may be transferred from capillary tube to the ambient air, before entering the CT-SLHX.

Bansal and Rupasinghe[18] developed an homogenous model for adiabatic capillary tubes.

This paper presents a homogeneous two-phase flow model, CAPIL, which is designed to study the performance of adiabatic capillary tubes in small vapour compression refrigeration systems, in particular household refrigerators and freezers. The model is based on the fundamental equations of conservation of mass, energy and momentum that are solved simultaneously through iterative procedure and Simpson's rule. The model uses empirical correlations for single-phase and two-phase friction factors and also accounts for the entrance effects. The model includes the effect of various design parameters, namely the tube diameter, tube relative roughness, tube length, level of subcooling and the refrigerant flow rate. The model is validated with earlier models over a range of operating conditions and is found to agree reasonably well with the available experimental data for HFC-134a.

Valladares[24] did numerical simulation of diabatic capillary tubes. Part I: Mathematical formulation and numerical model.

A detailed one-dimensional steady and transient numerical simulation of the thermal and fluid-dynamic behavior of capillary tube suction line heat exchangers has been carried out. The governing equations (continuity, momentum, energy and entropy) for fluid flows, together with the energy equation in solids, are solved iteratively in a segregated manner. The discretized governing equations in the zones with fluid flow are coupled using a fully implicit step-by-step method. An implicit central difference numerical scheme and a line-by-line solver were used in solids. A special treatment has been implemented in order to consider transitions. All the flow variables (enthalpies, temperatures, pressures, mass fractions, heat fluxes, etc.) together with the thermophysical and transport properties are evaluated at each point of the grid in which the domain is discretized. The numerical model allows analysis of aspects such as geometry, type of fluid, critical or non-critical flow conditions.

Khan, Kumar, Sahoo[11] developed a model based on FDM to refrigerant mass flow rate

Khan et al.[11] presented the performance of R-134a through a diabatic capillary tube with lateral configuration. The paper was divided into two sections: (1) an experimental investigation of straight and helical diabatic capillary tubes and (2) a numerical investigation of the straight diabatic capillary tube. In the experimental investigation, the effects of parameters such as capillary tube diameter, capillary tube length, coil pitch, and inlet subcooling on the refrigerant mass flow rate through a diabatic capillary tube were studied. In addition to the parameters mentioned above, the mass flow rate through a diabatic helical capillary tube was also found to be a function of suction-line inlet superheat and heat exchange length. The suction-line inlet superheat in the present investigation is not a controlled parameter. A comparison of the results of diabatic helical capillary and adiabatic helical capillary tubes was also made. On the basis of acquired experimental data, a correlation to predict the refrigerant mass flow rate was proposed.
It was found that the predictions of the proposed correlation are within ±5% agreement with the experimental data. In the numerical investigation, a mathematical model was developed by applying laws of conservation of mass, momentum, and energy to a straight

diabatic capillary tube. These differential equations were solved numerically using a finite difference method. The developed model was validated with experimental data from previous and present research.

Khan, Kumar, Sahoo[12] presented the experimental and numerical investigations systematically under different categories.

A comprehensive review of the literature on the flow of various refrigerants through the capillary tubes of different geometries viz. straight and coiled and flow configurations viz. adiabatic and diabatic, has been discussed in this paper. The paper presents in chronological order the experimental and numerical investigations systematically under different categories. The paper provides key information about the range of input parameters viz. tube diameter, tube length, surface roughness, coil pitch and coil diameter, inlet subcooling and condensing pressure or temperature. Other information includes type of refrigerants used, correlations proposed and methodology adopted in the analysis of flow through the capillary tubes of different geometries operating under adiabatic and diabatic flow conditions. It has been found from the review of the literature that there is a lot more to investigate for the flow of various refrigerants through different capillary tube geometries.

2.3 Problem Formulation

On the basis of the literature survey following points has been taken into account to carry out with the present research work.

1. Despite its simplicity, the capillary tube-suction line heat exchanger is one of the most difficult components of the system to design and up to now, 90% of the work is concentrated on adiabatic capillary tubes and it is difficult to investigate the two phase fluid problems.
2. Due to the public concerns on the depletion of the ozone layer and global warming, CFCs and HCFCs are being phased out from the refrigeration industry and there is a need to investigate the flow characteristics of new refrigerants like R-134a.
3. As stated earlier diabatic capillary tube has advantage over adiabatic capillary tube and is mostly used in all the refrigeration systems.
4. Proper prediction of the capillary tube performance required several preparation activities due to the usage of uncommon refrigerants and large number of capillary tubes having different dimensions so we will use the software for this.
5. No work has been reported on the modeling of diabatic capillary tube using the commercially available softwares like ANSYS-CFX.

Chapter 3

Modeling Procedure

In this chapter, the mathematical model has been developed by applying laws of conservation of mass, momentum and energy on capillary tube and compressor suction-line. The mathematical model obtained is a set of differential equation. A geometric model is also developed in Pro-E and solved with Ansys CFX.

3.1 Finite Difference Method

Finite Difference methods are used to solve differential equations numerically. Physical domain is converted to computational domain by discretizing it into a number of linear elements. Following steps describe the procedure of solving differential equation.

- Governing differential equations are obtained by applying the laws of conservation of energy momentum and mass.
- Using finite difference approximation to transform a given differential equations into difference equations.
- Algebraic Equations in nodal unknowns are thus obtained.
- These simultaneous algebraic equations can be solved by any numerical method.
- The solution of these algebraic is the solution at the nodes.

The finite difference approximations using Taylor Series

$$f(x_0 + \Delta x) = f(x_0) + \Delta x f'(x) + \frac{\Delta x^2}{2!} f''(x) + \ldots\ldots \tag{3.1}$$

$$f(x_0 - \Delta x) = f(x_0) - \Delta x f'(x) + \frac{\Delta x^2}{2!} f''(x) + \ldots\ldots \tag{3.2}$$

Approximation for first Derivative (forward difference formulation)

From equation (1)

$$f'(x_0) = \frac{f(x_0 + \Delta x) - f(x_0)}{\Delta x} - f''(x)$$

$$f'(x_0) = \frac{f(x_0 + \Delta x) - f(x_0)}{\Delta x} - 0(\Delta x)$$

or

$$f'(x_0) \approx f(x_0 + \Delta x) - f(x_0)$$

$$f_i \approx \frac{f_{i+1} - f_i}{\Delta x}$$

Backward difference formulation

From equation (2)

$$f'(x_0) = \frac{f(x) - f(x_0 - \Delta x)}{\Delta x} + f''(x).\frac{\Delta x}{2} \tag{3.3}$$

$$f_i' = \frac{f_i - f_{i-1}}{\Delta x} + 0(\Delta x) \qquad \text{where } 0(\Delta x) \text{ contains higher order terms.}$$

$$f_i' \approx \frac{f_i - f_{i-1}}{\Delta x} \quad \text{having an order of accuracy } 0(\Delta x)$$

Central Difference formulation

$$f(x_0 + \Delta x) - f(x_0 - \Delta x) = 2\Delta x f'(x_0) + 2\frac{\Delta x^3}{3!} f'''(x_0)$$

$$f'(x_0) = \frac{f(x_0 + \Delta x) - f(x_0 - \Delta x)}{2\Delta x} - \frac{\Delta x^2}{3} f'''(x_0) \tag{3.4}$$

$$f_i' \approx \frac{f_{i+1} - f_{i-1}}{2\Delta x} \quad \text{having an order of accuracy } 0(\Delta x)$$

Approximation for second derivative (Central difference formulation)

Adding Equation (1) and (2) we get

$$f(x_0 + \Delta x) + f(x_0 - \Delta x) = 2f(x_0) + 2\frac{\Delta x^2}{2!} f''(x_0) + \ldots\ldots \tag{3.5}$$

$$f''(x_0) \approx \frac{f(x_0 + \Delta x) - 2f(x_0) + f(x_0 - \Delta x)}{\Delta x^2} - 0(h^2)$$

$$f_i'' = \frac{f_{i+1} - 2f_i + f_{i-1}}{\Delta x^2}$$

3.2 Mathematical Modeling

The diabatic capillary tube of lateral configuration is shown in Fig 3.1. In lateral configuration, the capillary tube is brazed on the suction line and then the assembly is wrapped with copper tape. The capillary tube is insulated to avoid heat transfer to the surroundings. For the purpose of analysis, capillary tube has been divided into three regions: the initial adiabatic length (L_{in}), the intermediary region length or the heat exchange region length (L_{hx}), and the final adiabatic length (L_f).

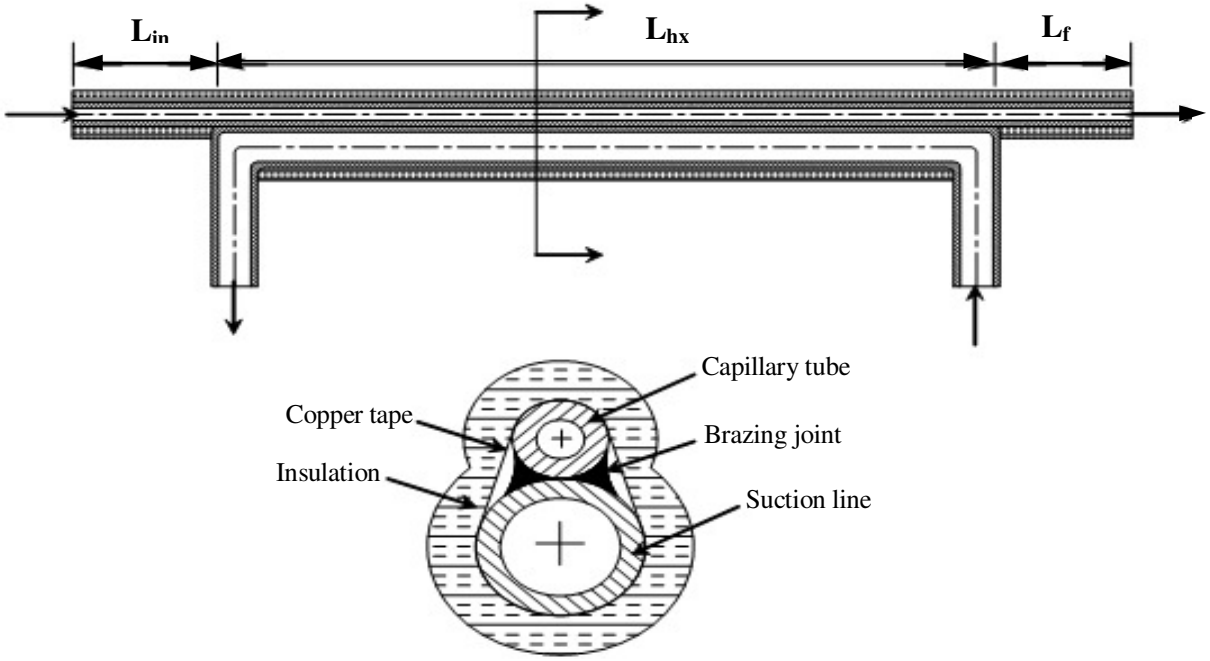

Fig. 3.1 Sectional views of diabatic straight capillary tube

The developed mathematical model is based on the following assumptions:

– straight, horizontal and constant inner diameter and roughness of the capillary tube

– negligible thermal resistance at the contact of the capillary tube and suction line

– one-dimensional and steady turbulent flow through the capillary tube

– homogenous two-phase flow

– no heat exchange with the surroundings

Table 3.1 shows the governing equations for both capillary tube and suction line fluid flow using principle of mass, momentum and energy conservations.

Table 3.1: Governing Equations

Conservation Equations	Capillary Tube	Suction Line
Mass	$G_c = m/A_c$	$G_s = m/A_s$
Momentum	$-\frac{dP}{dZ} = f\frac{G_c^2}{2d_c} + G_c^2\frac{dv}{dz}$	$-\frac{dP}{dZ} = f\frac{G_s^2}{2d_s} + G_s^2\frac{dv}{dz}$
Energy	$\frac{dT_c}{dZ} = \frac{-h_c\pi d_c(T_c - T_w)}{mc_{pc}} - \frac{G_c^2}{2}\frac{d_v^2}{dz}$	$\frac{dT_s}{dZ} = \frac{-h_s\pi d_s(T_w - T_s)}{mc_{ps}} - \frac{G_s^2}{2}\frac{d_v^2}{dz}$

Heat balance at the tube wall can be expressed by considering the fluid flow in the capillary tube and suction line. Therefore,

$$h_c\pi d_c(T_c - T_w) = h_s\pi d_s(T_w - T_s) \tag{3.6}$$

where, heat transfer coefficients h_c and h_s can be determined from the following equation:

$$h = \frac{N_u.k}{d} \tag{3.7}$$

where *Nu* is the Nusselt number is given by Gnielinski[10] correlation :

$$N_u = \frac{\left(\frac{f}{8}\right)(R_e - 1000)Pr}{1 + 12.7\sqrt{\frac{f}{8}}\left(Pr^{\frac{2}{3}} - 1\right)} \tag{3.8}$$

where, *Pr* is Prandtl number given by the following relationship:

$$Pr = \frac{c_p\mu}{k} \tag{3.9}$$

The friction factor *f* is evaluated using Moody[15] correlation given by

$$f = \frac{1.325}{\left[\ln\left(\frac{e/d}{3.7} + \frac{5.74}{R_e^{\,2}}\right)\right]^2} \tag{3.10}$$

For the saturated or superheated vapor flowing through the suction line, neglecting the elevation difference and external work in the capillary tube, term $\frac{G_s^2}{2}\frac{dv^2}{dz}$ is dropped from the energy equation.

Inside the suction line, thermophysical properties of superheated vapor have not been assumed constant and are developed as the function of suction line temperature. For different suction line temperatures, thermophysical properties are plotted as a function of suction line temperature. The best fit line is fitted and the equation for each thermophysical property is derived and then is used in the computer program.

After the development of mathematical model, as described in the previous section, the physical domain shown in Fig. 3.1 is converted into computational domain by discretizing the heat exchange region into 'N' number of infinitesimal elements of equal lengths. The governing differential equations of momentum and energy have been converted into the difference equations using forward difference method of the Finite Differences. These difference equations have been solved simultaneously to obtain the pressure and temperature distribution along the capillary tube. Further, the capillary tube lengths in the adiabatic regions of the capillary tube are calculated. In the adiabatic regions of the capillary tube, refrigerant temperature is constant when the flow is single phase flow while it falls sharply in the two-phase flow.

Heat exchange process in the single phase flow region

Fig 3.2 shows the schematic diagram of the capillary tube and suction line heat exchanger with the heat transfer starts in the single phase region. As can be seen from the figure that refrigerant enters the capillary tube in a subcooled liquid state. There is a drop in pressure at the inlet of capillary tube due to sudden contraction. The pressure at point 2 is given by

$$P_2 = P_1 - k\frac{G_c^2 v}{2} \tag{3.11}$$

where *k* is the entrance loss coefficient and its value has been taken as 1.5.

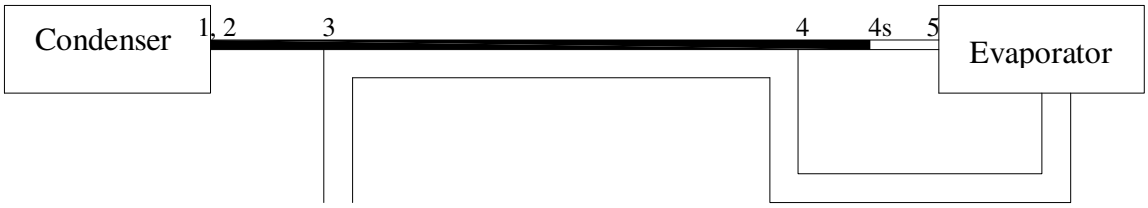

Fig. 3.2 Schematic diagram of capillary tube-suction line heat exchanger

The pressure drop in the initial length is evaluated using the momentum equation, therefore, pressure at point 3 can be written as

$$P_3 = P_2 - \frac{f_{sp}\, v G_c^2 L_{in}}{2 d_c} \tag{3.12}$$

Since the flow in the capillary tube is adiabatic in the section 1-3, the refrigerant temperature will be constant in section 1-3.

$$T_3 = T_1 \tag{3.13}$$

In section 3-4, the flow is diabatic, the temperature will not be constant and will vary along the length of capillary tube and in the suction line depending upon the rate of heat transfer. Since it is not known where the flash point location will lie in the heat exchange region, the single phase heat exchange region has been discretized into a number of infinitesimal elements of constant length ($\Delta z = z_{i+1} - z_i$). Therefore, after each elemental length, the computer program checks the state of refrigerant. Later on all these infinitesimal elements are summed up to get the single phase heat exchange length.

The pressure after each elemental length can be evaluated by converting the differential momentum equation into the difference equation using the forward difference formulation as:

$$-\frac{P_{i+1}-P_i}{z_{i+1}-z_i} = f\frac{G_c^2 v_i}{2 d_c} + G_c^2 \frac{v_{i+1}-v_i}{z_{i+1}-z_i} \tag{3.14}$$

The refrigerant temperature inside the capillary tube and the suction line can be calculated by applying the energy equation (shown in Table 3.1). As the energy equations are in differential form, they have been first converted difference equations as follows:

$$\frac{T_{c_{i+1}} - T_{c_i}}{Z_{i+1} - Z_i} = -\frac{h_c \pi d_c (T_{c_i} - T_{w_i})}{m_c c_{pc}} - \frac{G_c^2}{2} \frac{(v_{i+1}^2 - v_i^2)}{Z_{i+1} - Z_i} \tag{3.15}$$

$$\frac{T_{s_{i+1}} - T_{s_i}}{Z_{i+1} - Z_i} = -\frac{h_s \pi d_s (T_{w_i} - T_{s_i})}{m_s c_{ps}} \tag{3.16}$$

The wall temperature T_w has been calculated by the wall heat balance equation (3.6) as follows:

$$T_{w_i} = \frac{h_c d_c T_{c_i} + h_s d_s T_{s_i}}{h_c d_c + h_s d_s} \tag{3.17}$$

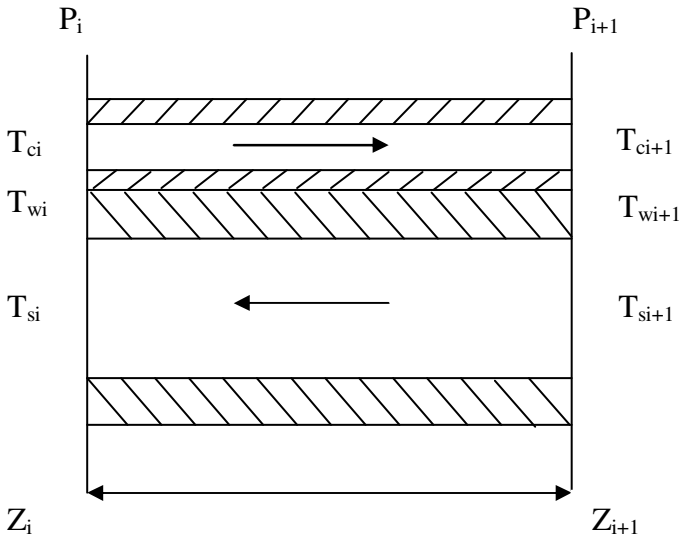

Fig. 3.3 Infinitesimal fluid element in the heat exchange region

The equations (3.15) to (3.17) have been solved simultaneously to obtain the distribution of temperature along the capillary tube-suction line heat exchanger. The temperature at the end of the heat exchange region i.e., T_4, will be known in this way. From 4 to 4s the single-phase flow is again adiabatic. Therefore,

$$T_{4_s} = T_4 \tag{3.18}$$

In the section 4s-5, the flow of refrigerant is two-phase adiabatic flow. This section is again discretized into '*n*' number of infinitesimal elements having constant pressure difference across them.

The pressure at any section '*i*' is given by

$$P_i = P_{4s} - idP \tag{3.19}$$

where, P_{4s} is the saturation pressure corresponding to the refrigerant temperature inside the capillary tube at the end heat exchange region, i.e., T_4. With the pressure P_i corresponding quality, x_i can be calculated and the entropy at the i-th section can be determined from

$$s_i = s_f + x_i s_{fg} \tag{3.20}$$

The incremental length, *dL*, is calculated from section after section. For each section, pressure, temperature, vapour quality, viscosity, friction factor and entropy are calculated. For calculating viscosity McAdams[13] Correlation was used as it gives the best two phase length for validation with Ansys CFX.

$$\frac{1}{\mu_{tp}} = \frac{x}{\mu_g} + \frac{1-x}{\mu_f} \tag{3.21}$$

It has been found that the entropy kept on increasing and after attaining certain value it started decreasing The calculations are done up to the point of maximum entropy. The pressure of the elemental section where entropy is maximum ($P_{i,smax}$), is then compared to the evaporator pressure (P_{evap})

$$\text{if } P_{i,smax} = P_e \text{ then } P_5 = P_e$$

$$\text{if } P_{i,smax} \neq P_e \text{ then } P_5 = P_{i,smax}$$

Integrating momentum equation from table 3.1 for the section 4 – 5

$$L_{tp} = 2d\left(\frac{-1}{G^2}\int_{P4}^{P_{smax}} \frac{\rho}{f_{tp}} dP + \int_{P_4}^{P_{smax}} \frac{dP}{\rho f_{tp}}\right) \tag{3.22}$$

The incremental length of each section is calculated using

$$\Delta L_i = \frac{2d}{f_{tp,i}}\left(\frac{-\rho_i \Delta P}{G^2} + \frac{\Delta \rho}{\rho_i}\right) \tag{3.23}$$

The total length of two-phase region is

$$L_{4s5} = L_{tp} = \sum_{i=1}^{n} \Delta L_i \tag{3.24}$$

The total length of capillary tubes is the sum of single and two-phase lengths, i.e.,

$$L = L_{13} + L_{34} + L_{44s} + L_{4s5} \tag{3.25}$$

Following flow chart depicts the step by step procedure followed to obtain results with mathematical model.

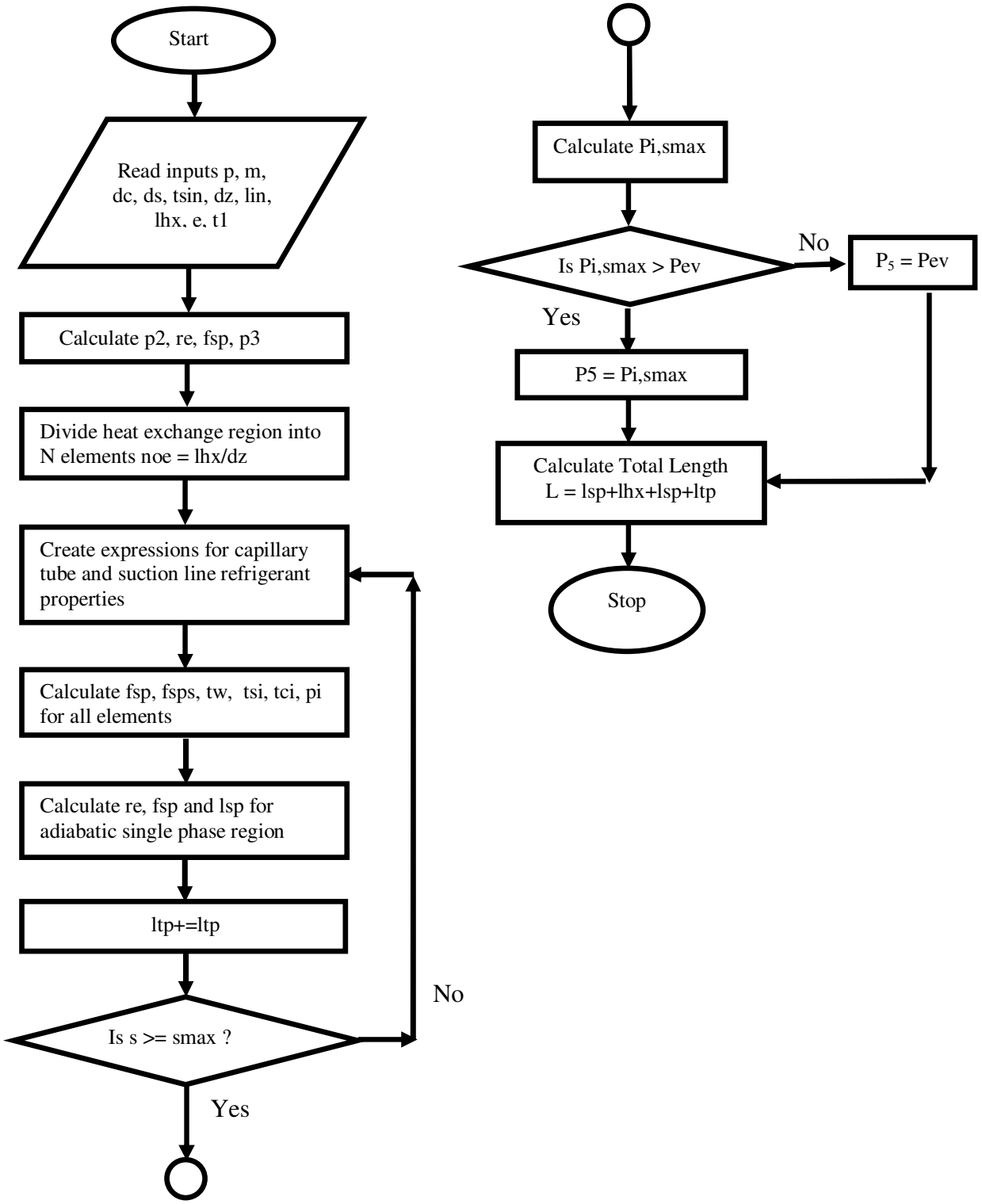

Fig. 3.4 Flow Chart for the computation of diabatic capillary length with Mathematical Model

3.3 ANSYS CFX Workflow

First we need to create the geometry of the model of capillary tube-suction tube heat exchanger. So, model it in the Pro Engineer. But for Ansys CFX we also need the fluid volume, therefore fill the hollow passages of capillary tube and suction tube with fluid volume and saved it in the iges format.

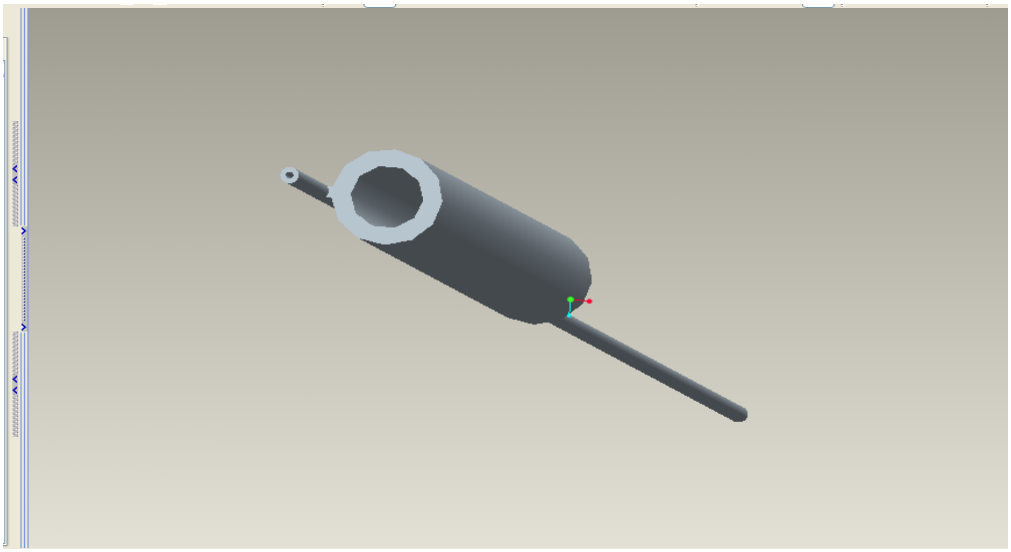

Fig.3.5 Physical model of capillary tube suction line heat exchanger

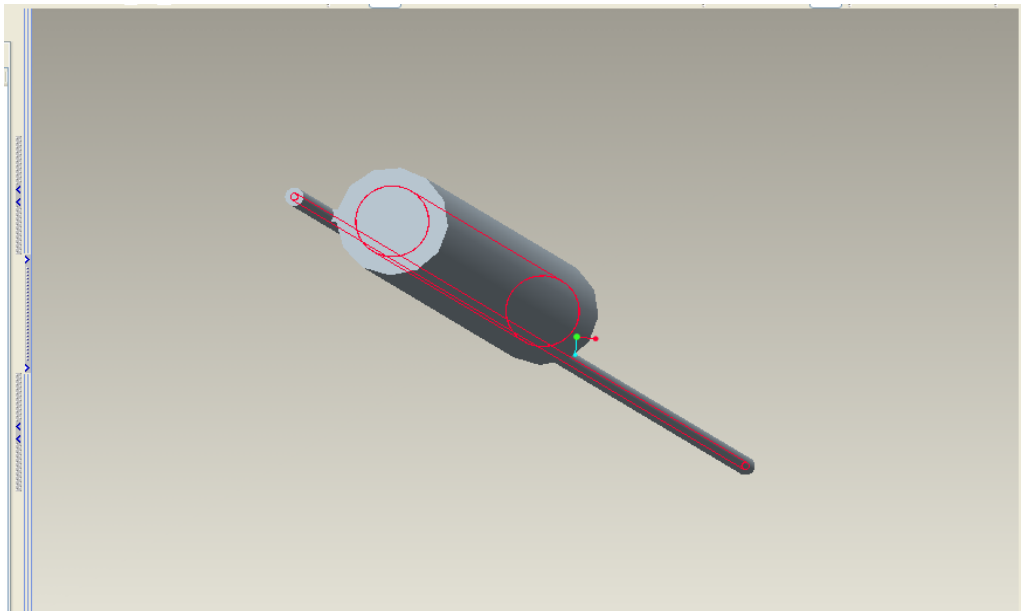

Fig.3.6 Physical model of capillary tube suction line heat exchanger filled with fluid volume

Now open the entire assembly in Ansys Workbench Meshing Module. Then opt for CFD in the preferences and CFX-Mesh option. In the CFX-Mesh module create the four regions namely, in1, in2, out1 and out2 for two inlets and two outlets in the counter flow direction.

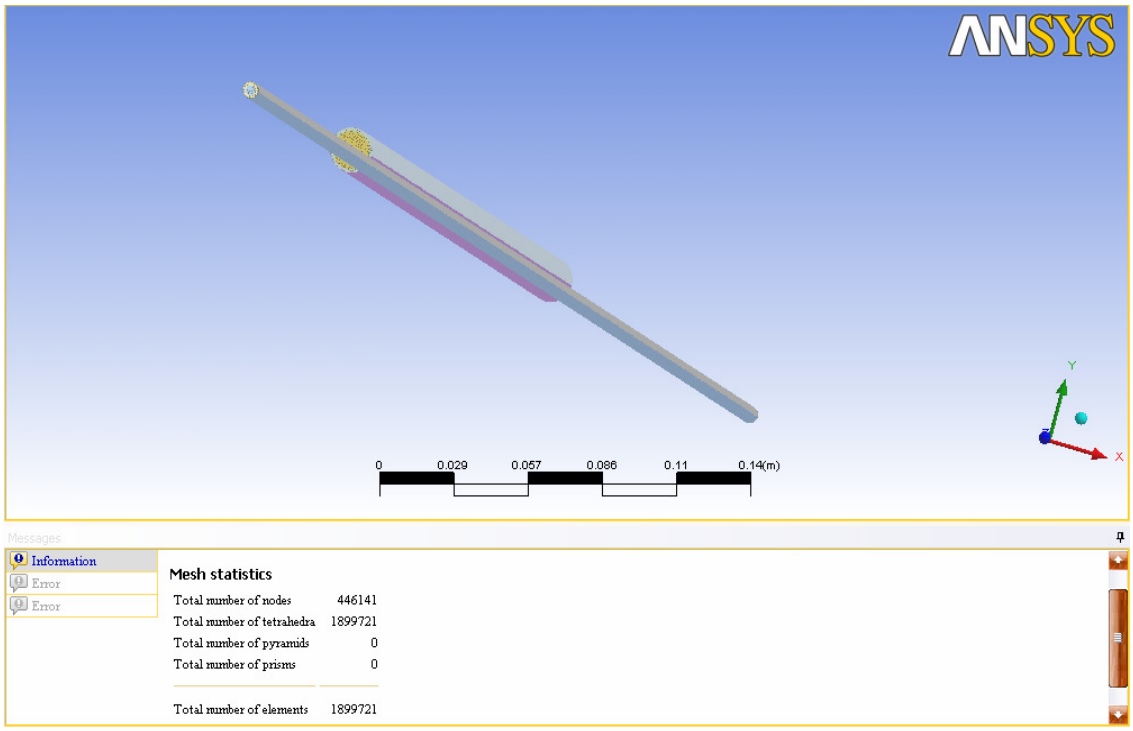

Fig.3.7 Mesh of capillary tube suction line heat exchanger model

Next create the inflated boundary (0.0001m), which is recommended for analyzing pressure drop in narrow hollow pipes. After that specify the Default Body Spacing and Default Face Spacing to 0.0003m and generated the volume mesh. Mesh is saved in .gtm format.

3.3.1 Ansys ICEM CFD

Alternatively, the mesh can be made in the Ansys ICEM CFD in the same way as in CFX-Mesh. This software has a great advantage over the CFX-Mesh, is that it can create unstructured mesh. This approach is very useful in our case i.e. meshing of capillary tube because the diameter of capillary tube is very small, which poses a great problem for CFX-Mesh as it can only decrease the size of the mesh element for adjusting to the small size of capillary tube. On the other hand Ansys ICEM CFD can not only decrease the size of mesh elements but also the increase the order of mesh elements as well as it can create the unstructured mesh. So for all these reasons Ansys ICEM CFD takes less time as compared to CFX-Mesh to create the same mesh and the number of elements require for meshing also reduces. Thus size of the mesh generated is less as compared to CFX-Mesh, this also helps in reducing the time for opening the file in Ansys CFX, for solving and for post processing also.

Meshing modules available in Ansys ICEM CFD

- Tetra
- Hexa
- Prism
- Hybrid meshes
- Shell meshing
- Shrinkwrap
- Patch independent shell meshing
- Patch based shell meshing

Tetra

Ansys ICEM CFD Tetra takes full advantage of object-oriented unstructured meshing technology. With no tedious up-front triangular surface meshing required providing well-balanced start meshes, ANSYS ICEM CFD Tetra works directly from the CAD surfaces and fills the volume with tetrahedral elements using the Octree approach. A powerful smoothing algorithm provides the element quality. Options are available to

automatically refine and coarsen the mesh both on geometry and within the volume. Tetra module has been used for mesh generation in this case.

Advantages of Tetra: -

Intelligent Geometry in ANSYS ICEM CFD Tetra

Using ANSYS ICEM CFD's Direct CAD Interfaces, which maintain the parametric description of the geometry throughout the CAD model and the grid generation process, unstructured grids can be directly remeshed on the modified geometry.The geometry is selected in the CAD system and tagged with information for grid generation such as boundary conditions and mesh element sizes. This intelligent geometry information is saved with the master geometry. Parametric changes in the geometry simply require the user to write the updated geometry file for grid generation. The user can then immediately re-calculate the unstructured tetrahedral grids.

The Octree Approach

- Tetra's mesh generation from surfaces is based on the following spatial subdivision algorithm: This algorithm ensures refinement of the mesh wherever necessary, but maintains larger elements wherever possible, allowing for faster computation.
- Once the "root" tetrahedron, which encloses the entire geometry, has been initialized, Tetra subdivides the root tetrahedron until all element size requirements are met.
- At this point, the Tetra mesher balances the mesh so that elements sharing an edge or face do not differ in size by more than a factor of 2.
- After this is done, Tetra makes the mesh conformal – i.e., it guarantees that each pair of adjacent elements will share an entire face.
- The mesh does not yet match the given geometry, so the mesher next rounds the nodes of the mesh to the geometry surfaces, curves, and prescribed points.
- The mesher then determines which portion of the mesh is enclosed by surfaces bounding a Body or Material Point (based on mesh connectivity). The remainder of the mesh is deleted.

- Finally, the mesh is smoothed by moving nodes (preserving geometry associations), merging nodes, swapping edges and in some cases, deleting bad elements.

Parts Creation, Material Points, and Prescribed Points

The grouping of the geometric entities into parts in the mesher interface allows the user to define different parameters on the individual parts. Aside from assigning unique boundary condition information to the various parts, the user can also define the parameters, which govern the element size for each part: maximum size, initial height and height ratio. Additionally, users can define element size on individual curves and surfaces. With the definition of prescribed points and curves in the mesher interface, the user can control the locations of tetrahedral nodes and edges in critical areas of the mesh. As described above in the mesh generation process (The Octree Approach) the mesher rounds the nodes of the mesh to match the given geometry, it first tries to project them onto the nearest prescribed points and curves. For the cutting step of the mesh generation, Tetra requires that a material point be defined for each distinct material that is needed for analysis. (The mesher can create these automatically if none are defined.) A material point might be used to define a fluid region for CFD analysis, a solid region for FEA analysis or both fluid and solid regions for conjugate heat transfer analysis.

Important Features in ANSYS ICEM CFD Tetra

Curvature /Proximity Based Refinement

If the maximum tetrahedral size defined on surface parts is larger than a geometric entity in the specified part, the user must employ the Curvature/Proximity Based Refinement limit. The user can specify a size that is proportional to the scale factor. It should be assigned a value that is slightly smaller than the smallest gap in the model, so that the mesher will further subdivide the tetrahedral to match this geometric feature. The Curvature/Proximity Based Refinement is the minimum size of any tetrahedral achieved via automatic subdivision for the entire model. If the user defines a smaller max element size on a geometry entity, Tetra does continue to subdivide until it meets the maximum size request. The effect of the Curvature/Proximity Based

Refinement is a geometry-based adaptation of the mesh based on feature curvature and proximity.

Tetrahedral Mesh Smoother

In smoothing the mesh, the tetrahedral smoother calculates individual element quality – based on the selected criterion. Referring then to the user specified element quality lower bound, the smoother modifies all elements below this quality criterion -- nodes are moved and merged, edges are swapped and in some cases, elements are deleted. This operation is then repeated on the improved grid, up to the specified number of iterations. To exclude particular parts from the smoothing, ICEM CFD offers the utility to smooth the mesh only on visible parts. Also, the user can smooth only specific element without affecting the others

Tetrahedral Mesh Coarsener

The mesh coarsener allows the element count to be decreased while still capturing the major features of the geometry. Users can choose to freeze surface elements during the coarsening process. If the mesh has multiple material domains and the user does not want to coarsen some of them, he/she can exclude individual material domains by specifying them in the frozen parts option. If the size checks option is used during coarsening, the resulting mesh does satisfy the selected mesh size criteria on all of the geometric entities. Furthermore, Tetra includes a complete set of projection and smoothing tools, as well as tools for element creation, deletion, and splitting, swapping and uniform enforcement of orientation.

Triangular Surface Mesh Smoother

The triangular surface mesh inherent in the Tetra mesh generation process can also be smoothed independently of the volume mesh. The triangular smoother marks all elements that are initially below the quality criterion and then runs the specified number of smoothing steps on the elements. Nodes are moved on the actual CAD surfaces to improve the aspect ratio of the elements.

Triangular Surface Mesh Coarsener

In the interest of minimizing grid points, the coarsener reduces the number of triangles in a mesh by merging triangles. This operation is based on the maximum

deviation of the resultant triangle center from the surface, the aspect ratio of the merged triangle and the maximum size of the merged triangle.

Triangular Surface Editing Tools

For the interactive editing of surface meshes, ANSYS ICEM CFD Tetra offers a mesh editor in which nodes can be moved on the underlying CAD surfaces, merged, or even deleted. Individual triangles of the mesh can be subdivided or added to different parts. The user can perform the quality checks, as well as local smoothing. Diagnostic tools for surface meshes allow the user to fill holes easily in the surface mesh. Also there are tools for the detection of overlapping triangles and non-manifold vertices, as well as detection of single/multiple edges and duplicate elements.

Mesh Periodicity

Periodicity definition for ANSYS ICEM CFD Tetra meshes is well suited for rotating turbomachinery flow solutions. Meshes for any rotational or translational cyclic geometry can be generated with ease.

Mesh Density Control

The mesh Density definition for ANSYS ICEM CFD Tetra allows users to control the tetra size locally where no geometry is present. Densities can be of different shapes: point, sphere, line, arbitrary volume.

Editing the Tetra Mesh

The two main criteria in validating a Tetra mesh are Check mesh and Smooth mesh globally, both of which are found under the Edit mesh menu.

Check Mesh

Go to **Edit mesh> Check mesh**, and press Apply**.**

The user can Check/fix each of the problems at this time, or can opt to create subsets for each of them so that they can be fixed later. Using subset manipulation and mesh editing techniques diagnose the problem and resolve it by merging nodes, splitting edges, swapping edges, delete/create elements, etc.

After eliminating errors/possible problems from a tetra grid, the user needs to smooth the grid to improve the quality. To do this, select **Edit mesh > Smooth mesh Globally Smoothing iterations:** This value is the number of times the smoothing process will be

performed. Displays with a more complicated geometry will require a greater number of iterations to obtain the desired quality, which is assigned in Up to quality.

Up to quality: As mentioned previously, the Min value represents the worst quality of elements, while the Max value represents the highest quality elements. Usually, the Min is set at 0.0 and the Max is set at 1.0. The Up to quality value gives the smoother a quality to aim for. Ideally, after smoothing, the quality of the elements should be higher than or equal to this value. If this does not happen, the user should find other methods of improving the quality, such as merging nodes and splitting edges. For most models, the elements should all have ratios of greater than 0.3, while a ratio of 0.15 for complicated models is usually sufficient.

Criterion: User can select any criterion to display from pull down menu.

Smooth: If the Smooth option is toggled on for a particular element type, then this element will be smoothed in order to produce a higher grid quality. Element types that have the Smooth option selected will have their qualities appear in the associated histogram.

Freeze: If the Freeze option is selected for an element type, the nodes of this element type will be fixed during the smoothing operation; thus, the element type will not be displayed in the histogram.

Float: If the Float option is selected for an element type, the nodes of the element type are capable of moving freely, allowing nodes that are common with another type of element to be smoothed. The nodes of this type of element, however, are not affected during the smoothing process and so the quality of these elements is not displayed in the histogram.

3.3.2 Ansys CFX

After creating the mesh, open CFX-Pre. Then insert the mesh created before (**File > Import Mesh**). Now we have to import the two materials namely, R-134al (liquid) and R-134av (vapour). (**Materials > Import Library Data > Browse > Materials-redkw.ccl**). A number of refrigerants are available in the library of Ansys CFX, even if the desired refrigerant is not available we can create it by giving the values of different variables or an expression for the variable properties (**Insert > Material**).

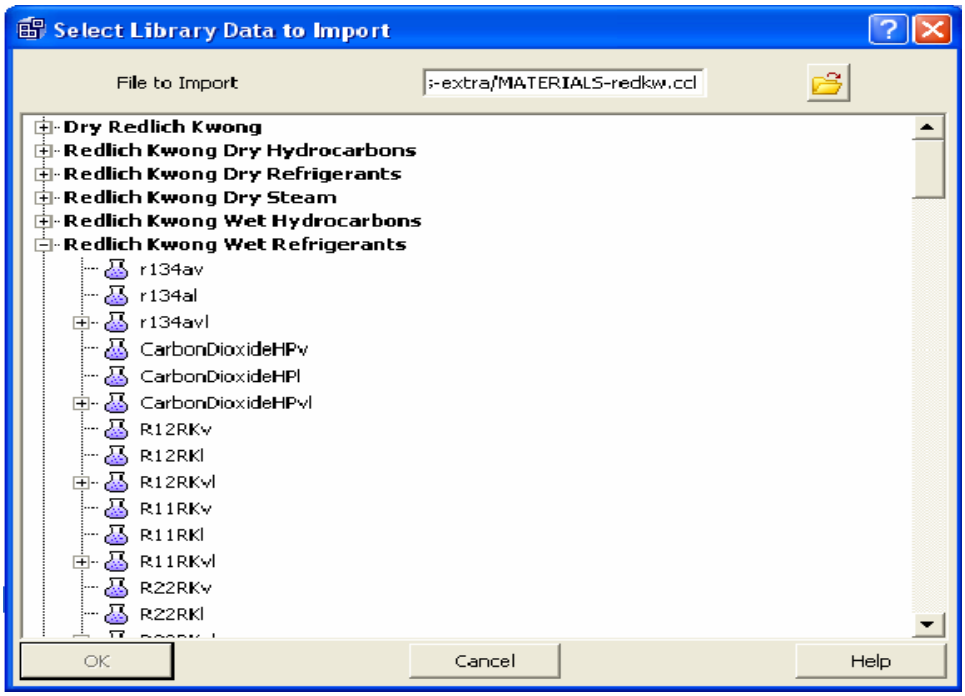

Fig. 3.8 CFX-Pre window showing different refrigerants available

The refrigerants which have been imported use Redlich-Kwong equation of state.

The Redlich-Kwong equation is considered by many to be the best of the two-constant equations of state. The Redlich-Kwong equations is somewhat more difficult to manipulate mathematically than the van der waals equation, it is more accurate, particularly at higher pressures. The two-constant Redlich-Kwong equation performs better than some equations of state having several adjustable constants, still, two-constant equations of state tend to be limited in accuracy as pressure (or density) increases.

After importing the material we need to create three domains one fluid domain for capillary volume, second fluid domain for suction volume and third solid domain for copper joint between them. And then we have to set up the physics for solving and post processing.

This is how the Ansys CFX-Pre workspace looks like **>**

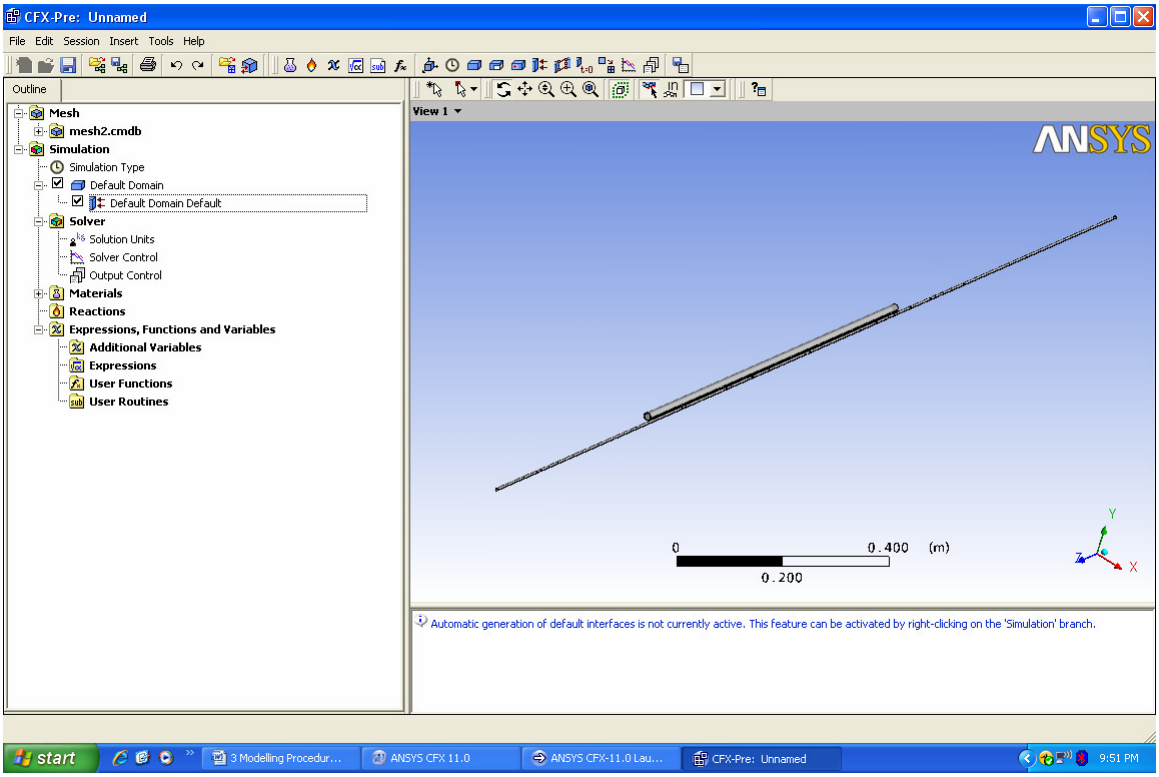

Fig.3.9 Mesh of capillary tube suction line heat exchanger in CFX-Pre

Capillary Domain:

For creating the domain, click **Insert > Domain**, give it a name, say capillary.

We need to fill information written below, some options are the default values and need not to change i.e. the only values which need to alter are written below.

General Options Tab:

Location > select Capillary

Domain Type > select Fluid Domain

Fluid List > select r134al, r134av

Fluid Model Tab:

Fluid Models > Multiphase Options > Homogenous Model

Heat Transfer > Option > Fluid Dependent

Turbulence Model > k-epsilon

Fluid Details Tab:

Fluid Details > r134al > Morphology > Continuous Fluid

Fluid Details > r134al > Heat Transfer > Total Energy

Fluid Details > r134av > Morphology > Dispersed Fluid

Fluid Details > r134av > Heat Transfer > Saturation Temperature

Fluid Pairs Tab:

Surface Tension Coefficient > 0.00792 N/m (approximate from Ashrae handbook)

Mass Transfer > Phase Change

Initialization Tab:

We need to give the initial guess values of following:

Initial Conditions > Velocity Type > Cartesian

Initial Conditions > Cartesian Velocity Components > Options > Automatic with Values

U > 0 m s^-1

V > 7 m s^-1

W > 0 m s^-1

Static Pressure > Option > Automatic with value

Static Pressure > Relative Pressure > 900 KPa

Turbulence Eddy Dissipation > Automatic

Fluid Specific Information > r134al > Initial conditions > Temperature > 30 c

Fluid Specific Information > r134al > Initial conditions > Volume Fraction > 1.00

Fluid Specific Information > r134av > Initial conditions > Temperature > 30 c

Fluid Specific Information > r134av > Initial conditions > Volume Fraction > 0.00

Solid Domain:

Fill the following information.

General Tab:

Basic Settings > Location > select the outer body of capillary and the joint between the capillary tube and suction line

Domain Type > Solid Domain

Solids List > Copper

Solids Models:

Heat Transfer > Option > Thermal Energy

Initialization Tab:

Initial Conditions > Temperature > 30 c (initial guess)

Suction Domain:

Fill the following information.

General Tab:

Basic Settings > Location > select the suction line

Domain Type > Fluid Domain

Fluids List > select r134al, r134av

Fluid Model Tab:

Fluid Models > Multiphase Options > Homogenous Model

Heat Transfer > Option > Fluid Dependent

Turbulence Model > k-epsilon

Fluid Details Tab:

Fluid Details > r134al > Morphology > Continuous Fluid

Fluid Details > r134al > Heat Transfer > Total Energy

Fluid Details > r134av > Morphology > Dispersed Fluid

Fluid Details > r134av > Heat Transfer > Saturation Temperature

Fluid Pairs Tab:

Surface Tension Coefficient > 0.00792 N/m (approximate from Ashrae handbook)

Mass Transfer > Phase Change

Initialization Tab:

We need to give the initial guess values of following:

Initial Conditions > Velocity Type > Cartesian

Initial Conditions > Cartesian Velocity Components > Options > Automatic with Values

U > 0 m s^-1

V > 1 m s^-1

W > 0 m s^-1

Static Pressure > Option > Automatic with value

Static Pressure > Relative Pressure > 200 KPa

Turbulence Eddy Dissipation > Automatic

Fluid Specific Information > r134al > Initial conditions > Temperature > 10 c

Fluid Specific Information > r134al > Initial conditions > Volume Fraction > 0.00

Fluid Specific Information > r134av > Initial conditions > Temperature > 10 c

Fluid Specific Information > r134av > Initial conditions > Volume Fraction > 1.00

Boundary Conditions:

Now we need to give boundary conditions for capillary tube and suction line.

1. **Capillary tube:**

There are two boundary conditions for capillary tube, one is inlet, second is outlet.

   A. **Inlet:**

      Insert > Boundary Condition > Name > in1

      Insert > Boundary Condition > Domain > select Capillary

      Basic Settings Tab:

      Boundary Type > Inlet

      Location > select that face of capillary tube which we want to make the inlet.

      Boundary Details:

      Flow Regime > Subsonic

      Mass and Momentum > Option > Static Pressure > 900 KPa

      Flow Direction > Zero Gradient

      Turbulence > Zero Gradient

      Heat Transfer > Static Temperature > 30 c

      Fluid Values:

      Boundary Conditions > r134al > Volume Fraction > 1.00

      Boundary Conditions > r134av > Volume Fraction > 0.00

   B. **Outlet:**

Insert > Boundary Condition > Name > out1

Insert > Boundary Condition > Domain > select Capillary

Basic Settings Tab:

Boundary Type > Outlet

Location > select that face of capillary tube which we want to make the outlet.

Boundary Details:

Flow Regime > Subsonic

Mass and Momentum > Option > Relative Pressure > 200 KPa (approximate)

2. **Suction Line:**

There are two boundary conditions for suction line, for inlet and outlet.

A. Inlet:

Insert > Boundary Condition > Name > in2

Insert > Boundary Condition > Domain > select Suction

Basic Settings Tab:

Boundary Type > Inlet

Location > select that face of suction line which we want to make the inlet.

Boundary Details:

Flow Regime > Subsonic

Mass and Momentum > Option > Static Pressure > 200 KPa

Flow Direction > Zero Gradient

Turbulence > Zero Gradient

Heat Transfer > Static Temperature > -10 c

Fluid Values:

Boundary Conditions > r134al > Volume Fraction > 0.00

Boundary Conditions > r134av > Volume Fraction > 1.00

B. Outlet:

Insert > Boundary Condition > Name > out2

Insert > Boundary Condition > Domain > select Suction

Basic Settings Tab:

Boundary Type > Outlet

Location > select that face of suction line which we want to make the outlet.

Boundary Details:

Flow Regime > Subsonic

Mass and Momentum > Option > Relative Pressure > 150 KPa (approximate)

Interface:

We need to create two interfaces also, one is between capillary tube and solid copper joint and other is between suction line and solid copper joint. To create a domain interface click **Insert > Domain Interface** and give it a name

1. Capillary Tube – Joint Interface:

Basic Settings Tab:

Interface Type > Fluid Solid

Interface Side 1 > Domain (filter) > select capillary

Interface Side 1 > Region List > select that face of capillary which is opposite to solid joint face i.e. which will be responsible for exchange of heat energy with solid joint.

Interface Side 2 > Domain (filter) > select the solid joint

Interface Side 2 > Region List > select that face of sold joint which is opposite to above selected face of capillary.

Interface Models > Option > General Connection

Mesh Connection Method > Automatic

Boundary Details:

Boundary Details > Wall Roughness > Rough Wall > 0.003 mm

Heat Transfer > Conservative Interface Flux

2. Suction Line – Joint Interface:

Basic Settings Tab:

Interface Type > Fluid Solid

Interface Side 1 > Domain (filter) > select suction

Interface Side 1 > Region List > select that face of suction line which is opposite to solid joint face i.e. which will be responsible for exchange of heat energy with solid joint.

Interface Side 2 > Domain (filter) > select the solid joint

Interface Side 2 > Region List > select that face of sold joint which is opposite to above selected face of suction.

Interface Models > Option > General Connection

Mesh Connection Method > Automatic

Boundary Details:

Boundary Details > Wall Roughness > Rough Wall > 0.0003 mm

Heat Transfer > Conservative Interface Flux

Automatic Wall Boundary Generation:

The faces which have not been given any boundary condition will be assigned wall boundary condition by default that means there is no flow of mass or heat energy.

Now all the physics has been setup, so we can save the CFX-Pre file. **File > Save Simulation As.** For starting the solver, click **File > Write Definition File** it will automatically start the solver. On the right hand side of workspace of Solver, iterations will be shown and on the left hand side convergence of different variables (mass, momentum, energy, volume fraction etc.) will be shown. When the desired convergence is reached, a pop-up menu will be displayed, asking for post-processing of the results, click YES to post-process the results. This will open the Post – Processor module of the Ansys CFX called CFX-Post. For the purpose of validating the results of our Visual C++ Program, we need to create the graphs of different properties like temperature versus length, pressure versus length and for that we need to create a Streamline passing through the center of the capillary from inlet to outlet.

Click**, Insert > Streamline**, give it a name.

Now click, **Domains > select capillary**

Start From > select inlet of capillary tube i.e. in1

# of Point > 1

We can select any property to be shown with the help of this streamline using different colors to represent the magnitude of that property. To do this,

Variable > select the desired property

Now we need to create the graphs, for that click **Insert > Chart**, give it a name. On the tab of Chart Line, select the following

Location > Streamline

X Axis > Select the desired property

Y Axis > Select the desired property

Click **Apply**, and the graph will be shown.

Following flow chart depicts the step by step procedure followed to obtain results with Ansys CFX.

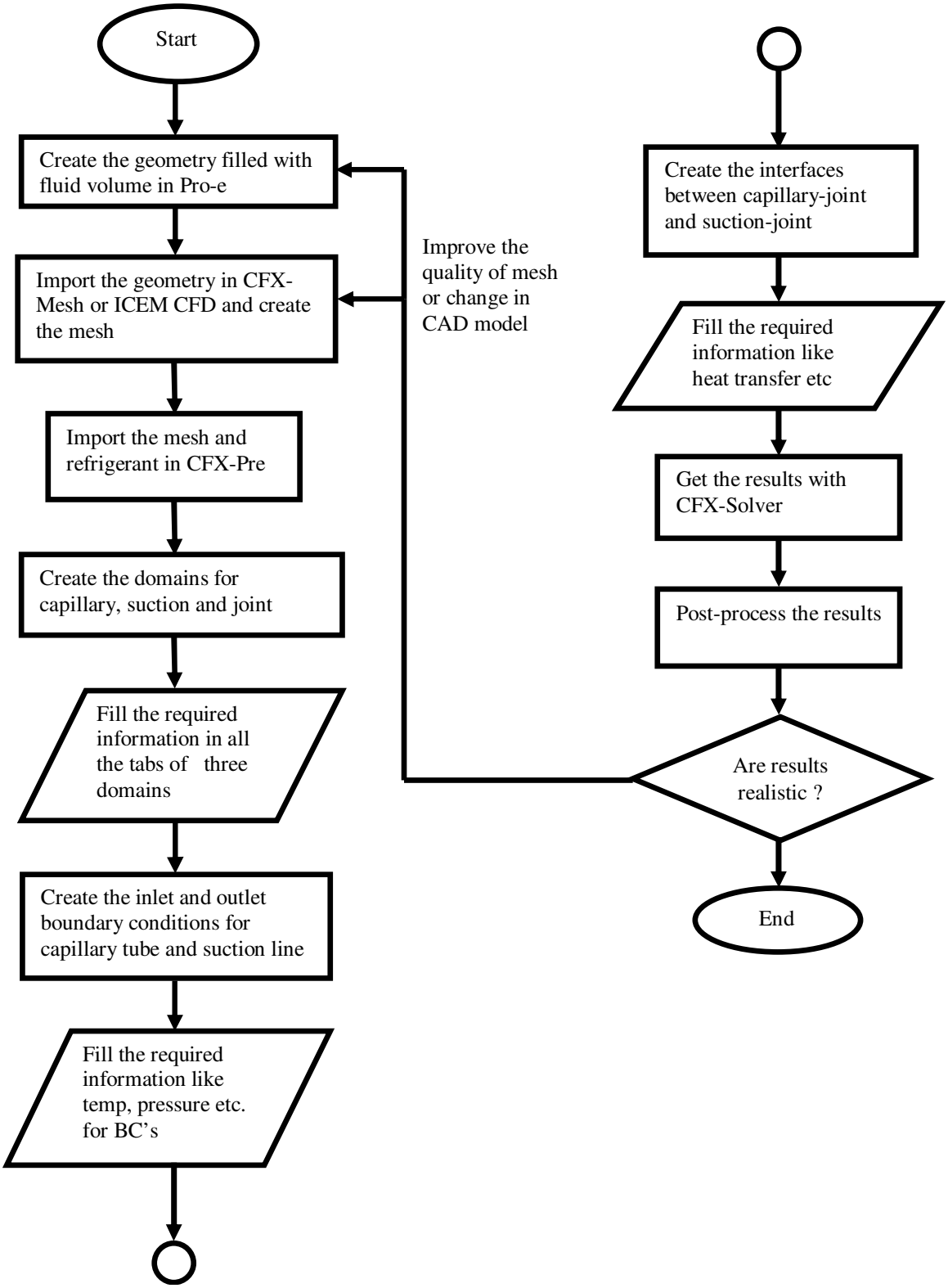

Fig. 3.10 Flow Chart representing linkages between geometry modeler, mesher, CFX-Pre, Solver and CFX-Post.

Chapter 4

Results and Discussion

4.1 Model Validation

The results obtained from numerical model, developed for straight capillary tube has been validated with the results of Ansys CFX by taking the data of Mendoca et al [14]. And the results are in fair agreement with the results of Ansys CFX, which is widely used by the industry for CFD analysis. Data input of two cases of Mendoca et al.[14] was used as input.

Case 1:

Refrigerant Used: R-134a

Mass flow rate: 5.44 kg/hr

Diameter of Capillary Tube: 0.83 mm

Diameter of Suction Line: 7.86 mm

Roughness Ratio: 1.50 µm

Inlet Suction Line Temperature: 268.15 K

Adiabatic Capillary Tube Inlet Length: 1.07 m

Heat Exchanger Length: 1.60 m

Capillary Tube Inlet Pressure: 0.9 MPa

Capillary Tube Inlet Temperature: 298 K

Case 2:

Refrigerant Used: R-134a

Mass flow rate: 5.37 kg/hr

Diameter of Capillary Tube: 0.83 mm

Diameter of Suction Line: 4.8 mm

Roughness Ratio: 1.50 µm

Inlet Suction Line Temperature: 262.05 K

Adiabatic Capillary Tube Inlet Length: 0.53 m

Heat Exchanger Length: 1.60 m

Capillary Tube Inlet Pressure: 0.9 MPa

Capillary Tube Inlet Temperature: 298 K

Following observations can be made from the results of these two cases:

In the first case adiabatic capillary tube length is 1.07 m but in the second case it is only 0.53 m, which is almost half of the first. In the capillary tube, adiabatic length at inlet, refrigerant temperature remains constant because there is no heat exchange with surrounding or suction line, and the refrigerant has entered as single phase, and it continues to be in single phase throughout the initial adiabatic capillary tube length, so that means there is no decrease in temperature of refrigerant. In the heat exchange region there is drop in the temperature of refrigerant flowing inside the capillary tube , but the temperature of refrigerant, flowing inside the suction line in vapour form, increases because of heat exchange with capillary tube. In the last adiabatic region of the capillary tube, temperature again becomes constant until the start of two phase or we can say the, onset of vaporization. Once the vaporization has started, temperature falls sharply till the end of capillary tube length.

Second difference in these two cases was of suction line inlet temperature, in the first case it is more than in the second case i.e. 268.15 K and 262.05 K respectively. Therefore, the rate of heat transfer between capillary tube and suction line will be more in second case, which is evident from the results.

4.2 Graphs

Following graphs are made from the output of Visual C++ program and graphs generated from Ansys CFX and superimposing both in SigmaPlot software.

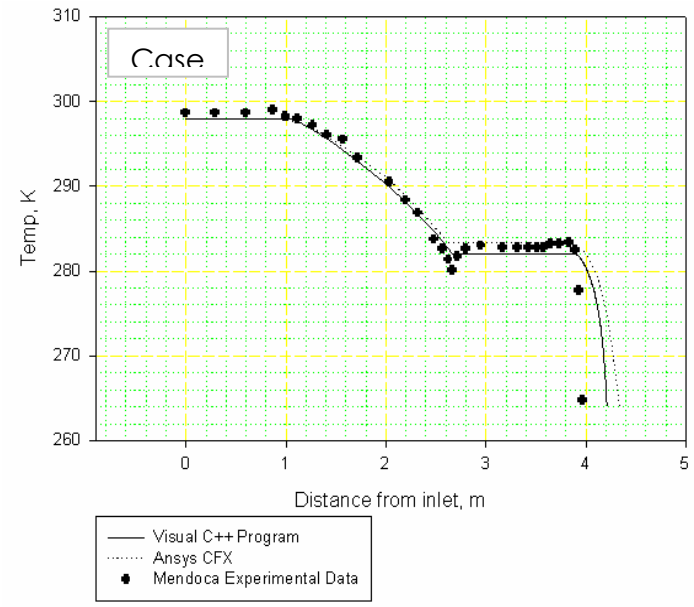

Fig. 4.1 (a)

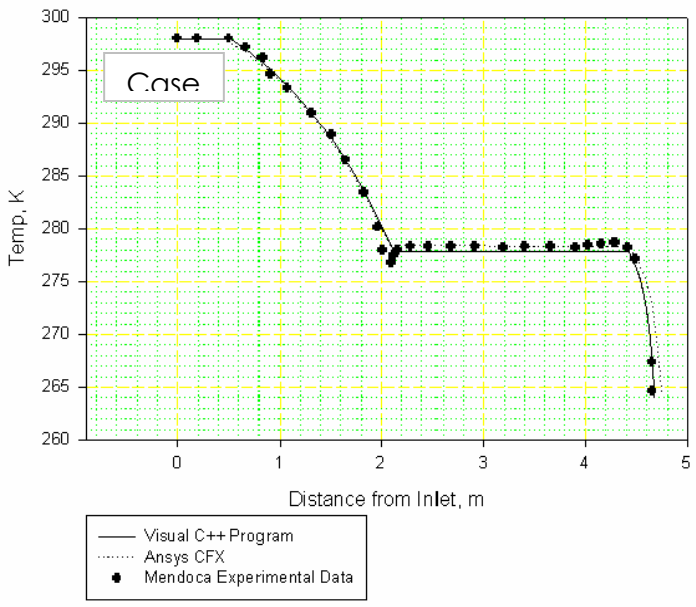

Fig. 4.1 (b)

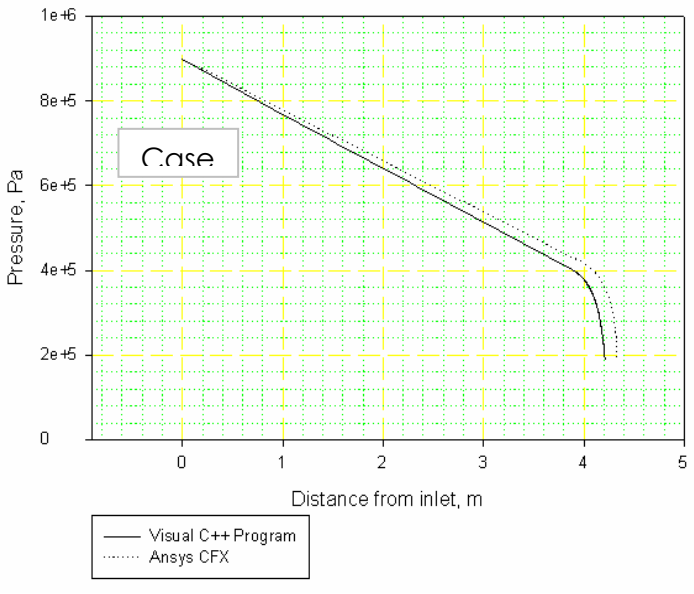

Fig. 4.2 (a)

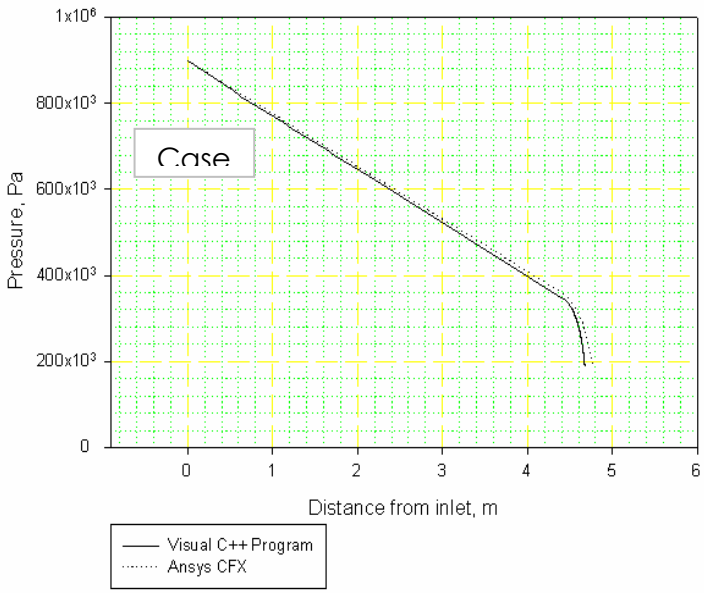

Fig. 4.2 (a)

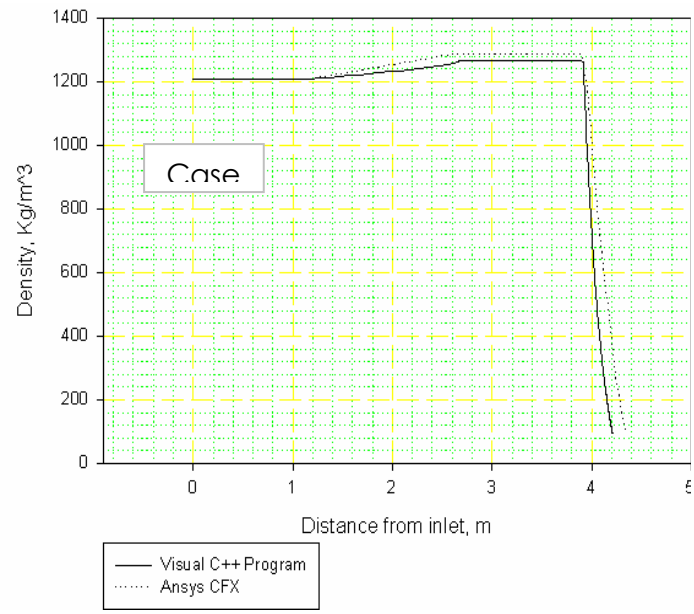

Fig. 4.3 (a)

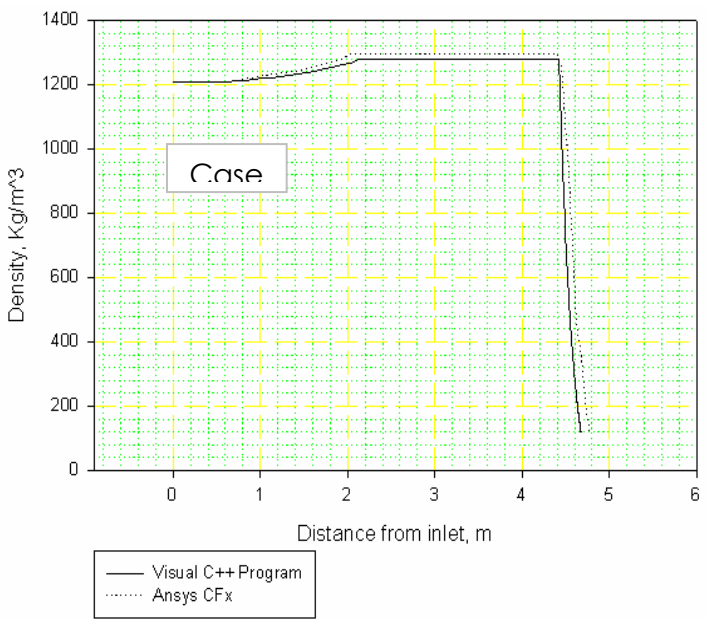

Fig. 4.3 (b)

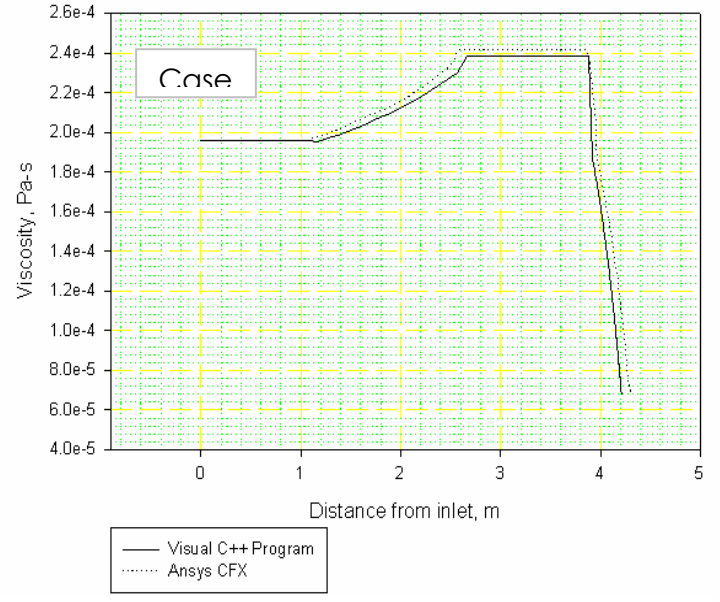

Fig. 4.4 (a)

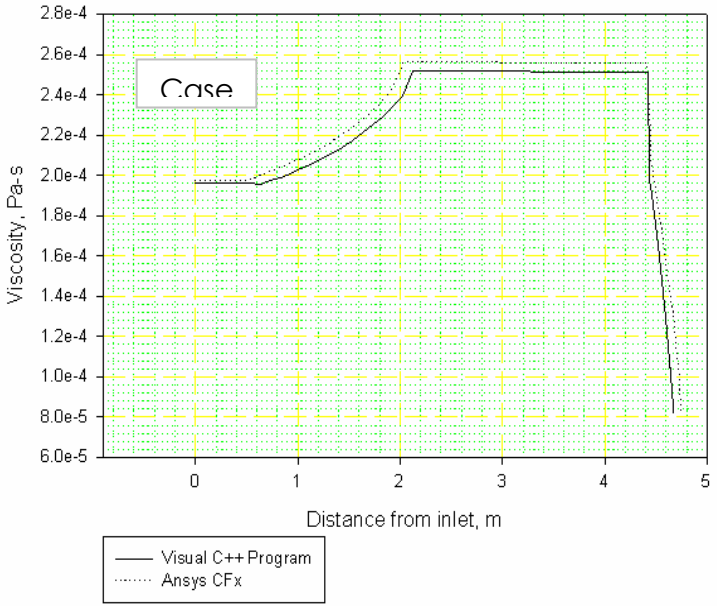

Fig. 4.4 (b)

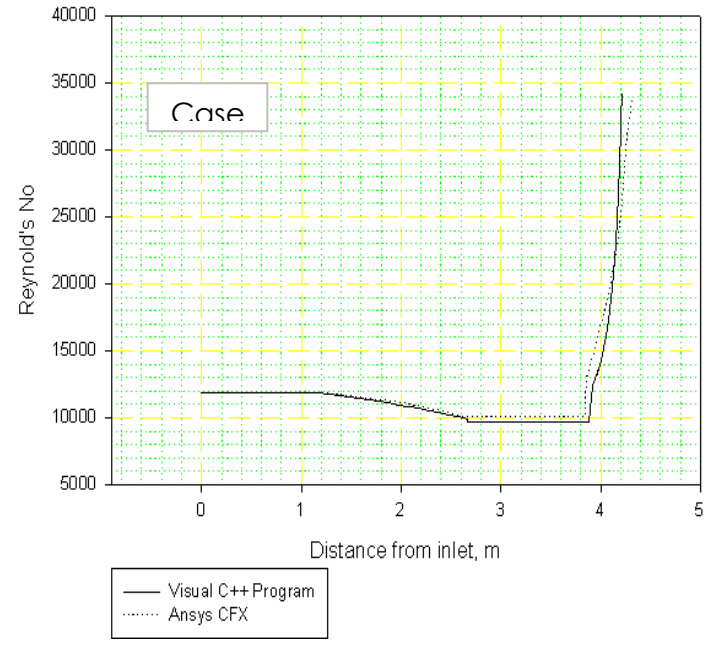

Fig. 4.5 (a)

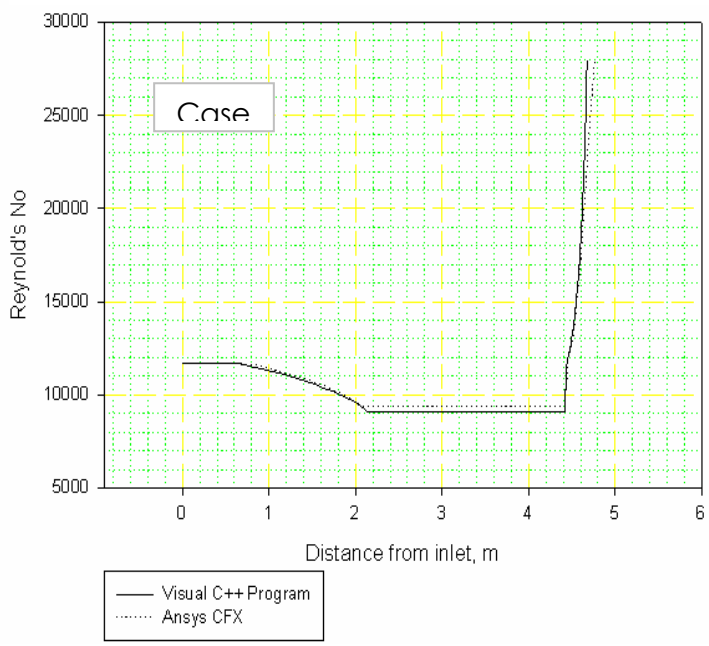

Fig. 4.5 (b)

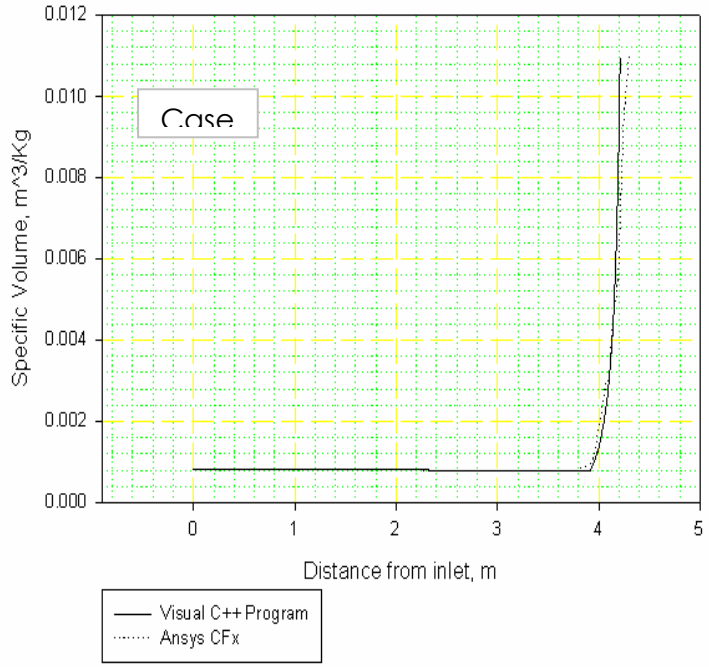

Fig. 4.6 (a)

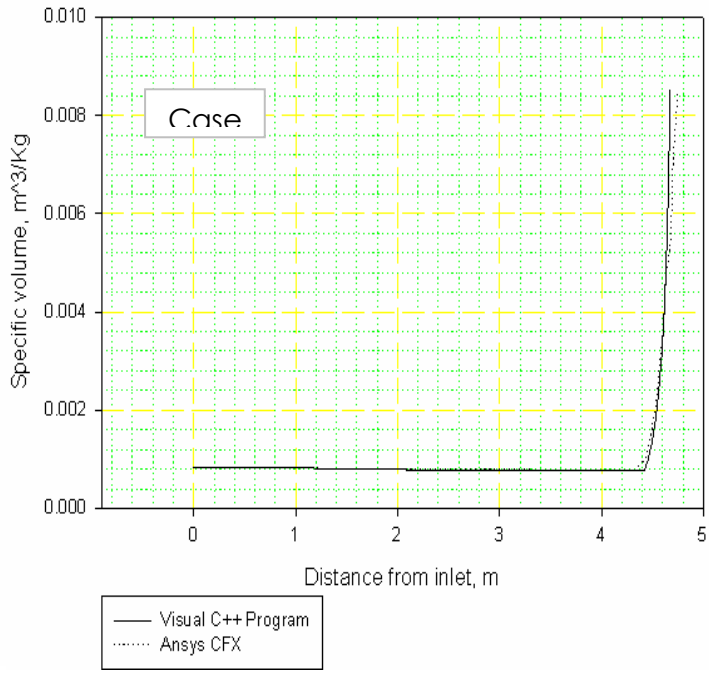

Fig. 4.6 (b)

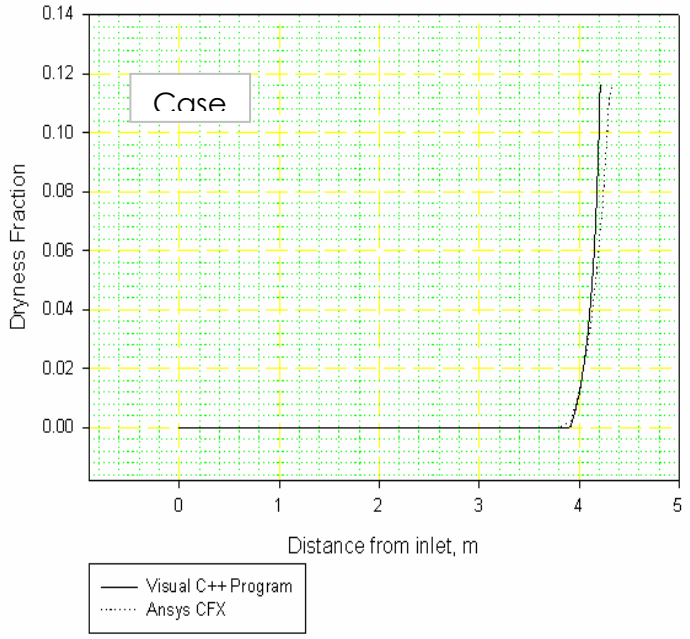

Fig. 4.7 (a)

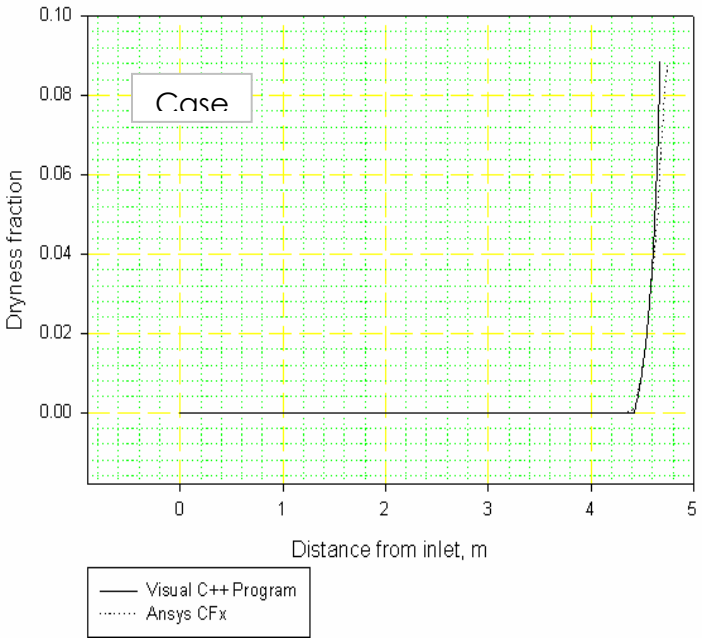

Fig. 4.7 (b)

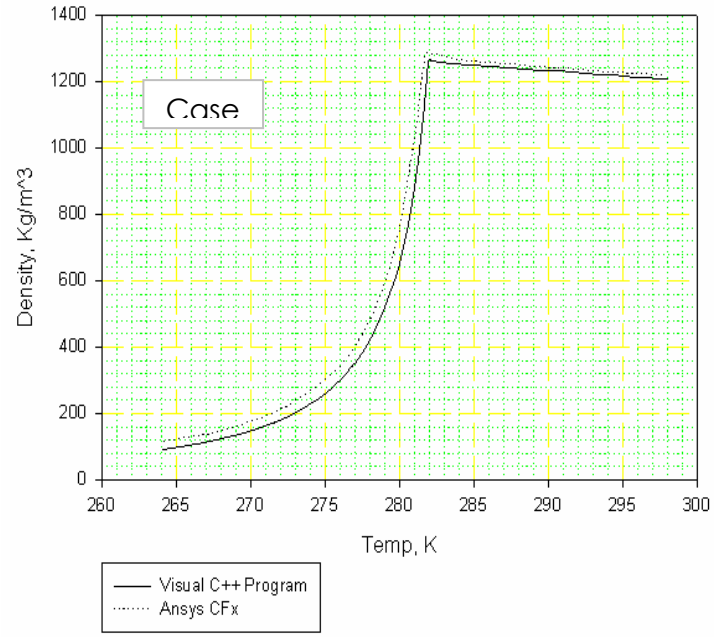

Fig. 4.8 (a)

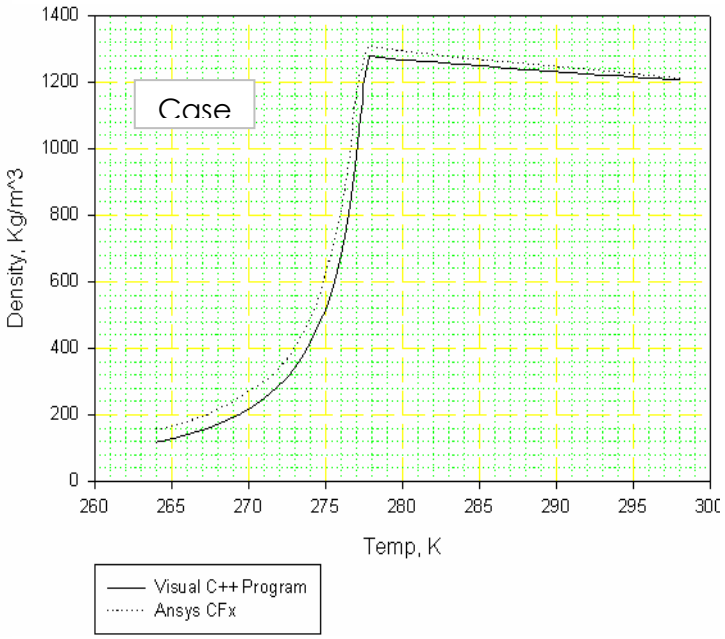

Fig. 4.8 (b)

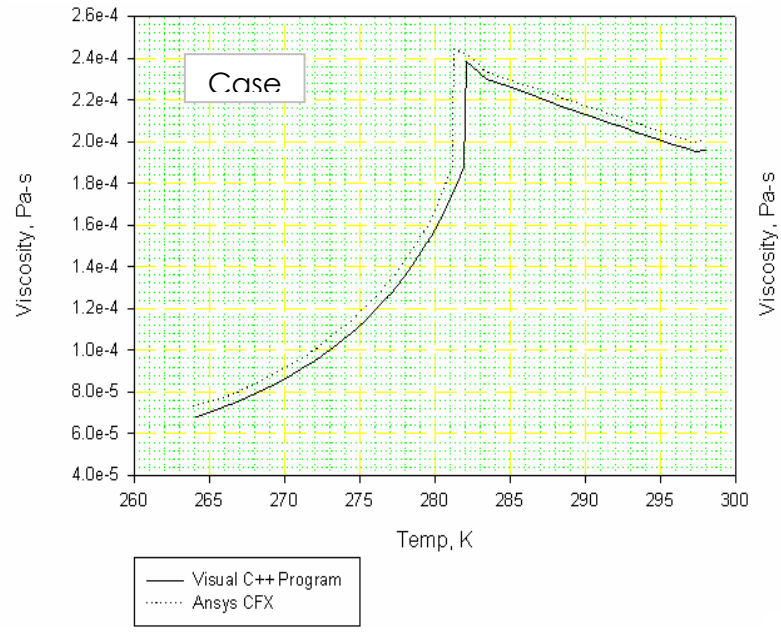

Fig. 4.9 (a)

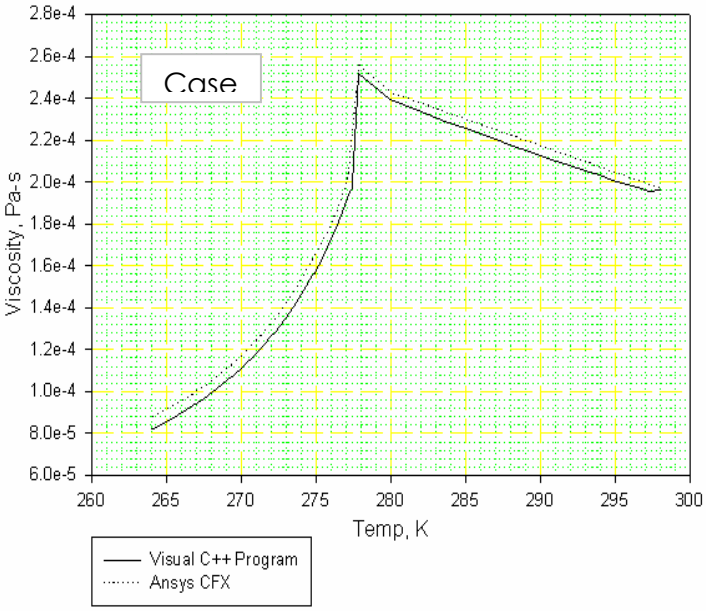

Fig. 4.9 (b)

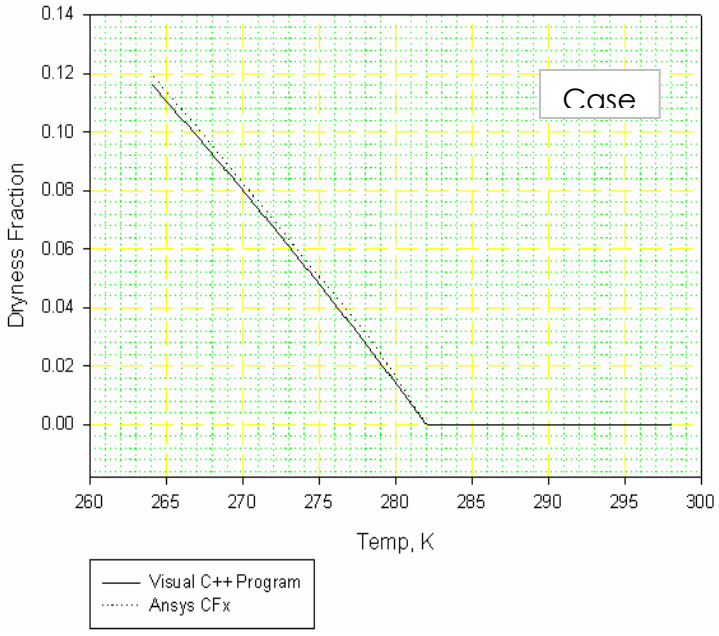

Fig. 4.10 (a)

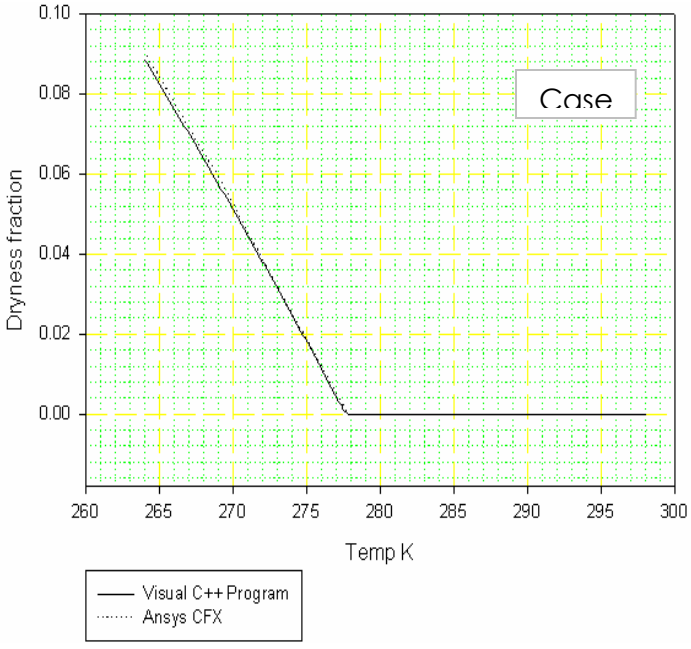

Fig. 4.10 (b)

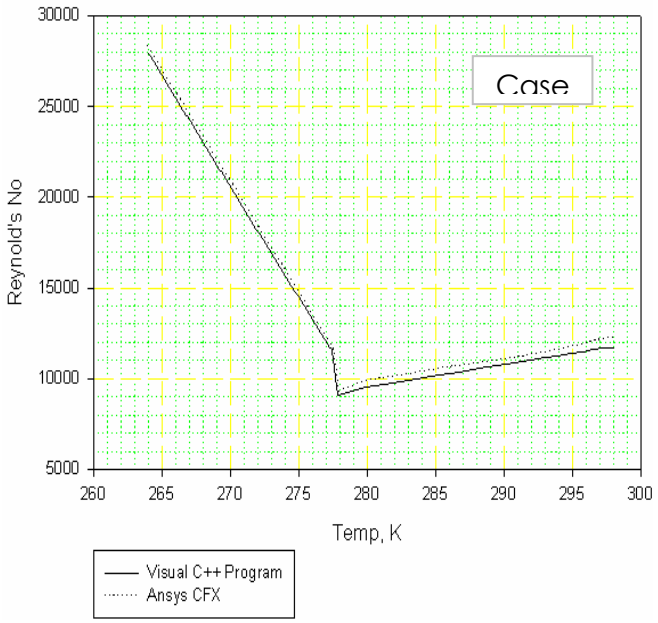

Fig. 4.11 (a)

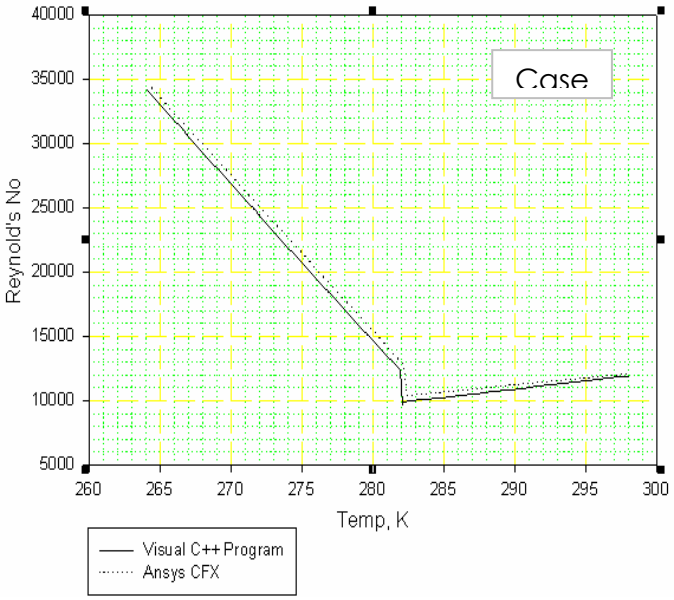

Fig. 4.11 (b)

4.3 Difference between Ansys CFX and Mathematical Model

- Ansys CFX uses Redlich Kwong equation of state for determining the properties of refrigerants whereas proposed mathematical model uses the properties from Ashrae Handbook[1], and then creating the expressions for them depending upon temperature or pressure and temperature.
- Ansys CFX is a general software available for CFD analysis whereas our mathematical model is written specifically for Diabatic Capillary Tube.
- Ansys CFX uses turbulence Model (k-ε) but our mathematical model does not, on the other hand our mathematical model uses friction factor and viscosity model but Ansys CFX does not.
- Ansys CFX uses FVM (Finite Volume Method) technique but our mathematical model uses FDM (Finite Difference Method) technique.
- Ansys CFX uses the physical (geometric model) model, created in Pro Engineer, filled with fluid volume, but our mathematical does not. Result of Ansys CFX depends upon the quality of the mesh generated. There may be possible loss of geometric information while moving from Pro Engineer to Ansys ICEM CFD and from Ansys ICEM CFD to Ansys CFX. There might be some loss of information within the three modules of Ansys CFX viz. Pre, Solver and Post Processing.

4.4 Limitations: -

- Creating the mesh for the size of a capillary tube is very difficult task because of the very small diameter and long length. It requires large processing power and lot of time. It becomes a iterative process i.e. we have to do a number of meshing operations to get a good quality mesh.
- Solver takes a lot of time and large amount of space is required because for each module a different file is made. On an average half GB space is required for one solution (one file for Pro-Engineer, one file for Ansys ICEM CFD, one each for

Pre, Solver and Post Processor) and one should remember that it is a iterative process.

– There is always a possibility of recondensation of regrigerant inside capillary tube if the suction line temperature is sufficiently low. Our model (both) does not consider this phenomenon.

4.5 Difference between Adiabatic and Diabatic Capillary Tube

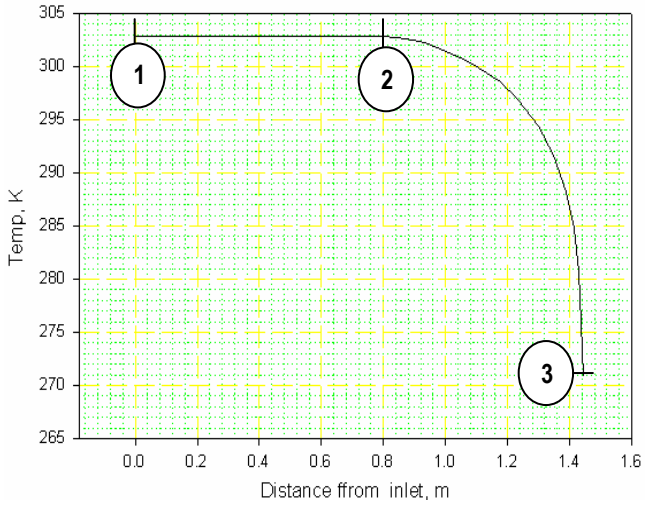

Fig. 4.12 (a)

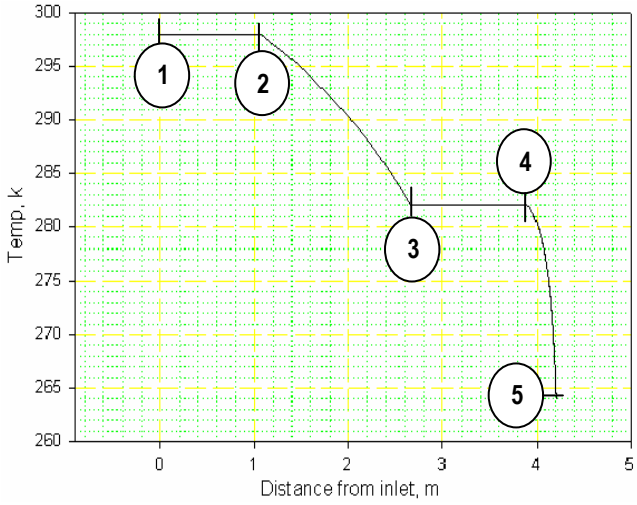

Fig. 4.12 (b)

Above figure shows typical temperature profile for adiabatic and diabatic capillary tube. Following observations can be made:

– The temperature profile for adiabatic capillary tube is divided into two regions, namely adiabatic single phase region and adiabatic two phase region, shown with the help of balloon markings 1, 2 and 3. Refrigerant is in single phase state when is between 1 and 2 and is in two phase when is between 2 and 3. Temperature remains constant when refrigerant is in single phase as there is no heat exchange with surroundings while it decreases sharply when refrigerant starts vaporizing.

- The temperature profile for diabatic capillary tube is divided into three regions, namely initial adiabatic single phase region, heat exchange region, adiabatic single phase region and adiabatic two phase region, shown with the help of balloon markings 1, 2, 3, 4 and 5. Refrigerant is in single phase state when is between 1 and 4, and is in two phase when is in between 4 and 5. Temperature remains constant in initial adiabatic single phase region i.e. between 1 and 2, and in adiabatic single phase region i.e. between 3 and 4. Between 2 and 3 is heat exchange with suction line which is cold, thus refrigerant losses heat to cold suction line and thereby decreasing its temperature. Temperature of suction line refrigerant increases. Nearing the end of capillary tube refrigerant starts vaporizing, hence the temperature decreases sharply between 4 and 5.
- In case of diabatic capillary tube, because of heat transfer between capillary tube and suction line, refrigerant in capillary tube losses heat to suction line and thus the refrigerant coming out of capillary tube will be able extract more heat from the evaporator. On the other hand, suction line gains heat from capillary tube and thus making the vapour superheated, which is favorable condition at the inlet of compressor because it increases the life by eliminating the probability of moisture entering the compressor.

4.6 Concluding Remarks

For Ansys CFX, first a physical (geometric) model is made in the Pro-Engineer, filled with fluid volume, then a mesh is generated in the Ansys ICEM CFD, and then this mesh is imported in Ansys CFX Pre. Then refrigerant R-134a is imported from its library and three domains are made for capillary tube, suction line and for joint between them. All the boundary and initial conditions are given, two interface were made between capillary tube and joint, and suction tube joint. After that solver starts and the solution is post processed.

In case of mathematical model of diabatic capillary tube, laws of conservation of mass, momentum and energy are used and lateral arrangement for capillary tube – suction

line counter flow heat exchange region is used. The differential equations are converted into difference equations using forward difference formulation of Finite Difference Approximations. The solution is obtained by solving these difference equations simultaneously. The numerical data has been validated with the results from Ansys CFX.

4.7 Future Scope

- The phenomenon for recondensation and metastability should be incorporated for future research work on the development of mathematical model for diabatic capillary tubes.
- Commercial software packages like Ansys ICEM CFD, Ansys CFX-Mesh should have separate algorithm for meshing of capillary sized small cylindrical pipes, which at present is very difficult work.
- Friction factor and viscosity model should be incorporated into commercial softwares for solution of capillary tube.

Appendix

A.1 Visual C++ Codes

Case 1:

```
// Diabatic.cpp : Defines the entry point for the console application.

#include "stdafx.h"
ofstream fout("output.txt");
ofstream gout("output2.txt");
void main()
{
        cout<<"\nProgram for Diabatic Capillary Tube"<<endl;
        double p1=900000,p2,p3,t1=25+273,t3,kloss=1.5,lin=1.07,lhx=1.60,
        lf=1.33,tsub=10,tci1,tci2,pi1,pi2,dc=0.83/1000,ds=7.86/1000,
        mfc=5.44/3600,vol=0.00082772,gc,gs,ac,as,res,fsps,vol2,ktc,ktcs,t4,p4,
        t4s,p4s, fsp,dz=0.1,rough=0.001807,re,rho=1208.1,vel,vis=0.00019575,
        noe,vels,rhos=26.934,pr,nu,hc,hs,nus,prs,enc=241720,visc=0.00018349,
        cpc=1445.1,cps=994.76,viss=0.000011448,tsi1=273+19.1,tsi2,tw,dx=0.0;

//-------------------------------------------
//Single-Phase Adiabatic Region
//-------------------------------------------

fout<<setprecision(8)<<setiosflags(ios::showpoint)<<"\n0.00"<<"\t\t"<<p1<<"\t"
      <<t1;
ac=3.14*dc*dc/4;
as=3.14*ds*ds/4;
gc=mfc/ac;
vel=gc/rho;                    fout<<"\t"<<vel;
gs=mfc/as;
vels=gs/rhos;
```

```
p2=p1-kloss*gc*gc*vol/2;
re=rho*vel*dc/vis;                fout<<"\t"<<re;
fsp=1.325/pow(log((rough/3.7)+(5.74/pow(re,0.9))),2);      fout<<"\t"<<fsp;
fout<<"\t"<<rho<<"\t"<<vol<<"\t"<<vis<<"\t"<<enc;
p3=p2-fsp*vol*gc*gc*lin/(2*dc);
fout<<"\n"<<lin<<"\t"<<p3;
t3=t1;                            fout<<"\t"<<t3<<endl;

//-------------------------------------------
//Single-Phase Heat-Exchange (Diabatic) Region
//-------------------------------------------

pi1=p3;          tci1=t3;          noe=lhx/dz;

for(int j=1;j<=noe;j++)
{
rho=exp(11.9599)*pow(tci1,-0.8592)*pow(pi1,0.0024);
visc=exp(12.2525)*pow(tci1,-3.6728)*pow(pi1,0.0097);
vol2=1/rho;
if(j==1) { vol=vol2; }
cpc=exp(2.9543)*pow(tci1,0.7642)*pow(pi1,-0.0036);
ktc=exp(6.0522)*pow(tci1,-1.5147)*pow(pi1,0.0050);
pr=cpc*visc/ktc;
enc=exp(2.0523)*pow(tci1,1.8094)*pow(pi1,0.0004);
vel=gc/rho;
re=gc*dc/visc;
fsp=1.325/pow(log((rough/3.7)+(5.74/pow(re,0.9))),2);
nu=(fsp/8)*(re-1000)*pr/(1+12.7*sqrt(fsp/8)*(pow(pr,2/3)-1));
hc=nu*ktc/dc;
rhos=-0.4836*tsi1+0.0020*tsi1*tsi1;
cps=1.6849*tsi1+0.0059*tsi1*tsi1;
viss=4.0863E-008*tsi1-5.7686E-012*tsi1*tsi1;
ktcs=-3.0583E-006*tsi1+1.6569E-007*tsi1*tsi1;
prs=cps*viss/ktcs;
```

```
vels=gs/rhos;
res=gs*ds/viss;
fsps=1.325/pow(log((rough/3.7)+(5.74/pow(res,0.9))),2);
nus=(fsps/8)*(res-1000)*prs/(1+12.7*sqrt(fsps/8)*(pow(prs,2/3)-1));
hs=nus*ktcs/ds;
tw=(hc*dc*tci1+hs*ds*tsi1)/(hc*dc+hs*ds);
tsi2=tsi1-(hs*3.141*ds*(tw-tsi1)*dz/(mfc*cps));
tci2=tci1-(hc*3.14*dc*(tci1-tw)*dz)/(mfc*cpc)-gc*gc*(vol2*vol2-vol*vol)/(2);
pi2=pi1-(fsp*gc*gc*vol*dz)/(2*dc)-(gc*gc*(vol2-vol));
tsi1=tsi2;        tci1=tci2;
pi1=pi2;          vol=vol2;                dx+=dz;
fout<<"\n"<<lin+dx<<"\t"<<pi2<<"\t"<<tci2<<"\t"<<vel<<"\t"<<re<<"\t"<<fsp;
fout<<"\t"<<rho<<"\t"<<vol2<<"\t"<<visc<<"\t"<<enc;
}

//-------------------------------
//Adiabatic Single-Phase Region
//-------------------------------

t4=tci2;          p4=pi2;
t4s=t4;           p4s=400940;
double rho4=1265,lsp;
vis=0.00023839;
vel=gc/rho4;
re=rho4*vel*dc/vis;
fsp=1.325/pow(log((rough/3.7)+(5.74/pow(re,0.9))),2);
lsp=2*dc*rho4*(p4-p4s)/(fsp*gc*gc);
fout<<"\n\n"<<lin+dx<<"\t"<<p4<<"\t"<<t4<<"\t"<<vel<<"\t"<<re<<"\t"<<fsp
    <<"\t"<<rho4;
fout<<"\n"<<lin+dx+lsp<<"\t"<<p4s<<"\t"<<t4s<<"\t"<<vel<<"\t"<<re<<"\t"
    <<fsp<<"\t"<<rho4<<endl;

//-----------------------------------
//Adiabatic Two-Phase Region
```

```
//-------------------------------------

double dp=1000,p,rhof,rhog,rhofg,hf,hg,hfg,sf,sg,sfg,muf,mug,mutp,
        vf,vg,vfg,s=0,smax=0,oldrho,h4s=212210,t,x=0,v,velocity,
        reytp,ftp,dl,ltp=0,y,h;

rho=rho4;
int i=1;
do
{
        p=p4s-dp;
        s=smax;         oldrho=rho;
        t=247.8017+8.6019E-005*p;
        vf=0.0007+1.7510E-010*p;            rhof=1/vf;
        vg=0.1230-1.8317E-007*p;            vfg=vg-vf;              rhog=1/vg;
        rhofg=rhog-rhof;
        hf=165913.8436+0.1164*p;
        hg=384092.9375+0.0495*p;            hfg=hg-hf;
        sf=877.5165+0.0004*p;
        sg=1740.1162-4.4446E-005*p;                 sfg=sg-sf;
        muf=0.0003-2.7942E-010*p;
        mug=9.7920E-006+3.1888E-012*p;
        y=pow(((gc*gc*vf*vfg)+hfg),2)-2*gc*gc*vfg*vfg*((-h4s+hf)
           +((gc*gc*vf*vf)/2)-((vel*vel)/2));
        x=(-hfg-gc*gc*vf*vfg+sqrt(y))/(gc*gc*vfg*vfg);
        mutp=mug*muf/(x*muf+(1-x)*mug);
        v=vf+x*vfg;
        rho=1/v;
        if(i==1)
        {
                oldrho=rho;
        }       i++;
        velocity=mfc/(ac*rho);
        smax=sf+x*sfg;
```

```
        h=hf+x*hfg;
        reytp=velocity*dc/(mutp*v);
        ftp=1.325/pow(log(rough/3.7+5.74/pow(reytp,0.9)),2);
        dl=fabs((2*dc/ftp)*(((-rho*dp)/(gc*gc))+((oldrho-rho)/(rho))));
        p4s=p;

        ltp+=dl;
        fout<<"\n"<<lin+dx+lsp+ltp<<"\t"<<p<<"\t"<<t<<"\t"<<velocity
            <<"\t"<<reytp<<"\t"<<ftp<<"\t"<<rho<<"\t"<<v<<"\t"
            <<mutp<<"\t"<<h<<"\t"<<x<<"\t"<<smax;
}while(s<smax && t>264);
getch();
}
```

Case 2:

```
// Diabatic.cpp : Defines the entry point for the console application.

        #include "stdafx.h"
        ofstream fout("output.txt");
        ofstream gout("output2.txt");

        void main()
        {
                cout<<"\nProgram for Diabatic Capillary Tube"<<endl;

                double p1=900000,p2,p3,t1=25+273,t3,kloss=1.5,lin=0.53,lhx=1.60,
                        tsub=10.5,tci1,tci2,pi1,pi2,dc=0.83/1000,ds=4.8/1000,
                        mfc=5.37/3600,vol=0.00082733,gc,gs,ac,as,res,fsps,vol2,
                        ktc,ktcs,t4,p4,t4s,p4s,fsp,dz=0.1,rough=0.001807,re,
                        rho=1208.7,vel,vis=0.00019612,noe,vels,rhos=27.652,pr,
                        nu,hc,hs,nus,prs,enc=234340,visc=0.00019586,cpc=1422.0,
                        cps=999.77,viss=0.000011482,tsi1=273+21,tsi2,tw,dx=0.00;

        //-------------------------------------------
        //Single-Phase Adiabatic Region
        //-------------------------------------------
        fout<<setprecision(8)<<setiosflags(ios::showpoint)<<"\n0.00"<<"\t\t"<<p1<<"\t"
              <<t1;
        ac=3.14*dc*dc/4;
        as=3.14*ds*ds/4;
        gc=mfc/ac;
        vel=gc/rho;                     fout<<"\t"<<vel;
        gs=mfc/as;
        vels=gs/rhos;
        p2=p1-kloss*gc*gc*vol/2;
        re=rho*vel*dc/vis;              fout<<"\t"<<re;
        fsp=1.325/pow(log((rough/3.7)+(5.74/pow(re,0.9))),2);       fout<<"\t"<<fsp;
```

```
fout<<"\t"<<rho<<"\t"<<vol<<"\t"<<vis<<"\t"<<enc;
p3=p2-fsp*vol*gc*gc*lin/(2*dc);
fout<<"\n"<<lin<<"\t"<<p3;
t3=t1;                              fout<<"\t"<<t3<<endl;

//-------------------------------------------
//Single-Phase Heat-Exchange (Diabatic) Region
//-------------------------------------------

pi1=p3;          tci1=t3;          noe=lhx/dz;

for(int j=1;j<=noe;j++)
{
        rho=exp(11.9599)*pow(tci1,-0.8592)*pow(pi1,0.0024);
        visc=exp(12.2525)*pow(tci1,-3.6728)*pow(pi1,0.0097);
        vol2=1/rho;
        if(j==1) { vol=vol2; }
        cpc=exp(2.9543)*pow(tci1,0.7642)*pow(pi1,-0.0036);
        ktc=exp(6.0522)*pow(tci1,-1.5147)*pow(pi1,0.0050);
        pr=cpc*visc/ktc;
        enc=exp(2.0523)*pow(tci1,1.8094)*pow(pi1,0.0004);
        vel=gc/rho;
        re=gc*dc/visc;
        fsp=1.325/pow(log((rough/3.7)+(5.74/pow(re,0.9))),2);
        nu=(fsp/8)*(re-1000)*pr/(1+12.7*sqrt(fsp/8)*(pow(pr,2/3)-1));
        hc=nu*ktc/dc;
        rhos=-0.4836*tsi1+0.0020*tsi1*tsi1;
        cps=1.6849*tsi1+0.0059*tsi1*tsi1;
        viss=4.0863E-008*tsi1-5.7686E-012*tsi1*tsi1;
        ktcs=-3.0583E-006*tsi1+1.6569E-007*tsi1*tsi1;
        prs=cps*viss/ktcs;
        vels=gs/rhos;
        res=gs*ds/viss;
        fsps=1.325/pow(log((rough/3.7)+(5.74/pow(res,0.9))),2);
```

```
        nus=(fsps/8)*(res-1000)*prs/(1+12.7*sqrt(fsps/8)*(pow(prs,2/3)-1));
        hs=nus*ktcs/ds;
        tw=(hc*dc*tci1+hs*ds*tsi1)/(hc*dc+hs*ds);
        tsi2=tsi1-(hs*3.141*ds*(tw-tsi1)*dz/(mfc*cps));
        tci2=tci1-(hc*3.14*dc*(tci1-tw)*dz)/(mfc*cpc)
              -gc*gc*(vol2*vol2-vol*vol)/(2);
        pi2=pi1-(fsp*gc*gc*vol*dz)/(2*dc)-(gc*gc*(vol2-vol));
        tsi1=tsi2;        tci1=tci2;
        pi1=pi2;          vol=vol2;                dx+=dz;
        fout<<"\n"<<lin+dx<<"\t"<<pi2<<"\t"<<tci2<<"\t"<<vel
            <<"\t"<<re<<"\t"<<fsp;
        fout<<"\t"<<rho<<"\t"<<vol2<<"\t"<<visc<<"\t"<<enc;
}

//-------------------------------
//Adiabatic Single-Phase Region
//-------------------------------

t4=tci2;          p4=pi2;
t4s=t4;           p4s=345740;
double rho4=1279.2,lsp;
vis=0.00025114;
vel=gc/rho4;
re=rho4*vel*dc/vis;
fsp=1.325/pow(log((rough/3.7)+(5.74/pow(re,0.9))),2);
lsp=2*dc*rho4*(p4-p4s)/(fsp*gc*gc);
fout<<"\n\n"<<lin+dx<<"\t"<<p4<<"\t"<<t4<<"\t"<<vel<<"\t"<<re
    <<"\t"<<fsp<<"\t"<<rho4;
fout<<"\n"<<lin+dx+lsp<<"\t"<<p4s<<"\t"<<t4s<<"\t"<<vel<<"\t"
    <<re<<"\t"<<fsp<<"\t"<<rho4<<endl;

//-------------------------------------
//Adiabatic Two-Phase Region
//-------------------------------------
```

```
double dp=1000,p,rhof,rhog,rhofg,hf,hg,hfg,sf,sg,sfg,muf,mug,mutp,
        vf,vg,vfg,s=0,smax=0,oldrho,h4s=206310,t,x=0,v,velocity,
        reytp,ftp,dl,ltp=0,y,h;

rho=rho4;
int i=1;
do
{
        p=p4s-dp;
        s=smax;         oldrho=rho;
        t=247.8017+8.6019E-005*p;
        vf=0.0007+1.7510E-010*p;            rhof=1/vf;
        vg=0.1230-1.8317E-007*p;            vfg=vg-vf;              rhog=1/vg;
        rhofg=rhog-rhof;
        hf=165913.8436+0.1164*p;
        hg=384092.9375+0.0495*p;            hfg=hg-hf;
        sf=877.5165+0.0004*p;
        sg=1740.1162-4.4446E-005*p;                 sfg=sg-sf;
        muf=0.0003-2.7942E-010*p;
        mug=9.7920E-006+3.1888E-012*p;
        y=pow(((gc*gc*vf*vfg)+hfg),2)-2*gc*gc*vfg*vfg*((-h4s+hf)
           +((gc*gc*vf*vf)/2)-((vel*vel)/2));
        x=(-hfg-gc*gc*vf*vfg+sqrt(y))/(gc*gc*vfg*vfg);
        mutp=mug*muf/(x*muf+(1-x)*mug);
        v=vf+x*vfg;
        rho=1/v;
        if(i==1)
        {
                oldrho=rho;
        }       i++;
        velocity=mfc/(ac*rho);
        smax=sf+x*sfg;
        h=hf+x*hfg;
```

```
        reytp=velocity*dc/(mutp*v);
        ftp=1.325/pow(log(rough/3.7+5.74/pow(reytp,0.9)),2);
        dl=fabs((2*dc/ftp)*(((-rho*dp)/(gc*gc))+((oldrho-rho)/(rho))));
        p4s=p;
        ltp+=dl;
        fout<<"\n"<<lin+dx+lsp+ltp<<"\t"<<p<<"\t"<<t<<"\t"<<velocity
            <<"\t"<<reytp<<"\t"<<ftp<<"\t"<<rho<<"\t"<<v<<"\t"<<mutp<<"\t"
            <<h<<"\t"<<x<<"\t"<<smax;
}while(s<smax+0.5 && t>264);
getch();
}
```

A.2 Data Generated

Case 1:

Table 5.1: Properties as calculated by Visual C++ Program

Length	Pressure	Temp	Vel	Rey No	f	Density	Volume	Viscosity	Enthalpy	x	Entropy
0	900000	298	2.313	11848.05	0.0327	1208.1	8.28E-04	1.96E-04	234340	0	1119
1.07	758774.57	298	2.313	11848.05	0.0327	1207.9	8.28E-04	1.96E-04	234340	0	1119
1.17	746041.39	297.3107	2.3115	11869.158	0.0327	1208.883	8.27E-04	1.95E-04	234693.8	0	1119
1.27	733299.19	296.5999	2.307	11770.572	0.0328	1211.241	8.26E-04	1.97E-04	233710.9	0	1119
1.37	720559.86	295.8545	2.3023	11669.488	0.0328	1213.685	8.24E-04	1.99E-04	232699.2	0	1119
1.47	707823.24	295.0731	2.2974	11564.11	0.0329	1216.26	8.22E-04	2.01E-04	231640.6	0	1119
1.57	695089.38	294.2537	2.2923	11454.306	0.033	1218.975	8.20E-04	2.02E-04	230533.1	0	1119
1.67	682358.34	293.3943	2.287	11339.909	0.033	1221.838	8.18E-04	2.05E-04	229374.3	0	1119
1.77	669630.15	292.4928	2.2813	11220.753	0.0331	1224.858	8.16E-04	2.07E-04	228161.9	0	1119
1.87	656904.84	291.5468	2.2754	11096.665	0.0332	1228.046	8.14E-04	2.09E-04	226893.3	0	1119
1.97	644182.44	290.5542	2.2692	10967.472	0.0333	1231.411	8.12E-04	2.11E-04	225565.6	0	1119
2.07	631462.96	289.5122	2.2626	10832.999	0.0333	1234.967	8.10E-04	2.14E-04	224176.1	0	1119
2.17	618746.38	288.4183	2.2558	10693.068	0.0334	1238.726	8.07E-04	2.17E-04	222721.8	0	1119
2.27	606032.69	287.2696	2.2486	10547.503	0.0335	1242.701	8.05E-04	2.20E-04	221199.7	0	1119
2.37	593321.84	286.0631	2.241	10396.126	0.0336	1246.907	8.02E-04	2.23E-04	219606.3	0	1119
2.47	580613.76	284.7956	2.233	10238.762	0.0337	1251.361	7.99E-04	2.27E-04	217938.4	0	1119
2.57	567908.36	283.4637	2.2246	10075.239	0.0339	1256.079	7.96E-04	2.30E-04	216192.4	0	1119
2.67	555205.52	282.0639	2.2158	9905.391	0.034	1261.081	7.93E-04	2.39E-04	214364.6	0	1119
2.6701	555205.52	282.0639	2.2089	9728.83	0.0341	1265	7.90E-04	2.39E-04	212120	0	1042.9
3.8859	400940	282.0639	2.2089	9728.83	0.0341	1265	7.90E-04	2.39E-04	212120	0	1042.9
3.9147	396940	281.9461	2.2169	12360.689	0.0325	1260.456	7.93E-04	1.88E-04	212210	4.82E-04	1036.62
3.920	395940	281.860	2.300	12462.35	0.032	1214.4	8.23E-	1.86E-	212209.	1.09E-	1036.

7		1	8	9	4	73	04	04	8	03	64
3.9265	394940	281.774	2.3853	12564.086	0.0324	1171.453	8.54E-04	1.85E-04	212209.6	1.69E-03	1036.66
3.9322	393940	281.688	2.4704	12665.869	0.0323	1131.123	8.84E-04	1.83E-04	212209.4	2.30E-03	1036.67
3.9376	392940	281.602	2.556	12767.708	0.0323	1093.24	9.15E-04	1.82E-04	212209.2	2.90E-03	1036.69
3.9428	391940	281.516	2.6421	12869.601	0.0322	1057.591	9.46E-04	1.80E-04	212209	3.51E-03	1036.71
3.9479	390940	281.43	2.7288	12971.549	0.0322	1023.986	9.77E-04	1.79E-04	212208.7	4.11E-03	1036.72
3.9528	389940	281.344	2.8161	13073.552	0.0321	992.256	1.01E-03	1.77E-04	212208.5	4.71E-03	1036.74
3.9576	388940	281.2579	2.9039	13175.608	0.0321	962.2506	1.04E-03	1.76E-04	212208.2	5.32E-03	1036.76
3.9622	387940	281.1719	2.9923	13277.718	0.032	933.8347	1.07E-03	1.75E-04	212208	5.92E-03	1036.78
3.9667	386940	281.0859	3.0812	13379.881	0.032	906.8871	1.10E-03	1.73E-04	212207.7	6.52E-03	1036.8
3.9711	385940	280.9999	3.1706	13482.096	0.0319	881.2984	1.13E-03	1.72E-04	212207.4	7.12E-03	1036.81
3.9753	384940	280.9139	3.2607	13584.364	0.0319	856.97	1.17E-03	1.71E-04	212207.1	7.72E-03	1036.83
3.9794	383940	280.8278	3.3512	13686.683	0.0318	833.8124	1.20E-03	1.69E-04	212206.8	8.32E-03	1036.85
3.9834	382940	280.7418	3.4423	13789.054	0.0318	811.7444	1.23E-03	1.68E-04	212206.5	8.92E-03	1036.87
3.9873	381940	280.6558	3.534	13891.475	0.0317	790.6922	1.26E-03	1.67E-04	212206.2	9.52E-03	1036.89
3.9911	380940	280.5698	3.6262	13993.947	0.0317	770.5884	1.30E-03	1.66E-04	212205.9	0.0101	1036.91
3.9949	379940	280.4838	3.7189	14096.47	0.0316	751.3716	1.33E-03	1.65E-04	212205.5	0.0107	1036.93
3.9985	378940	280.3977	3.8122	14199.042	0.0316	732.9853	1.36E-03	1.63E-04	212205.2	0.0113	1036.95
4.002	377940	280.3117	3.906	14301.663	0.0316	715.3779	1.40E-03	1.62E-04	212204.8	0.0119	1036.97
4.0054	376940	280.2257	4.0004	14404.333	0.0315	698.5018	1.43E-03	1.61E-04	212204.4	0.0125	1036.99
4.0088	375940	280.1397	4.0953	14507.052	0.0315	682.3134	1.47E-03	1.60E-04	212204.1	0.0131	1037.01
4.0121	374940	280.0537	4.1908	14609.819	0.0314	666.7722	1.50E-03	1.59E-04	212203.7	0.0137	1037.03
4.0153	373940	279.9676	4.2868	14712.634	0.0314	651.8412	1.53E-03	1.58E-04	212203.3	0.0143	1037.05
4.0184	372940	279.8816	4.3833	14815.496	0.0313	637.4858	1.57E-03	1.57E-04	212202.8	0.0149	1037.07
4.0215	371940	279.7956	4.4804	14918.405	0.0313	623.6741	1.60E-03	1.55E-04	212202.4	0.0155	1037.1
4.0245	370940	279.7096	4.578	15021.36	0.0313	610.3765	1.64E-03	1.54E-04	212202	0.0161	1037.12
4.0274	369940	279.6236	4.6761	15124.362	0.0312	597.5654	1.67E-03	1.53E-04	212201.5	0.0167	1037.14

4.0303	368940	279.5376	4.7748	15227.409	0.0312	585.2154	1.71E-03	1.52E-04	212201	0.0173	1037.16
4.0331	367940	279.4515	4.874	15330.501	0.0311	573.3025	1.74E-03	1.51E-04	212200.6	0.0179	1037.18
4.0358	366940	279.3655	4.9738	15433.639	0.0311	561.8046	1.78E-03	1.50E-04	212200.1	0.0185	1037.21
4.0385	365940	279.2795	5.0741	15536.821	0.0311	550.7009	1.82E-03	1.49E-04	212199.6	0.0191	1037.23
4.0411	364940	279.1935	5.1749	15640.048	0.031	539.9719	1.85E-03	1.48E-04	212199.1	0.0196	1037.25
4.0437	363940	279.1074	5.2762	15743.318	0.031	529.5996	1.89E-03	1.47E-04	212198.5	0.0202	1037.27
4.0463	362940	279.0214	5.3781	15846.631	0.031	519.5669	1.92E-03	1.46E-04	212198	0.0208	1037.3
4.0487	361940	278.9354	5.4805	15949.988	0.0309	509.8579	1.96E-03	1.45E-04	212197.4	0.0214	1037.32
4.0512	360940	278.8494	5.5835	16053.387	0.0309	500.4575	2.00E-03	1.44E-04	212196.9	0.022	1037.34
4.0536	359940	278.7634	5.6869	16156.828	0.0308	491.3519	2.04E-03	1.44E-04	212196.3	0.0226	1037.37
4.0559	358940	278.6774	5.7909	16260.312	0.0308	482.5276	2.07E-03	1.43E-04	212195.7	0.0232	1037.39
4.0582	357940	278.5913	5.8955	16363.836	0.0308	473.9722	2.11E-03	1.42E-04	212195.1	0.0238	1037.42
4.0605	356940	278.5053	6.0005	16467.402	0.0307	465.6741	2.15E-03	1.41E-04	212194.4	0.0244	1037.44
4.0627	355940	278.4193	6.1061	16571.009	0.0307	457.6221	2.19E-03	1.40E-04	212193.8	0.0249	1037.46
4.0649	354940	278.3333	6.2122	16674.656	0.0307	449.8058	2.22E-03	1.39E-04	212193.1	0.0255	1037.49
4.067	353940	278.2473	6.3188	16778.343	0.0306	442.2153	2.26E-03	1.38E-04	212192.5	0.0261	1037.51
4.0691	352940	278.1613	6.426	16882.069	0.0306	434.8413	2.30E-03	1.37E-04	212191.8	0.0267	1037.54
4.0712	351940	278.0752	6.5337	16985.835	0.0306	427.675	2.34E-03	1.37E-04	212191.1	0.0273	1037.56
4.0732	350940	277.9892	6.6419	17089.639	0.0305	420.708	2.38E-03	1.36E-04	212190.4	0.0279	1037.59
4.0752	349940	277.9032	6.7506	17193.483	0.0305	413.9323	2.42E-03	1.35E-04	212189.7	0.0285	1037.61
4.0771	348940	277.8172	6.8598	17297.364	0.0305	407.3406	2.45E-03	1.34E-04	212188.9	0.029	1037.64
4.0791	347940	277.7312	6.9696	17401.283	0.0304	400.9256	2.49E-03	1.33E-04	212188.2	0.0296	1037.67
4.081	346940	277.6451	7.0799	17505.239	0.0304	394.6806	2.53E-03	1.32E-04	212187.4	0.0302	1037.69
4.0828	345940	277.5591	7.1907	17609.232	0.0304	388.5992	2.57E-03	1.32E-04	212186.6	0.0308	1037.72
4.0847	344940	277.4731	7.302	17713.262	0.0303	382.6752	2.61E-03	1.31E-04	212185.8	0.0314	1037.75
4.0865	343940	277.3871	7.4138	17817.328	0.0303	376.9029	2.65E-03	1.30E-04	212185	0.032	1037.77
4.088	342940	277.301	7.526	17921.43	0.030	371.27	2.69E-	1.29E-	212184.	0.032	1037.

3		1	2		3	66	03	04	1	5	8
4.09	341940	277.215	7.639	18025.567	0.0303	365.7913	2.73E-03	1.29E-04	212183.3	0.0331	1037.83
4.0917	340940	277.129	7.7524	18129.74	0.0302	360.4417	2.77E-03	1.28E-04	212182.4	0.0337	1037.85
4.0934	339940	277.043	7.8663	18233.947	0.0302	355.2232	2.82E-03	1.27E-04	212181.5	0.0343	1037.88
4.0951	338940	276.957	7.9807	18338.189	0.0302	350.1312	2.86E-03	1.26E-04	212180.6	0.0349	1037.91
4.0967	337940	276.871	8.0956	18442.465	0.0301	345.1612	2.90E-03	1.26E-04	212179.7	0.0354	1037.93
4.0983	336940	276.7849	8.211	18546.775	0.0301	340.3092	2.94E-03	1.25E-04	212178.7	0.036	1037.96
4.0999	335940	276.6989	8.3269	18651.118	0.0301	335.5712	2.98E-03	1.24E-04	212177.8	0.0366	1037.99
4.1015	334940	276.6129	8.4434	18755.494	0.0301	330.9434	3.02E-03	1.24E-04	212176.8	0.0372	1038.02
4.103	333940	276.5269	8.5603	18859.903	0.03	326.422	3.06E-03	1.23E-04	212175.8	0.0377	1038.05
4.1046	332940	276.4409	8.6778	18964.344	0.03	322.0037	3.11E-03	1.22E-04	212174.8	0.0383	1038.08
4.1061	331940	276.3549	8.7958	19068.816	0.03	317.6851	3.15E-03	1.22E-04	212173.8	0.0389	1038.1
4.1075	330940	276.2688	8.9142	19173.321	0.0299	313.463	3.19E-03	1.21E-04	212172.7	0.0395	1038.13
4.109	329940	276.1828	9.0332	19277.857	0.0299	309.3344	3.23E-03	1.20E-04	212171.6	0.04	1038.16
4.1104	328940	276.0968	9.1527	19382.423	0.0299	305.2963	3.28E-03	1.20E-04	212170.6	0.0406	1038.19
4.1119	327940	276.0108	9.2727	19487.02	0.0299	301.3459	3.32E-03	1.19E-04	212169.5	0.0412	1038.22
4.1133	326940	275.9248	9.3932	19591.647	0.0298	297.4805	3.36E-03	1.18E-04	212168.3	0.0418	1038.25
4.1146	325940	275.8387	9.5142	19696.304	0.0298	293.6975	3.40E-03	1.18E-04	212167.2	0.0423	1038.28
4.116	324940	275.7527	9.6356	19800.991	0.0298	289.9944	3.45E-03	1.17E-04	212166	0.0429	1038.31
4.1173	323940	275.6667	9.7576	19905.706	0.0298	286.3689	3.49E-03	1.17E-04	212164.8	0.0435	1038.34
4.1187	322940	275.5807	9.8801	20010.45	0.0297	282.8186	3.54E-03	1.16E-04	212163.6	0.0441	1038.37
4.12	321940	275.4947	10.003	20115.223	0.0297	279.3413	3.58E-03	1.15E-04	212162.4	0.0446	1038.4
4.1212	320940	275.4086	10.127	20220.024	0.0297	275.935	3.62E-03	1.15E-04	212161.2	0.0452	1038.43
4.1225	319940	275.3226	10.251	20324.853	0.0297	272.5975	3.67E-03	1.14E-04	212159.9	0.0458	1038.46
4.1238	318940	275.2366	10.375	20429.708	0.0296	269.3269	3.71E-03	1.14E-04	212158.6	0.0463	1038.49
4.125	317940	275.1506	10.5	20534.591	0.0296	266.1213	3.76E-03	1.13E-04	212157.3	0.0469	1038.52
4.1262	316940	275.0646	10.626	20639.501	0.0296	262.9788	3.80E-03	1.12E-04	212156	0.0475	1038.55

4.1274	315940	274.9785	10.752	20744.437	0.0296	259.8978	3.85E-03	1.12E-04	212154.6	0.048	1038.58
4.1286	314940	274.8925	10.878	20849.399	0.0295	256.8765	3.89E-03	1.11E-04	212153.3	0.0486	1038.62
4.1298	313940	274.8065	11.005	20954.387	0.0295	253.9133	3.94E-03	1.11E-04	212151.9	0.0492	1038.65
4.1309	312940	274.7205	11.132	21059.4	0.0295	251.0066	3.98E-03	1.10E-04	212150.5	0.0497	1038.68
4.1321	311940	274.6345	11.26	21164.438	0.0295	248.1548	4.03E-03	1.10E-04	212149	0.0503	1038.71
4.1332	310940	274.5485	11.389	21269.501	0.0294	245.3566	4.08E-03	1.09E-04	212147.6	0.0509	1038.74
4.1343	309940	274.4624	11.518	21374.588	0.0294	242.6106	4.12E-03	1.09E-04	212146.1	0.0514	1038.77
4.1354	308940	274.3764	11.647	21479.699	0.0294	239.9152	4.17E-03	1.08E-04	212144.6	0.052	1038.81
4.1365	307940	274.2904	11.777	21584.833	0.0294	237.2693	4.21E-03	1.07E-04	212143.1	0.0526	1038.84
4.1376	306940	274.2044	11.907	21689.991	0.0293	234.6715	4.26E-03	1.07E-04	212141.6	0.0531	1038.87
4.1387	305940	274.1184	12.038	21795.172	0.0293	232.1206	4.31E-03	1.06E-04	212140	0.0537	1038.9
4.1397	304940	274.0323	12.169	21900.376	0.0293	229.6155	4.36E-03	1.06E-04	212138.4	0.0543	1038.94
4.1407	303940	273.9463	12.301	22005.602	0.0293	227.1549	4.40E-03	1.05E-04	212136.8	0.0548	1038.97
4.1418	302940	273.8603	12.434	22110.85	0.0293	224.7377	4.45E-03	1.05E-04	212135.1	0.0554	1039
4.1428	301940	273.7743	12.566	22216.119	0.0292	222.363	4.50E-03	1.04E-04	212133.5	0.0559	1039.04
4.1438	300940	273.6883	12.7	22321.41	0.0292	220.0295	4.54E-03	1.04E-04	212131.8	0.0565	1039.07
4.1448	299940	273.6022	12.833	22426.722	0.0292	217.7364	4.59E-03	1.03E-04	212130.1	0.0571	1039.1
4.1457	298940	273.5162	12.968	22532.055	0.0292	215.4826	4.64E-03	1.03E-04	212128.4	0.0576	1039.14
4.1467	297940	273.4302	13.102	22637.408	0.0291	213.2672	4.69E-03	1.02E-04	212126.6	0.0582	1039.17
4.1476	296940	273.3442	13.238	22742.781	0.0291	211.0893	4.74E-03	1.02E-04	212124.8	0.0587	1039.2
4.1486	295940	273.2582	13.373	22848.174	0.0291	208.9479	4.79E-03	1.02E-04	212123	0.0593	1039.24
4.1495	294940	273.1721	13.509	22953.586	0.0291	206.8423	4.83E-03	1.01E-04	212121.2	0.0598	1039.27
4.1504	293940	273.0861	13.646	23059.017	0.0291	204.7716	4.88E-03	1.01E-04	212119.3	0.0604	1039.31
4.1514	292940	273.0001	13.783	23164.467	0.029	202.7349	4.93E-03	1.00E-04	212117.5	0.061	1039.34
4.1523	291940	272.9141	13.921	23269.936	0.029	200.7315	4.98E-03	9.97E-05	212115.6	0.0615	1039.37
4.1531	290940	272.8281	14.059	23375.422	0.029	198.7606	5.03E-03	9.92E-05	212113.6	0.0621	1039.41
4.154	289940	272.742	14.19	23480.92	0.029	196.82	5.08E-	9.88E-	212111.	0.062	1039.

		1	7	6		16	03	05	7	6	44
4.1549	288940	272.656	14.336	23586.448	0.029	194.9136	5.13E-03	9.83E-05	212109.7	0.0632	1039.48
4.1558	287940	272.57	14.476	23691.987	0.0289	193.0359	5.18E-03	9.79E-05	212107.7	0.0637	1039.51
4.1566	286940	272.484	14.615	23797.542	0.0289	191.188	5.23E-03	9.75E-05	212105.6	0.0643	1039.55
4.1574	285940	272.398	14.756	23903.115	0.0289	189.3691	5.28E-03	9.70E-05	212103.6	0.0648	1039.58
4.1583	284940	272.312	14.897	24008.703	0.0289	187.5786	5.33E-03	9.66E-05	212101.5	0.0654	1039.62
4.1591	283940	272.2259	15.038	24114.307	0.0289	185.8158	5.38E-03	9.62E-05	212099.4	0.0659	1039.65
4.1599	282940	272.1399	15.18	24219.927	0.0288	184.0802	5.43E-03	9.58E-05	212097.2	0.0665	1039.69
4.1607	281940	272.0539	15.322	24325.562	0.0288	182.3713	5.48E-03	9.53E-05	212095.1	0.067	1039.72
4.1615	280940	271.9679	15.465	24431.212	0.0288	180.6883	5.53E-03	9.49E-05	212092.9	0.0676	1039.76
4.1623	279940	271.8819	15.608	24536.876	0.0288	179.0308	5.59E-03	9.45E-05	212090.6	0.0681	1039.8
4.1631	278940	271.7958	15.752	24642.555	0.0288	177.3982	5.64E-03	9.41E-05	212088.4	0.0687	1039.83
4.1639	277940	271.7098	15.896	24748.248	0.0287	175.7901	5.69E-03	9.37E-05	212086.1	0.0692	1039.87
4.1646	276940	271.6238	16.04	24853.955	0.0287	174.2058	5.74E-03	9.33E-05	212083.8	0.0698	1039.9
4.1654	275940	271.5378	16.185	24959.675	0.0287	172.6449	5.79E-03	9.29E-05	212081.5	0.0703	1039.94
4.1661	274940	271.4518	16.331	25065.408	0.0287	171.107	5.84E-03	9.25E-05	212079.1	0.0709	1039.98
4.1669	273940	271.3657	16.477	25171.153	0.0287	169.5914	5.90E-03	9.21E-05	212076.7	0.0714	1040.01
4.1676	272940	271.2797	16.623	25276.912	0.0287	168.0979	5.95E-03	9.18E-05	212074.3	0.072	1040.05
4.1683	271940	271.1937	16.77	25382.682	0.0286	166.6259	6.00E-03	9.14E-05	212071.8	0.0725	1040.09
4.169	270940	271.1077	16.917	25488.464	0.0286	165.175	6.05E-03	9.10E-05	212069.4	0.0731	1040.12
4.1697	269940	271.0217	17.065	25594.258	0.0286	163.7448	6.11E-03	9.06E-05	212066.8	0.0736	1040.16
4.1705	268940	270.9357	17.213	25700.063	0.0286	162.3349	6.16E-03	9.02E-05	212064.3	0.0742	1040.2
4.1711	267940	270.8496	17.362	25805.879	0.0286	160.9449	6.21E-03	8.99E-05	212061.7	0.0747	1040.24
4.1718	266940	270.7636	17.511	25911.706	0.0286	159.5743	6.27E-03	8.95E-05	212059.1	0.0752	1040.27
4.1725	265940	270.6776	17.66	26017.543	0.0285	158.2229	6.32E-03	8.91E-05	212056.5	0.0758	1040.31
4.1732	264940	270.5916	17.811	26123.39	0.0285	156.8902	6.37E-03	8.88E-05	212053.8	0.0763	1040.35
4.1739	263940	270.5056	17.961	26229.246	0.0285	155.5758	6.43E-03	8.84E-05	212051.1	0.0769	1040.39

4.1745	262940	270.4195	18.112	26335.112	0.0285	154.2795	6.48E-03	8.81E-05	212048.4	0.0774	1040.42
4.1752	261940	270.3335	18.263	26440.988	0.0285	153.0008	6.54E-03	8.77E-05	212045.7	0.078	1040.46
4.1758	260940	270.2475	18.415	26546.872	0.0285	151.7395	6.59E-03	8.74E-05	212042.9	0.0785	1040.5
4.1765	259940	270.1615	18.567	26652.764	0.0284	150.4952	6.64E-03	8.70E-05	212040.1	0.079	1040.54
4.1771	258940	270.0755	18.72	26758.665	0.0284	149.2676	6.70E-03	8.67E-05	212037.2	0.0796	1040.57
4.1777	257940	269.9894	18.873	26864.574	0.0284	148.0564	6.75E-03	8.63E-05	212034.3	0.0801	1040.61
4.1784	256940	269.9034	19.027	26970.491	0.0284	146.8612	6.81E-03	8.60E-05	212031.4	0.0806	1040.65
4.179	255940	269.8174	19.181	27076.415	0.0284	145.6819	6.86E-03	8.57E-05	212028.5	0.0812	1040.69
4.1796	254940	269.7314	19.335	27182.345	0.0284	144.518	6.92E-03	8.53E-05	212025.5	0.0817	1040.73
4.1802	253940	269.6454	19.49	27288.283	0.0283	143.3693	6.98E-03	8.50E-05	212022.5	0.0823	1040.77
4.1808	252940	269.5594	19.646	27394.227	0.0283	142.2356	7.03E-03	8.47E-05	212019.5	0.0828	1040.8
4.1814	251940	269.4733	19.801	27500.178	0.0283	141.1165	7.09E-03	8.43E-05	212016.4	0.0833	1040.84
4.182	250940	269.3873	19.958	27606.134	0.0283	140.0119	7.14E-03	8.40E-05	212013.3	0.0839	1040.88
4.1826	249940	269.3013	20.114	27712.096	0.0283	138.9214	7.20E-03	8.37E-05	212010.2	0.0844	1040.92
4.1831	248940	269.2153	20.271	27818.063	0.0283	137.8447	7.25E-03	8.34E-05	212007	0.0849	1040.96
4.1837	247940	269.1293	20.429	27924.035	0.0282	136.7817	7.31E-03	8.31E-05	212003.8	0.0855	1041
4.1843	246940	269.0432	20.587	28030.013	0.0282	135.7322	7.37E-03	8.27E-05	212000.5	0.086	1041.04
4.1848	245940	268.9572	20.745	28135.994	0.0282	134.6958	7.42E-03	8.24E-05	211997.3	0.0865	1041.08
4.1854	244940	268.8712	20.904	28241.98	0.0282	133.6723	7.48E-03	8.21E-05	211994	0.0871	1041.12
4.186	243940	268.7852	21.063	28347.969	0.0282	132.6615	7.54E-03	8.18E-05	211990.6	0.0876	1041.16
4.1865	242940	268.6992	21.223	28453.963	0.0282	131.6633	7.60E-03	8.15E-05	211987.2	0.0881	1041.2
4.187	241940	268.6131	21.383	28559.959	0.0282	130.6773	7.65E-03	8.12E-05	211983.8	0.0887	1041.23
4.1876	240940	268.5271	21.544	28665.959	0.0281	129.7034	7.71E-03	8.09E-05	211980.4	0.0892	1041.27
4.1881	239940	268.4411	21.705	28771.961	0.0281	128.7414	7.77E-03	8.06E-05	211976.9	0.0897	1041.31
4.1886	238940	268.3551	21.866	28877.966	0.0281	127.791	7.83E-03	8.03E-05	211973.4	0.0902	1041.35
4.1892	237940	268.2691	22.028	28983.973	0.0281	126.8522	7.88E-03	8.00E-05	211969.8	0.0908	1041.39
4.189	236940	268.183	22.19	29089.98	0.028	125.92	7.94E-	7.97E-	211966.	0.091	1041.

7				2	1	46	03	05	2	3	43
4.1902	235940	268.097	22.353	29195.992	0.0281	125.0081	8.00E-03	7.94E-05	211962.6	0.0918	1041.47
4.1907	234940	268.011	22.516	29302.004	0.0281	124.1025	8.06E-03	7.92E-05	211959	0.0924	1041.51
4.1912	233940	267.925	22.68	29408.017	0.028	123.2076	8.12E-03	7.89E-05	211955.3	0.0929	1041.55
4.1917	232940	267.839	22.843	29514.031	0.028	122.3233	8.18E-03	7.86E-05	211951.5	0.0934	1041.59
4.1922	231940	267.753	23.008	29620.046	0.028	121.4494	8.23E-03	7.83E-05	211947.8	0.0939	1041.63
4.1927	230940	267.6669	23.173	29726.06	0.028	120.5857	8.29E-03	7.80E-05	211944	0.0945	1041.67
4.1932	229940	267.5809	23.338	29832.075	0.028	119.732	8.35E-03	7.77E-05	211940.1	0.095	1041.71
4.1937	228940	267.4949	23.504	29938.089	0.028	118.8882	8.41E-03	7.75E-05	211936.2	0.0955	1041.75
4.1941	227940	267.4089	23.67	30044.103	0.028	118.0542	8.47E-03	7.72E-05	211932.3	0.096	1041.8
4.1946	226940	267.3229	23.836	30150.116	0.0279	117.2297	8.53E-03	7.69E-05	211928.4	0.0965	1041.84
4.1951	225940	267.2368	24.003	30256.128	0.0279	116.4146	8.59E-03	7.67E-05	211924.4	0.0971	1041.88
4.1955	224940	267.1508	24.17	30362.139	0.0279	115.6088	8.65E-03	7.64E-05	211920.3	0.0976	1041.92
4.196	223940	267.0648	24.338	30468.148	0.0279	114.8122	8.71E-03	7.61E-05	211916.3	0.0981	1041.96
4.1965	222940	266.9788	24.506	30574.155	0.0279	114.0245	8.77E-03	7.59E-05	211912.2	0.0986	1042
4.1969	221940	266.8928	24.675	30680.159	0.0279	113.2457	8.83E-03	7.56E-05	211908	0.0992	1042.04
4.1974	220940	266.8067	24.844	30786.162	0.0279	112.4756	8.89E-03	7.53E-05	211903.8	0.0997	1042.08
4.1978	219940	266.7207	25.013	30892.162	0.0279	111.714	8.95E-03	7.51E-05	211899.6	0.1002	1042.12
4.1983	218940	266.6347	25.183	30998.158	0.0278	110.9609	9.01E-03	7.48E-05	211895.4	0.1007	1042.16
4.1987	217940	266.5487	25.353	31104.152	0.0278	110.2161	9.07E-03	7.46E-05	211891.1	0.1012	1042.2
4.1991	216940	266.4627	25.523	31210.142	0.0278	109.4795	9.13E-03	7.43E-05	211886.7	0.1017	1042.24
4.1996	215940	266.3766	25.694	31316.128	0.0278	108.7509	9.20E-03	7.41E-05	211882.3	0.1023	1042.29
4.2	214940	266.2906	25.866	31422.11	0.0278	108.0303	9.26E-03	7.38E-05	211877.9	0.1028	1042.33
4.2004	213940	266.2046	26.038	31528.088	0.0278	107.3175	9.32E-03	7.36E-05	211873.5	0.1033	1042.37
4.2008	212940	266.1186	26.21	31634.061	0.0278	106.6124	9.38E-03	7.33E-05	211869	0.1038	1042.41
4.2013	211940	266.0326	26.382	31740.029	0.0278	105.9149	9.44E-03	7.31E-05	211864.4	0.1043	1042.45
4.2017	210940	265.9466	26.555	31845.993	0.0277	105.2249	9.50E-03	7.28E-05	211859.9	0.1048	1042.49

4.2021	209940	265.8605	26.729	31951.951	0.0277	104.5422	9.57E-03	7.26E-05	211855.2	0.1053	1042.53
4.2025	208940	265.7745	26.903	32057.903	0.0277	103.8668	9.63E-03	7.23E-05	211850.6	0.1059	1042.57
4.2029	207940	265.6885	27.077	32163.85	0.0277	103.1986	9.69E-03	7.21E-05	211845.9	0.1064	1042.62
4.2033	206940	265.6025	27.251	32269.79	0.0277	102.5374	9.75E-03	7.19E-05	211841.1	0.1069	1042.66
4.2037	205940	265.5165	27.426	32375.724	0.0277	101.8831	9.82E-03	7.16E-05	211836.3	0.1074	1042.7
4.2041	204940	265.4304	27.602	32481.652	0.0277	101.2357	9.88E-03	7.14E-05	211831.5	0.1079	1042.74
4.2045	203940	265.3444	27.778	32587.572	0.0277	100.595	9.94E-03	7.12E-05	211826.6	0.1084	1042.78
4.2049	202940	265.2584	27.954	32693.486	0.0276	99.9609	0.01	7.09E-05	211821.7	0.1089	1042.82
4.2053	201940	265.1724	28.13	32799.392	0.0276	99.3335	0.0101	7.07E-05	211816.8	0.1094	1042.87
4.2056	200940	265.0864	28.307	32905.29	0.0276	98.7124	0.0101	7.05E-05	211811.8	0.1099	1042.91
4.206	199940	265.0003	28.485	33011.181	0.0276	98.0978	0.0102	7.03E-05	211806.8	0.1104	1042.95
4.2064	198940	264.9143	28.662	33117.063	0.0276	97.4894	0.0103	7.00E-05	211801.7	0.111	1042.99
4.2068	197940	264.8283	28.841	33222.937	0.0276	96.8872	0.0103	6.98E-05	211796.6	0.1115	1043.03
4.2071	196940	264.7423	29.019	33328.803	0.0276	96.2911	0.0104	6.96E-05	211791.4	0.112	1043.08
4.2075	195940	264.6563	29.198	33434.659	0.0276	95.7011	0.0104	6.94E-05	211786.2	0.1125	1043.12
4.2079	194940	264.5702	29.377	33540.507	0.0276	95.1169	0.0105	6.91E-05	211780.9	0.113	1043.16
4.2082	193940	264.4842	29.557	33646.345	0.0275	94.5386	0.0106	6.89E-05	211775.6	0.1135	1043.2
4.2086	192940	264.3982	29.737	33752.173	0.0275	93.9661	0.0106	6.87E-05	211770.3	0.114	1043.24
4.2089	191940	264.3122	29.918	33857.991	0.0275	93.3993	0.0107	6.85E-05	211764.9	0.1145	1043.29
4.2093	190940	264.2262	30.099	33963.8	0.0275	92.8381	0.0108	6.83E-05	211759.5	0.115	1043.33
4.2096	189940	264.1402	30.28	34069.597	0.0275	92.2824	0.0108	6.81E-05	211754	0.1155	1043.37
4.21	188940	264.0541	30.461	34175.385	0.0275	91.7322	0.0109	6.79E-05	211748.5	0.116	1043.41
4.2103	187940	263.9681	30.643	34281.161	0.0275	91.1874	0.011	6.77E-05	211742.9	0.1165	1043.45

Case 2:

Table 5.2: Properties as calculated by Visual C++ Program

Length	Pressure	Temp	Vel	Rey No	f	Density	Volume	Viscosity	Enthalpy	x	s
0.0000	900000.0000	298.0000	2.2821	11673.5290	0.0328	1208.7000	8.2733e-4	1.9612e-4	234340.0000	0.0000	1118.6
0.5300	829286.5500	298.0000	2.2821	11673.5290	0.0328	1208.7000	8.2733e-4	1.9612e-4	234340.0000	0.0000	1118.6
0.6300	816846.7200	297.2908	2.2812	11706.3350	0.0328	1209.1407	8.2703e-4	1.9557e-4	234702.0900	0.0000	1118.6
0.7300	804397.6700	296.5426	2.2766	11606.0470	0.0329	1211.5745	8.2537e-4	1.9726e-4	233691.0700	0.0000	1118.6
0.8300	791951.1600	295.7399	2.2718	11500.8340	0.0329	1214.1559	8.2362e-4	1.9906e-4	232626.4800	0.0000	1118.6
0.9300	779507.0700	294.8786	2.2666	11388.6230	0.0330	1216.9415	8.2173e-4	2.0103e-4	231486.8500	0.0000	1118.6
1.0300	767065.4800	293.9542	2.2610	11269.0120	0.0331	1219.9485	8.1971e-4	2.0316e-4	230267.0100	0.0000	1118.6
1.1300	754626.4600	292.9618	2.2550	11141.5490	0.0332	1223.1967	8.1753e-4	2.0548e-4	228961.1100	0.0000	1118.6
1.2300	742190.0800	291.8958	2.2486	11005.7600	0.0332	1226.7080	8.1519e-4	2.0802e-4	227562.8300	0.0000	1118.6
1.3300	729756.3600	290.7505	2.2416	10861.1510	0.0333	1230.5068	8.1267e-4	2.1079e-4	226065.4000	0.0000	1118.6
1.4300	717325.3200	289.5195	2.2342	10707.2090	0.0334	1234.6202	8.0997e-4	2.1382e-4	224461.5100	0.0000	1118.6
1.5300	704896.9500	288.1957	2.2261	10543.4000	0.0335	1239.0782	8.0705e-4	2.1714e-4	222743.3100	0.0000	1118.6
1.6300	692471.2000	286.7715	2.2175	10369.1760	0.0337	1243.9147	8.0391e-4	2.2079e-4	220902.3500	0.0000	1118.6
1.7300	680047.9700	285.2387	2.2081	10183.9740	0.0338	1249.1673	8.0053e-4	2.2481e-4	218929.5600	0.0000	1118.6
1.8300	667627.0900	283.5881	2.1981	9987.2220	0.0339	1254.8783	7.9689e-4	2.2923e-4	216815.1700	0.0000	1118.6
1.9300	655208.3400	281.8098	2.1872	9778.3431	0.0341	1261.0954	7.9296e-4	2.3413e-4	214548.7500	0.0000	1118.6
2.0300	642791.4000	279.8931	2.1756	9556.7643	0.0343	1267.8725	7.8872e-4	2.3956e-4	212119.0800	0.0000	1118.6
2.1300	630375.8100	277.8262	2.1563	9116.0804	0.0346	1279.2000	7.8103e-4	2.5218e-4	206370.0000	0.0000	1118.6
4.4252	345740.0000	277.8262	2.1563	9116.0804	0.0346	1279.2000	7.8176e-4	2.5114e-4	206310.0000	0.0000	1118.6
4.4331	344740.0000	277.4559	2.3213	11513.9800	0.0329	1188.2878	8.4155e-4	1.9884e-4	206309.6300	1.3738e-3	1016.3871
4.4386	343740.0000	277.3699	2.4187	11617.0580	0.0329	1140.4116	8.7688e-4	1.9707e-4	206309.4000	1.9685e-3	1016.4098
4.4438	342740.0000	277.2838	2.5167	11720.1780	0.0328	1096.0150	9.1240e-4	1.9534e-4	206309.1600	2.5628e-3	1016.4328
4.4488	341740.0000	277.1978	2.6152	11823.3380	0.0328	1054.7339	9.4811e-4	1.9364e-4	206308.9100	3.1565e-3	1016.4559

4.4537	340740.0000	277.1118	2.7142	11926.5390	0.0327	1016.2533	9.8401e-4	1.9196e-4	206308.6400	3.7499e-3	1016.4792
4.4584	339740.0000	277.0258	2.8138	12029.7810	0.0326	980.2994	1.0201e-3	1.9031e-4	206308.3700	4.3427e-3	1016.5028
4.4629	338740.0000	276.9398	2.9138	12133.0630	0.0326	946.6328	1.0564e-3	1.8869e-4	206308.0800	4.9351e-3	1016.5265
4.4673	337740.0000	276.8538	3.0144	12236.3840	0.0325	915.0434	1.0928e-3	1.8710e-4	206307.7800	5.5270e-3	1016.5505
4.4715	336740.0000	276.7677	3.1155	12339.7450	0.0325	885.3461	1.1295e-3	1.8553e-4	206307.4700	6.1185e-3	1016.5746
4.4756	335740.0000	276.6817	3.2172	12443.1450	0.0324	857.3771	1.1663e-3	1.8399e-4	206307.1500	6.7095e-3	1016.5989
4.4796	334740.0000	276.5957	3.3193	12546.5830	0.0324	830.9911	1.2034e-3	1.8247e-4	206306.8200	7.3000e-3	1016.6234
4.4834	333740.0000	276.5097	3.4220	12650.0600	0.0323	806.0584	1.2406e-3	1.8098e-4	206306.4700	7.8901e-3	1016.6482
4.4872	332740.0000	276.4237	3.5252	12753.5750	0.0323	782.4633	1.2780e-3	1.7951e-4	206306.1100	8.4797e-3	1016.6731
4.4908	331740.0000	276.3376	3.6289	12857.1280	0.0322	760.1020	1.3156e-3	1.7807e-4	206305.7400	9.0688e-3	1016.6982
4.4944	330740.0000	276.2516	3.7331	12960.7180	0.0322	738.8809	1.3534e-3	1.7664e-4	206305.3600	9.6575e-3	1016.7234
4.4978	329740.0000	276.1656	3.8379	13064.3450	0.0321	718.7160	1.3914e-3	1.7524e-4	206304.9600	0.0102	1016.7489
4.5011	328740.0000	276.0796	3.9431	13168.0090	0.0321	699.5312	1.4295e-3	1.7386e-4	206304.5500	0.0108	1016.7746
4.5044	327740.0000	275.9936	4.0489	13271.7090	0.0320	681.2574	1.4679e-3	1.7250e-4	206304.1300	0.0114	1016.8004
4.5075	326740.0000	275.9076	4.1552	13375.4450	0.0320	663.8320	1.5064e-3	1.7117e-4	206303.6900	0.0120	1016.8264
4.5106	325740.0000	275.8215	4.2620	13479.2160	0.0319	647.1979	1.5451e-3	1.6985e-4	206303.2400	0.0126	1016.8527
4.5136	324740.0000	275.7355	4.3693	13583.0230	0.0319	631.3031	1.5840e-3	1.6855e-4	206302.7800	0.0132	1016.8791
4.5166	323740.0000	275.6495	4.4771	13686.8650	0.0318	616.1000	1.6231e-3	1.6727e-4	206302.3000	0.0138	1016.9057
4.5194	322740.0000	275.5635	4.5854	13790.7410	0.0318	601.5449	1.6624e-3	1.6601e-4	206301.8100	0.0143	1016.9324
4.5222	321740.0000	275.4774	4.6942	13894.6520	0.0317	587.5979	1.7018e-3	1.6477e-4	206301.3100	0.0149	1016.9594
4.5250	320740.0000	275.3914	4.8036	13998.5970	0.0317	574.2221	1.7415e-3	1.6355e-4	206300.7900	0.0155	1016.9865
4.5277	319740.0	275.30	4.913	14102.5	0.031	561.383	1.7813e	1.6234e	206300.	0.01	1017.01

	000	54	4	750	6	7	-3	-4	2500	61	38
4.5303	318740.0000	275.2194	5.0238	14206.5870	0.0316	549.0514	1.8213e-3	1.6115e-4	206299.7100	0.0167	1017.0413
4.5328	317740.0000	275.1334	5.1347	14310.6320	0.0315	537.1962	1.8615e-3	1.5998e-4	206299.1400	0.0173	1017.0690
4.5353	316740.0000	275.0474	5.2460	14414.7090	0.0315	525.7915	1.9019e-3	1.5882e-4	206298.5600	0.0178	1017.0968
4.5378	315740.0000	274.9613	5.3579	14518.8190	0.0315	514.8125	1.9425e-3	1.5769e-4	206297.9700	0.0184	1017.1249
4.5402	314740.0000	274.8753	5.4703	14622.9600	0.0314	504.2361	1.9832e-3	1.5656e-4	206297.3600	0.0190	1017.1530
4.5425	313740.0000	274.7893	5.5832	14727.1330	0.0314	494.0410	2.0241e-3	1.5546e-4	206296.7400	0.0196	1017.1814
4.5448	312740.0000	274.7033	5.6966	14831.3380	0.0313	484.2073	2.0652e-3	1.5436e-4	206296.1000	0.0202	1017.2100
4.5470	311740.0000	274.6173	5.8105	14935.5740	0.0313	474.7164	2.1065e-3	1.5329e-4	206295.4400	0.0208	1017.2387
4.5492	310740.0000	274.5312	5.9249	15039.8400	0.0313	465.5510	2.1480e-3	1.5222e-4	206294.7700	0.0213	1017.2676
4.5514	309740.0000	274.4452	6.0398	15144.1370	0.0312	456.6950	2.1896e-3	1.5117e-4	206294.0900	0.0219	1017.2966
4.5535	308740.0000	274.3592	6.1552	15248.4630	0.0312	448.1333	2.2315e-3	1.5014e-4	206293.3800	0.0225	1017.3259
4.5556	307740.0000	274.2732	6.2710	15352.8200	0.0311	439.8517	2.2735e-3	1.4912e-4	206292.6600	0.0231	1017.3553
4.5576	306740.0000	274.1872	6.3874	15457.2050	0.0311	431.8370	2.3157e-3	1.4811e-4	206291.9300	0.0236	1017.3849
4.5596	305740.0000	274.1012	6.5043	15561.6200	0.0311	424.0767	2.3581e-3	1.4712e-4	206291.1700	0.0242	1017.4146
4.5616	304740.0000	274.0151	6.6217	15666.0640	0.0310	416.5592	2.4006e-3	1.4614e-4	206290.4000	0.0248	1017.4445
4.5635	303740.0000	273.9291	6.7396	15770.5360	0.0310	409.2735	2.4434e-3	1.4517e-4	206289.6100	0.0254	1017.4746
4.5654	302740.0000	273.8431	6.8579	15875.0360	0.0309	402.2093	2.4863e-3	1.4421e-4	206288.8100	0.0259	1017.5048
4.5673	301740.0000	273.7571	6.9768	15979.5640	0.0309	395.3567	2.5294e-3	1.4327e-4	206287.9900	0.0265	1017.5352
4.5691	300740.0000	273.6710	7.0962	16084.1190	0.0309	388.7068	2.5726e-3	1.4234e-4	206287.1500	0.0271	1017.5658
4.5709	299740.0000	273.5850	7.2160	16188.7020	0.0308	382.2508	2.6161e-3	1.4142e-4	206286.2900	0.0277	1017.5965
4.5727	298740.0000	273.4990	7.3364	16293.3110	0.0308	375.9805	2.6597e-3	1.4051e-4	206285.4100	0.0282	1017.6274
4.5744	297740.0000	273.4130	7.4572	16397.9470	0.0308	369.8883	2.7035e-3	1.3962e-4	206284.5200	0.0288	1017.6584
4.5761	296740.0000	273.3270	7.5785	16502.6090	0.0307	363.9668	2.7475e-3	1.3873e-4	206283.6100	0.0294	1017.6897
4.5778	295740.0000	273.2410	7.7003	16607.2970	0.0307	358.2092	2.7917e-3	1.3786e-4	206282.6800	0.0300	1017.7210
4.5794	294740.0000	273.1549	7.8226	16712.0110	0.0307	352.6089	2.8360e-3	1.3699e-4	206281.7300	0.0305	1017.7525
4.5811	293740.0000	273.0689	7.9454	16816.7500	0.0306	347.1597	2.8805e-3	1.3614e-4	206280.7600	0.0311	1017.7842

4.5827	292740.0000	272.9829	8.0687	16921.5140	0.0306	341.8557	2.9252e-3	1.3530e-4	206279.7700	0.0317	1017.8161
4.5842	291740.0000	272.8969	8.1925	17026.3020	0.0306	336.6914	2.9701e-3	1.3446e-4	206278.7700	0.0322	1017.8481
4.5858	290740.0000	272.8109	8.3167	17131.1150	0.0305	331.6615	3.0151e-3	1.3364e-4	206277.7400	0.0328	1017.8802
4.5873	289740.0000	272.7249	8.4414	17235.9520	0.0305	326.7609	3.0603e-3	1.3283e-4	206276.7000	0.0334	1017.9125
4.5888	288740.0000	272.6388	8.5666	17340.8120	0.0305	321.9848	3.1057e-3	1.3202e-4	206275.6300	0.0340	1017.9449
4.5903	287740.0000	272.5528	8.6923	17445.6960	0.0304	317.3287	3.1513e-3	1.3123e-4	206274.5500	0.0345	1017.9775
4.5917	286740.0000	272.4668	8.8185	17550.6030	0.0304	312.7883	3.1971e-3	1.3045e-4	206273.4400	0.0351	1018.0103
4.5932	285740.0000	272.3808	8.9452	17655.5330	0.0304	308.3594	3.2430e-3	1.2967e-4	206272.3200	0.0357	1018.0432
4.5946	284740.0000	272.2948	9.0723	17760.4850	0.0303	304.0380	3.2891e-3	1.2890e-4	206271.1700	0.0362	1018.0762
4.5960	283740.0000	272.2087	9.1999	17865.4600	0.0303	299.8205	3.3353e-3	1.2815e-4	206270.0100	0.0368	1018.1094
4.5973	282740.0000	272.1227	9.3280	17970.4560	0.0303	295.7032	3.3818e-3	1.2740e-4	206268.8200	0.0374	1018.1428
4.5987	281740.0000	272.0367	9.4566	18075.4740	0.0302	291.6827	3.4284e-3	1.2666e-4	206267.6100	0.0379	1018.1763
4.6000	280740.0000	271.9507	9.5857	18180.5130	0.0302	287.7557	3.4752e-3	1.2593e-4	206266.3800	0.0385	1018.2099
4.6013	279740.0000	271.8647	9.7152	18285.5730	0.0302	283.9192	3.5221e-3	1.2520e-4	206265.1300	0.0391	1018.2437
4.6026	278740.0000	271.7786	9.8452	18390.6540	0.0302	280.1701	3.5693e-3	1.2449e-4	206263.8600	0.0396	1018.2776
4.6039	277740.0000	271.6926	9.9757	18495.7550	0.0301	276.5055	3.6166e-3	1.2378e-4	206262.5700	0.0402	1018.3117
4.6051	276740.0000	271.6066	10.1066	18600.8770	0.0301	272.9228	3.6640e-3	1.2308e-4	206261.2500	0.0407	1018.3459
4.6064	275740.0000	271.5206	10.2380	18706.0180	0.0301	269.4193	3.7117e-3	1.2239e-4	206259.9200	0.0413	1018.3802
4.6076	274740.0000	271.4346	10.3699	18811.1780	0.0300	265.9925	3.7595e-3	1.2170e-4	206258.5600	0.0419	1018.4147
4.6088	273740.0000	271.3485	10.5023	18916.3580	0.0300	262.6400	3.8075e-3	1.2103e-4	206257.1800	0.0424	1018.4493
4.6100	272740.0000	271.2625	10.6352	19021.5560	0.0300	259.3595	3.8557e-3	1.2036e-4	206255.7700	0.0430	1018.4841
4.6111	271740.0000	271.1765	10.7685	19126.7730	0.0300	256.1487	3.9040e-3	1.1970e-4	206254.3400	0.0435	1018.5189
4.6123	270740.0000	271.0905	10.9022	19232.0090	0.0299	253.0056	3.9525e-3	1.1904e-4	206252.9000	0.0441	1018.5540
4.6134	269740.0000	271.0045	11.0365	19337.2620	0.0299	249.9281	4.0012e-3	1.1839e-4	206251.4200	0.0447	1018.5891
4.6146	268740.0000	270.9185	11.1712	19442.5330	0.0299	246.9142	4.0500e-3	1.1775e-4	206249.9300	0.0452	1018.6244
4.6157	267740.0000	270.8324	11.3064	19547.8210	0.0298	243.9621	4.0990e-3	1.1712e-4	206248.4100	0.0458	1018.6598
4.6168	266740.0	270.74	11.44	19653.1	0.029	241.069	4.1482e	1.1649e	206246.	0.04	1018.69

	000	64	20	260	8	9	-3	-4	8600	63	54
4.6179	265740.0000	270.6604	11.5781	19758.4490	0.0298	238.2359	4.1975e-3	1.1587e-4	206245.3000	0.0469	1018.7311
4.6189	264740.0000	270.5744	11.7147	19863.7870	0.0298	235.4585	4.2470e-3	1.1526e-4	206243.7100	0.0475	1018.7669
4.6200	263740.0000	270.4884	11.8517	19969.1420	0.0297	232.7360	4.2967e-3	1.1465e-4	206242.0900	0.0480	1018.8029
4.6210	262740.0000	270.4023	11.9892	20074.5130	0.0297	230.0668	4.3466e-3	1.1405e-4	206240.4500	0.0486	1018.8389
4.6220	261740.0000	270.3163	12.1272	20179.9000	0.0297	227.4496	4.3966e-3	1.1345e-4	206238.7900	0.0491	1018.8751
4.6231	260740.0000	270.2303	12.2656	20285.3010	0.0297	224.8827	4.4468e-3	1.1286e-4	206237.1000	0.0497	1018.9114
4.6241	259740.0000	270.1443	12.4045	20390.7180	0.0296	222.3650	4.4971e-3	1.1228e-4	206235.3900	0.0502	1018.9479
4.6251	258740.0000	270.0583	12.5439	20496.1500	0.0296	219.8949	4.5476e-3	1.1170e-4	206233.6500	0.0508	1018.9845
4.6260	257740.0000	269.9722	12.6836	20601.5960	0.0296	217.4712	4.5983e-3	1.1113e-4	206231.8900	0.0513	1019.0212
4.6270	256740.0000	269.8862	12.8239	20707.0560	0.0296	215.0927	4.6492e-3	1.1056e-4	206230.1000	0.0519	1019.0580
4.6280	255740.0000	269.8002	12.9646	20812.5300	0.0295	212.7582	4.7002e-3	1.1000e-4	206228.2800	0.0525	1019.0949
4.6289	254740.0000	269.7142	13.1058	20918.0180	0.0295	210.4665	4.7513e-3	1.0945e-4	206226.4400	0.0530	1019.1320
4.6298	253740.0000	269.6282	13.2474	21023.5190	0.0295	208.2165	4.8027e-3	1.0890e-4	206224.5800	0.0536	1019.1691
4.6308	252740.0000	269.5421	13.3895	21129.0330	0.0295	206.0071	4.8542e-3	1.0835e-4	206222.6900	0.0541	1019.2064
4.6317	251740.0000	269.4561	13.5320	21234.5600	0.0294	203.8373	4.9059e-3	1.0782e-4	206220.7700	0.0547	1019.2439
4.6326	250740.0000	269.3701	13.6750	21340.0990	0.0294	201.7061	4.9577e-3	1.0728e-4	206218.8200	0.0552	1019.2814
4.6334	249740.0000	269.2841	13.8184	21445.6500	0.0294	199.6124	5.0097e-3	1.0675e-4	206216.8500	0.0558	1019.3190
4.6343	248740.0000	269.1981	13.9623	21551.2140	0.0294	197.5554	5.0619e-3	1.0623e-4	206214.8500	0.0563	1019.3568
4.6352	247740.0000	269.1121	14.1066	21656.7890	0.0293	195.5341	5.1142e-3	1.0571e-4	206212.8300	0.0569	1019.3946
4.6361	246740.0000	269.0260	14.2514	21762.3750	0.0293	193.5476	5.1667e-3	1.0520e-4	206210.7700	0.0574	1019.4326
4.6369	245740.0000	268.9400	14.3966	21867.9720	0.0293	191.5952	5.2193e-3	1.0469e-4	206208.6900	0.0579	1019.4707
4.6377	244740.0000	268.8540	14.5423	21973.5800	0.0293	189.6759	5.2722e-3	1.0419e-4	206206.5900	0.0585	1019.5089
4.6386	243740.0000	268.7680	14.6884	22079.1990	0.0293	187.7890	5.3251e-3	1.0369e-4	206204.4500	0.0590	1019.5472
4.6394	242740.0000	268.6819	14.8350	22184.8280	0.0292	185.9336	5.3783e-3	1.0320e-4	206202.2900	0.0596	1019.5856
4.6402	241740.0000	268.5959	14.9820	22290.4670	0.0292	184.1091	5.4316e-3	1.0271e-4	206200.0900	0.0601	1019.6242
4.6410	240740.0000	268.5099	15.1295	22396.1150	0.0292	182.3147	5.4850e-3	1.0222e-4	206197.8700	0.0607	1019.6628

4.6418	239740.0000	268.4239	15.2774	22501.7730	0.0292	180.5498	5.5386e-3	1.0174e-4	206195.6300	0.0612	1019.7015
4.6426	238740.0000	268.3379	15.4257	22607.4400	0.0292	178.8135	5.5924e-3	1.0127e-4	206193.3500	0.0618	1019.7404
4.6434	237740.0000	268.2519	15.5745	22713.1160	0.0291	177.1053	5.6464e-3	1.0080e-4	206191.0400	0.0623	1019.7793
4.6441	236740.0000	268.1658	15.7237	22818.8000	0.0291	175.4245	5.7005e-3	1.0033e-4	206188.7100	0.0629	1019.8184
4.6449	235740.0000	268.0798	15.8734	22924.4930	0.0291	173.7705	5.7547e-3	9.9868e-5	206186.3400	0.0634	1019.8575
4.6456	234740.0000	267.9938	16.0235	23030.1930	0.0291	172.1427	5.8091e-3	9.9409e-5	206183.9500	0.0639	1019.8968
4.6464	233740.0000	267.9078	16.1740	23135.9020	0.0290	170.5405	5.8637e-3	9.8955e-5	206181.5300	0.0645	1019.9361
4.6471	232740.0000	267.8218	16.3250	23241.6170	0.0290	168.9633	5.9184e-3	9.8505e-5	206179.0700	0.0650	1019.9755
4.6479	231740.0000	267.7357	16.4764	23347.3400	0.0290	167.4106	5.9733e-3	9.8059e-5	206176.5900	0.0656	1020.0151
4.6486	230740.0000	267.6497	16.6283	23453.0700	0.0290	165.8818	6.0284e-3	9.7617e-5	206174.0800	0.0661	1020.0547
4.6493	229740.0000	267.5637	16.7806	23558.8070	0.0290	164.3764	6.0836e-3	9.7179e-5	206171.5300	0.0666	1020.0945
4.6500	228740.0000	267.4777	16.9333	23664.5500	0.0289	162.8940	6.1390e-3	9.6744e-5	206168.9600	0.0672	1020.1343
4.6507	227740.0000	267.3917	17.0864	23770.2990	0.0289	161.4339	6.1945e-3	9.6314e-5	206166.3500	0.0677	1020.1742
4.6514	226740.0000	267.3057	17.2400	23876.0540	0.0289	159.9958	6.2502e-3	9.5887e-5	206163.7200	0.0683	1020.2142
4.6521	225740.0000	267.2196	17.3940	23981.8140	0.0289	158.5792	6.3060e-3	9.5465e-5	206161.0500	0.0688	1020.2543
4.6527	224740.0000	267.1336	17.5485	24087.5800	0.0289	157.1836	6.3620e-3	9.5045e-5	206158.3500	0.0693	1020.2945
4.6534	223740.0000	267.0476	17.7033	24193.3510	0.0288	155.8085	6.4181e-3	9.4630e-5	206155.6200	0.0699	1020.3348
4.6541	222740.0000	266.9616	17.8586	24299.1270	0.0288	154.4536	6.4744e-3	9.4218e-5	206152.8600	0.0704	1020.3752
4.6547	221740.0000	266.8755	18.0143	24404.9070	0.0288	153.1184	6.5309e-3	9.3810e-5	206150.0700	0.0709	1020.4156
4.6554	220740.0000	266.7895	18.1705	24510.6910	0.0288	151.8025	6.5875e-3	9.3405e-5	206147.2400	0.0715	1020.4562
4.6560	219740.0000	266.7035	18.3271	24616.4790	0.0288	150.5056	6.6443e-3	9.3003e-5	206144.3800	0.0720	1020.4968
4.6567	218740.0000	266.6175	18.4841	24722.2720	0.0288	149.2272	6.7012e-3	9.2605e-5	206141.4900	0.0725	1020.5375
4.6573	217740.0000	266.5315	18.6415	24828.0670	0.0287	147.9670	6.7583e-3	9.2211e-5	206138.5700	0.0731	1020.5783
4.6579	216740.0000	266.4455	18.7994	24933.8660	0.0287	146.7246	6.8155e-3	9.1819e-5	206135.6200	0.0736	1020.6192
4.6585	215740.0000	266.3594	18.9576	25039.6670	0.0287	145.4996	6.8729e-3	9.1431e-5	206132.6300	0.0741	1020.6602
4.6592	214740.0000	266.2734	19.1163	25145.4720	0.0287	144.2917	6.9304e-3	9.1047e-5	206129.6100	0.0747	1020.7012
4.6598	213740.0	266.18	19.27	25251.2	0.028	143.100	6.9881e	9.0665e	206126.	0.07	1020.74

	000	74	54	790	7	6	-3	-5	5500	52	24
4.6604	212740.0000	266.1014	19.4350	25357.0870	0.0286	141.9260	7.0459e-3	9.0287e-5	206123.4700	0.0757	1020.7836
4.6610	211740.0000	266.0154	19.5949	25462.8980	0.0286	140.7674	7.1039e-3	8.9912e-5	206120.3400	0.0763	1020.8248
4.6616	210740.0000	265.9293	19.7553	25568.7110	0.0286	139.6247	7.1621e-3	8.9540e-5	206117.1900	0.0768	1020.8662
4.6621	209740.0000	265.8433	19.9161	25674.5240	0.0286	138.4975	7.2203e-3	8.9171e-5	206114.0000	0.0773	1020.9076
4.6627	208740.0000	265.7573	20.0773	25780.3390	0.0286	137.3854	7.2788e-3	8.8805e-5	206110.7800	0.0779	1020.9491
4.6633	207740.0000	265.6713	20.2389	25886.1550	0.0286	136.2883	7.3374e-3	8.8442e-5	206107.5200	0.0784	1020.9907
4.6639	206740.0000	265.5853	20.4010	25991.9710	0.0285	135.2059	7.3961e-3	8.8082e-5	206104.2300	0.0789	1021.0324
4.6644	205740.0000	265.4993	20.5634	26097.7880	0.0285	134.1377	7.4550e-3	8.7724e-5	206100.9000	0.0794	1021.0741
4.6650	204740.0000	265.4132	20.7263	26203.6050	0.0285	133.0837	7.5141e-3	8.7370e-5	206097.5400	0.0800	1021.1159
4.6655	203740.0000	265.3272	20.8895	26309.4220	0.0285	132.0435	7.5733e-3	8.7019e-5	206094.1400	0.0805	1021.1578
4.6661	202740.0000	265.2412	21.0532	26415.2380	0.0285	131.0169	7.6326e-3	8.6670e-5	206090.7100	0.0810	1021.1997
4.6666	201740.0000	265.1552	21.2173	26521.0540	0.0285	130.0037	7.6921e-3	8.6324e-5	206087.2400	0.0815	1021.2417
4.6672	200740.0000	265.0691	21.3818	26626.8680	0.0284	129.0034	7.7517e-3	8.5981e-5	206083.7300	0.0821	1021.2838
4.6677	199740.0000	264.9831	21.5467	26732.6820	0.0284	128.0161	7.8115e-3	8.5641e-5	206080.1900	0.0826	1021.3259
4.6682	198740.0000	264.8971	21.7120	26838.4940	0.0284	127.0414	7.8715e-3	8.5303e-5	206076.6200	0.0831	1021.3681
4.6687	197740.0000	264.8111	21.8778	26944.3040	0.0284	126.0790	7.9315e-3	8.4968e-5	206073.0100	0.0836	1021.4104
4.6693	196740.0000	264.7251	22.0439	27050.1130	0.0284	125.1288	7.9918e-3	8.4636e-5	206069.3600	0.0842	1021.4527
4.6698	195740.0000	264.6391	22.2104	27155.9190	0.0284	124.1906	8.0521e-3	8.4306e-5	206065.6700	0.0847	1021.4951
4.6703	194740.0000	264.5530	22.3774	27261.7230	0.0283	123.2641	8.1127e-3	8.3979e-5	206061.9500	0.0852	1021.5375
4.6708	193740.0000	264.4670	22.5447	27367.5240	0.0283	122.3492	8.1733e-3	8.3654e-5	206058.1900	0.0857	1021.5800
4.6713	192740.0000	264.3810	22.7125	27473.3230	0.0283	121.4455	8.2341e-3	8.3332e-5	206054.4000	0.0862	1021.6226
4.6718	191740.0000	264.2950	22.8806	27579.1180	0.0283	120.5530	8.2951e-3	8.3013e-5	206050.5600	0.0868	1021.6652
4.6723	190740.0000	264.2090	23.0492	27684.9100	0.0283	119.6715	8.3562e-3	8.2695e-5	206046.6900	0.0873	1021.7079
4.6728	189740.0000	264.1230	23.2181	27790.6980	0.0283	118.8007	8.4175e-3	8.2381e-5	206042.7800	0.0878	1021.7506
4.6732	188740.0000	264.0369	23.3875	27896.4820	0.0283	117.9405	8.4789e-3	8.2068e-5	206038.8400	0.0883	1021.7934
4.6737	187740.0000	263.9509	23.5572	28002.2630	0.0282	117.0907	8.5404e-3	8.1758e-5	206034.8500	0.0888	1021.8363

REFERENCES

1. ASHRAE. ASHRAE handbook— refrigeration. Atlanta,CA: American Society of Heating, Refrigerating and Air-Conditioning Engineers, Inc., 1998.
2. Bansal, P.K. and Xu, B., A Parametric Study of Refrigerant Flow in Non-Adiabatic Capillary Tube, *Applied Thermal Engineering*, Vol. 23, pp. 397-408, 2003.
3. Bansal, P.K. and Yang, C., Numerical Investigation of Capillary Tube-Suction Line Heat Exchanger Performance, *Applied Thermal Engineering*, Vol. 25, pp. 2014-2028, 2005.
4. Bansal, P.K. and Yang, C., Reverse Heat Transfer and Recondensation Phenomena in Non-Adiabatic Capillary Tubes, *Applied Thermal Engineering*, Vol.25, pp.3187-3202, 2005.
5. Bolstad, M.M. and Jordan, R.C., Theory and Use of the Capillary Tube Expansion Device: Part II – Non-Adiabatic, *Refrigerating Engineering*, Vol. 57, pp. 519-523, 1949.
6. Chen, Y. and Gu, J., Non-Adiabatic Capillary Tube Flow of Carbon Dioxide in a Novel Refrigeration Cycle, *Applied Thermal Engineering*, Vol. 25, pp.1670-1683, 2005.
7. Chunlu Zhang, Guoliang Ding., Approximate analytic solutions of adiabatic capillary tube, *International Journal of Refrigeration,* Vol. 27, pp.17–24, 2004
8. C. Yang, P.K. Bansal., Numerical investigation of capillary tube-suction line heat exchanger performance, *Applied Thermal Engineering,* Vol.25, pp. 2014–2028, 2005.
9. Chunlu Zhang, Guoliang Ding., 2002. Approximate analytic solutions of adiabatic capillary tube, *Int. J. Refrigeration*, Vol. 27, pp. 17-24, 2004.

10. Gnielinski, V., New Equations for Heat and Mass Transfer in Turbulent Pipe and Channel Flow, *International Chemical Engineering*, Vol.16, pp.359-368, 1976.

11. Khan, M. K**.**, Kumar, R., Sahoo, P.K., 2008. Experimental and Numerical Investigations of the Flow of R-134a Through Lateral Type Diabatic Capillary Tube, *HVAC&R Research ASHRAE*, Vol. 14, issue 6, pp. xxx-xxx. (in press).

12. Khan, M.K**.**, Kumar, R., Sahoo, P.K., Flow Characteristics of Refrigerants Flowing through Capillary Tubes - A Review, *Applied Thermal Engineering*, (available online on http://sciencedirect.com) 2007.

13. McAdams, W.H., Wood, W.K. and Bryan, R.L, Vaporization inside Horizontal Tubes- Part II: Benzene-Oil Mixture, *Trans. ASME*, Vol. 64, p. 193, 1942.

14. Mendoca, K.C., Melo, C., Ferreira, R.T.S. and Pereira, R.H., Experimental Study on Lateral Capillary Tube-Suction Line Heat Exchangers, in: *Proceedings of International Refrigeration Conference, Purdue*, pp. 437-442, 1998.

15. Moody, L.F., Friction Factors for Pipe Flow, *ASME,* Vol. 66, pp. 671-684, 1944.

16. Pate, M.B. and Tree, D.R., A Linear Quality Model for Capillary Tube-Suction Line Heat Exchangers, *ASHRAE Trans.*, Vol.90, pp. 3-17, 1984.

17. P. K. Bansal and A. S. Rupasinghe., 1996. An empirical model for sizing capillary tubes, *Int. J. Refrigeration*, 19, 497 –505, 1996.

18. P. K**.** Bansal and A. S. Rupasinghe., An homogenous model for adiabatic capillary tubes *Applied Thermal Engineerin,* Vol.25, pp. 3187–3202, 2005.

19. S. M. Sami, Ph.D., P.E., H. Maltais and D. E. Desjardins., Influence of Geometrical Parameters on Capillary Behavior with New Alternative Refrigerants, *Applied Thermal Engineering*, Vol. 18, No. 6, pp. 491-502, 1998.

20. Staeblar, L.A., Theory and Use of a Capillary Tube for Liquid Refrigerant Control, *Refrigerating Engineering*, pp. 55-59, 1948.

21. Swalla, D.M. and Sherif, S.A., Thermodynamic Analysis of a Combined Vapor Compression/Absorption Refrigeration System, *Proceedings of the 16th World Energy Engineering Congress and the 3rd Environmental Technology Congress*,

Atlanta, October 26-28, pp. 557-561, 1993.

22. Sinpiboon, J. and Wongwises, S., Numerical Investigation of refrigerant flow through non-adiabatic capillary tubes, *Applied Thermal Engineering*, Vol. 22, pp.2015-2032, 2002.

23. S. Wongwiscs, T. Songnetichaovalit, N. Lokathada, P. Kritsadathikarn, M. Suchatawat and W. Pirompak A comparison of the flow characteristics of refrigerants flowing through adiabatic capillary tubes, *Int. Comm. Heat Mass Transfer*, Vol. 27, No. 5, pp. 611-621, 2000.

24. Valladares, G., Numerical Simulation of Non-Adiabatic Capillary Tubes Considering Metastable Region. Part I: Mathematical Formulation and Numerical Model, *Int. J. Refrigeration*, Vol. 30, pp. 642-653, 2007.

25. Valladares, G., Numerical Simulation of Capillary Expansion Devices Behaviour with Pure and Mixed Refrigerants Considering Metastable Region. Part II: Experimental Validation, *Int. J. Refrigeration*, Vol. 30, pp. 654-663, 2007.

26. Valladares, G., Review of numerical simulation of capillary tube using refrigerant mixtures, *Applied Thermal Engineering*, Vol. 24, pp.949-966, 2004.

27. Xu, B. and Bansal, P.K., Non-Adiabatic Capillary Tube Flow: A Homogeneous Model and Process Description, *Applied Thermal Engineering*, Vol. 22, 1801-1819, 2002.